# EEG correlates and methods for learning in brain-computer interaction.

**Mushfika Sultana**

School of Computer Science and Electronic Engineering

University of Essex

A thesis submitted for the degree of

*Doctor of Philosophy*

December 2023

# Acknowledgements

First and foremost, I would like to express my heartfelt gratitude to my supervisor, Dr. Serafeim Perdiks, for accepting me as a BCI PhD student. His consideration opened the door for me to work in this amazing research field. I am deeply grateful for his endless patience, generosity, guidance, teaching, help, and support throughout my PhD journey. His continuous encouragement and guidance have been instrumental in deepening my understanding of my research area and in my growth as a BCI research student. I only wish I could have had more time to learn from his vast knowledge and experience. This thesis would not have been achievable without his invaluable contribution.

It is a great pleasure to have been a part of the Brain-Computer Interfaces and Neural Engineering Laboratory (BCI-NE) at the University of Essex, a place filled with welcoming, friendly people and exceptional researchers. I am grateful to everyone from the BCI-NE lab. My fellow lab mates deserve special thanks for the stimulating discussions and productive work we shared over the last four years. To name just a few, I extend my gratitude to Idorenyin A. Amaunam, Yiyuan Han, Federica Armani, Lena Marreel, Ryber Milan, Ahmet C. Mercimek, Zilu Wang, and Alberto S. Tates Puetate.

Special thanks are also due to Evangelia P. Christodoulaki, Dr. Jacobo Fernandez Vargas, Dr. Amirul Islam, and other research students who participated in my experiments, especially during the challenging COVID times when finding participants was difficult.

My deepest gratitude goes to my colleagues Dr. Nihan Ari, Parisa Rahimi, and Evangelia P. Christodoulaki. With them, I shared not just work but also my free time, creating strong bonds that I believe will last forever

I am also thankful to my Supervisory Panel (SP) Meeting Chair, Dr. Mays Al-Naday, for her constructive feedback and suggestions during my panel meetings.

Last but not least, I would like to thank my sister, Dr. Zakia Sultana; my brother, Dr. Rifat Hasan Mazumder; and my niece, Rumaisa Fareesa Naome, for their unconditional help, sacrifice, and encouragement in pursuing and completing my PhD studies. Without their help, starting my PhD journey would not have been possible.

I dedicate my thesis to my late parents, Masuda Begum and Abdur Rab. Their unconditional love, sacrifice, and upbringing have shaped my life. I believe that wherever they are now, they are also happy for me to have completed this journey.

# Abstract

Motor Imagery (MI)-based Brain-Computer Interface (BCI) has emerged as a promising approach to provide an alternative means of communication and control and of restoring motor function for people with severe motor impairments. However, the efficiency and efficacy of BCI systems remain to date rather limited, preventing their out-of-lab implementation. The current lack of usability could be explained by the fact that significant efforts to improve decoding accuracy have not been coupled with an equally intensive strive to account for and exploit human and co-adaptive learning in the BCI loop. BCI research is nowadays still biased towards data-driven, exclusively Machine Learning (ML)-oriented methods.

This thesis aspires to offer a few stepping stones towards more user-oriented BCI, shifting the focus to subject learning, neuroplasticity monitoring and the co-adaptation between the human and the ML BCI decoder.

Along these lines, first, I seek to identify the electroencephalography (EEG) correlates of learning to drive a racing car, an example of complex and fine motor skills. Additionally, I explore the role of anodal transcranial Direct Current Stimulation (tDCS) in enhancing race-driving training. My work determines that theta EEG rhythms and alpha-band effective functional connectivity between frontocentral and occipital cortical areas are salient neuromarkers of the acquisition of racing skills. I also discern a possible tDCS effect in accelerating the pace of learning. Future research can build

upon these findings in order to establish innovative race-driving training protocols using neurotechnology.

Furthermore, my thesis presents a novel feature selection method which combines the conventional data-driven approach with BCI expert knowledge thanks to Fuzzy Logic (FL) theory and practice. Specifically, the proposed methodology balances the features' separability with their suitability derived from prior neurophysiological knowledge accounted in the relevant neuroscience literature. I show that my algorithm achieves considerable and statistically significant improvement in terms of classification accuracy, feature stability and class bias, thanks to a fuzzy controller formulation. I posit that the application of this method can promote subject learning during BCI training thanks to keeping the selected features within a "learnable", physiologically relevant manifold, thus potentially boosting the overall BCI efficiency beyond the immediate classification accuracy gains extracted here.

Adaptive/co-adaptive BCI systems play a pivotal role in achieving consistent and effective control of MI BCIs by integrating learning for both the user and the machine. One of the main motivations behind co-adaptative BCI has been the avoidance of the boring and laborious open-loop calibration sessions that are conventionally imposed at the onset of user/system training in order to collect data for training the ML BCI model, or intermittently to re-adapt the model with recent data to address performance degradation and fluctuations. In the context of BCI-based rehabilitation, these issues become particularly pressing, as time-consuming and tedious recalibration will not only demotivate the patients but also hard to fit logistically into a strict clinical schedule. In addition to that, recalibration sessions occupy time that could have been dedicated to therapeutic sessions, thus reducing the intensity and efficacy of an intervention. Towards alleviating this issue, this thesis identifies and compares different methods for calibration-free BCI-based rehabilitation. My results indicate that calibration-less

BCI-based rehabilitation algorithms are possible without compromising performance with respect to calibration-based regimes. The proposed methods thus lift a major barrier currently obstructing the translation of BCI-based therapies.

**Keywords:** brain-computer interface, electroencephalography, motor imagery, sensorimotor rhythms, Adaptive/co-adaptive BCI, machine learning, neuromarkers, Mamdani Fuzzy controller, transcranial Direct Current Stimulation.

# Table of contents

# List of figures

# List of tables

# List of acronyms

**EEG** electroencephalography

**EOG** Electrooculography

**MRCP** Movement-related Cortical Potentials

**CNV** Contingent Negative Variation

**UoE** University of Essex

**fMRI** functional Magnetic Resonance Imaging

**tDCS** transcranial Direct Current Stimulation

**CAR** Common Average Reference

**PSD** Power Spectral Density

**ROI** Region of Interest

**ROIs** Regions of Interest

**DTF** Directed Transfer Function

**IIR** Infinite Impulse Response

**BCI** Brain-Computer Interface

**SMR** Sensorimotor Rhythms

**ML** Machine Learning

**PR** Pattern Recognition

**DL** Deep Learning

**FL** Fuzzy Logic

**MI** Motor Imagery

**ERD/ERS** Event-Related Synchronization/Desynchronization

**ERSP** Event-Related Spectral Perturbation

**FES** Functional Electrical Stimulation

**QDA** Quadratic Discriminant Analysis

**MEG** Magnetoencephalography

**SNR** signal-to-noise ratio

**ERP** Event-Related Potential

**ERD** Event-Related Desynchronization

**ERS** Event-Related Synchronization

**SSVEP** Steady-State Visual Evoked Potential

**FS** Fisher Score

**LDA** Linear Discriminant Analysis

**FB** Frequency Band

**DP** Discriminant Power

**ff** Feature Fitness

# Chapter 1

# Introduction

Brain-Computer Interface (BCI) records brain activity, extracts the characteristics of specific mental states, and translates the recorded signal of interest into commands to external devices without any involvement of body movement (muscle control). Therefore, BCI plays an important role in restoring the communication and control capabilities of paralyzed people [3, 4] and is a promising tool for rehabilitation [5, 6]. Non-invasive BCI based on the modulation of sensorimotor brain rhythms (SMR) in electroencephalography (EEG) is one of the most popular, portable, safe, affordable, and self-placed BCI control paradigms, where a user can forward mental commands at will, in a self-paced manner, and without depending on external stimuli [7].

Despite progressive developments of BCI systems for different paradigms and applications, they still lack universality and robustness. Many prospective BCI users are unable to gain and maintain dexterous control of a BCI system. Various kinds of research have been conducted to address the issue by improving the signal processing and ML aspects of the BCI algorithms, or by establishing training and feedback protocols to exploit the human learning capacity. In particular, adaptive/co-adaptive BCIs using real-time, closed-loop BCI learning of the user and the machine have

proven effective in decreasing performance instability by identifying and adapting to non-stationarity effects present in brain signals [7].

This thesis studies methods, algorithms and practices designed to promote or investigate the effects of learning and brain plasticity in various BCI contexts, encompassing both learning of the machine and of the user in the BCI loop. Specifically, I first examine the EEG correlates of learning to drive a racing car, a particularly complex motor skill. Subsequently, I explore a FL-based approach for data-driven feature selection able to automatically exploit expert knowledge without requiring manual intervention. Finally, my thesis develops and evaluates algorithms for BCI-based rehabilitation that discard the need for time-consuming calibration sessions.

The remainder of this introductory chapter is organized as follows: Section 1.1 offers a general overview of BCI systems. Section 1.2 discusses the problem of learning in BCI and Section 1.3 presents the thesis objectives. Finally, Section 1.4 describes the structure of the thesis document and Section 1.5 presents the common experimental methods employed in two of the studies reported in this thesis.

## 1.1 General overview of BCI

BCI translates human intentions into commands to external devices from brain signals, without using the normal neuromuscular interaction pathways. Thus, people with impaired motor function can benefit from BCI, as the BCI system directly connects with the patient's intact brain tissue [7] bypassing lesions of the peripheral nervous system, the spinal cord and/or the muscular system. A non-invasive BCI system usually consists of the following modules:

- Brain activity measurement: targets either high temporal resolution (EEG, Magnetoencephalography (MEG)) or high spatial resolution (functional Magnetic Resonance Imaging (fMRI)).
- Signal pre-processing to filter brain signals and increase their signal-to-noise ratio (SNR).
- Feature extraction to extract attributes that characterize the targeted brain phenomena (depending on the BCI paradigm used).
- Classification to convert the extracted feature vectors into a mental state/class.
- Translation of each class of mental state to an action of the external device, like driving a robot, moving a cursor, etc.
- The user receives feedback (visual, auditory, tactile, multimodal, proprioceptive, etc.) informing him/her on their performance.

This thesis exclusively used EEG. EEG measures the electrical activity of the neuronal populations underneath the electrodes placed over the scalp. Hence, for EEG, the signal's spatial resolution is limited. EEG-based BCI allows for high temporal resolution able to support real-time decoding of fast-paced and quickly changing mental states. Four main paradigms are dominating the EEG BCI literature: SMR, Event-Related Potential (ERP)s, Slow Cortical Potentials, and Steady-State Visual Evoked Potential (SSVEP). For all the experiments this thesis used SMR-based BCI. SMR refers to spontaneous brain oscillations recorded over cortical regions in the $\mu$ [8–12 Hz] and $\beta$ [10-30 Hz] frequency bands associated with voluntary modulation of the motor cortex by motor execution or MI. Hence, learning is studied in this thesis mostly in the context of EEG MI-based BCI, but also concerning other brain rhythms involved in cognition and learning. MI is the mental rehearsal of a motor act without any overt

motor output, which involves similar brain regions and responses to those observed in programming and preparation of the associated real movements [8]. The replicability and thorough description of the identified MI-EEG-correlates, initially established in able-bodied individuals, along with their similarity to the correlates of Motor Execution (ME), suggest that natural motor circuits could potentially be leveraged through EEG monitoring, even for individuals with motor impairments. This naturally leads to the idea of utilizing these signals for BCI applications. The imagination of various types of movements results in amplitude suppression, known as ERD, or enhancement, known as ERS, of the Rolandic $\mu$ rhythm and the central $\beta$ rhythm recorded over the sensorimotor cortex of a BCI user. Consequently, MI-BCI is a particular sub-class of SMR-based BCI which is practical for the technology's main end-users: people with motor disabilities.

## 1.2 Problem definition and motivations

This thesis pertains to various topics on BCI learning in its most general sense, involving both human learning (and the associated brain plasticity) and parameter estimation of the BCI model. Learning and adaptation are central notions in BCI literature attracting considerable interest. Learning and co-adaptation in BCI have been attacked by several different angles, of which those that are directly related to my thesis work are briefly discussed below.

Many early approaches of BCI were based on the brain's ability to learn to regulate its activity through feedback provision. Feedback learning techniques are mainly based on neurofeedback research and represent a form of operant conditioning with brain signals [9–11]. This subject-learning process is followed by functional and structural transformations within the brain (neuroplasticity) [12–15] and needs prolonged training periods. However, more recently, one of the breakthroughs of BCI is the adoption of

Artificial Intelligence (mainly, ML algorithms) that enables the machine to learn in shorter time scales by decoding the high-dimensional, multivariate noisy patterns of various mental tasks [16]. With increased decoding accuracy by using ML algorithms, current research trends of non-invasive and invasive BCIs are heavily biased towards ML-oriented BCI training [17, 18].

However, despite the introduction and development of elaborate ML for BCI in the last 20 years, universal BCI and large-scale deployment of BCI technology in healthcare systems remain elusive. Even the most advanced ML-oriented BCI approaches are bound to fail to identify non-separable brain patterns. On the contrary, subject learning allows the creation of new neural circuits that generate discriminant task-dependent activity, which can then be easily decoded by the BCI model in a reasonable time scale [3].

Many studies indicate [17, 19–21] the importance of brain plasticity and the interactions between the machine and the human subject. However, research on subject-learning methodologies in BCI is still limited and often suffers from various shortcomings like the absence of longitudinal, closed-loop SMR BCI with adequately populated cohorts [22].

While initially BCI was envisioned as assistive technology [23] for communication [4, 9, 24], assistive mobility [25, 26], and motor substitution [27], based on more recent studies [28], it has been shown to have profound applicability in motor rehabilitation, where motor recovery is subserved by neural plasticity [5]. Hence, motor SMR BCI learning and motor recovery seem to share common mechanisms of brain plasticity. Closed-loop BCI training with real-time feedback is known to guide cortical plasticity within the aforementioned operant conditioning framework [3, 12]. Thus, similarly, BCI-based interventions for stroke or spinal cord injury rely on the contingency between sensory feedback and efferent brain commands. Functional electrical stimulation [5],

robots [29], and visual-based [30] treatments are examples of sensory feedback employed so far, where the BCI adds time contingency between afferent and efferent volleys, differentiating these therapies from previous ones, not including the BCI component. By doing this, BCI-based therapy promotes recovery by reinstating the intention-action-perception loop of natural motor control; the ability to manipulate the brain's plasticity through the BCI stands at the core of this kind of intervention.

Adaptive/co-adaptive training methods allow simultaneous adaptation for both learning agents involved in the BCI loop (subject and machine). Effective co-adaptation is hoped to gradually unlock the translational potential of BCI technology for both assistance [7] and as a tool for motor rehabilitation [22].

This thesis attempts to extend our knowledge on the abovementioned topics, investigating in-depth specific, selected aspects of the BCI learning problem lying at the cross-roads of machine and subject learning, co-adaptation, EEG plasticity monitoring, as well as the identification of the EEG correlates of learning complex motor skills.

## 1.3 Thesis Objectives

My thesis attempts to identify methods and algorithms to promote learning and plasticity in BCI. I further seek to understand EEG correlates of learning complex motor skills focusing in particular on acquiring and enhancing race-driving skills. Overall, I have defined three main objectives, each aspiring to address the following research questions:

- Is it possible to identify neuromarkers for acquiring and enhancing race-driving skills? Can the corresponding plasticity mechanisms be manipulated through

brain stimulation to give rise to faster and/or more effective motor training approaches for race driving?

- Does combining expert knowledge with a data-driven approach through FL facilitate feature selection to increase classification accuracy and promote user learning?
- Is it possible to eliminate calibration sessions in BCI-based stroke rehabilitation?

My thesis comprises a total of three EEG studies, each elaborated and discussed in its own dedicated chapter, as detailed below.

## 1.4 Thesis structure and contributions

The structure and the contents and contributions of each chapter in this thesis are as follows:

- Chapter 2 presents a thorough literature review of methods, practices, and algorithms designed to promote learning in BCI that are relevant to the research questions addressed. The respective literature is categorized per distinct topic and discusses current challenges associated with adaptive/co-adaptive training and methods for incorporating expert knowledge into popular data-driven parameter estimation approaches for BCI models. This chapter also includes a short review of adaptive methods devised to minimize the calibration procedures in BCI. Finally, it discusses works that sought to determine EEG correlates of learning various complex motor skills.
- Chapter 3 contributes the first, to my based knowledge, experimental investigation on the neural correlates of acquiring race driving skills.

- Chapter 4 proposes a novel feature selection method for BCI able to exploit both data-driven and expert knowledge through an FL-based controller.
- Chapter 5 investigates the possibility of calibration-free BCI-based methods for stroke rehabilitation to promote learning at the machine end.
- Chapter 6 provides a general discussion about the possible extensions and a reflection on the limitations of the presented thesis work.

## 1.5 General experimental apparatus

Two experiments of this thesis share a common experimental apparatus (Chapters 4 and 5). These are briefly described below.

### EEG and system configuration

The brain activity is acquired via 16 active EEG channels over the sensorimotor cortex: Fz, FC3, FC1, FCz, FC2, FC4, C3, C1, Cz, C2, C4, CP3, CP1, CPz, CP2, and CP4 according to the international 10-20 system with reference on the right ear and ground on AFz (see Fig. 1B). The EEG was recorded with a g.USBamp system at 512 Hz with a hardware bandpass filter whose passband was [0.1, 100] Hz, and a notch filter at the European power line frequency of 50 Hz. Raw signals were bandpassed between 0.1 Hz and 100 Hz, and notch-filtered at 50 Hz.

### General structure of training protocol

These two experiments involved MI (Chapter 4) or motor attempt (Chapter 5) tasks of different movements (e.g. right hand, left hand, and/or feet). In both cases, within an experimental session, users executed multiple training runs, with each run representing uninterrupted open or closed-loop BCI operation lasting approximately 5 to 15 minutes.

Effectively, a run corresponds to the duration required for a single execution of the training protocol, from initiation to completion or user/experimenter intervention. In general, each calibration run is composed of several trials. Each trial lasts for approximately 5 to 10 seconds. During each trial, the user is actively involved in a mental task, which includes short preparatory intervals preceding and following the central trial time. Notably, a trial encompasses numerous samples, typically ranging from 20 to 50, which refer to the brief subdivisions of a second. These samples are utilized to extract and classify individual feature vectors, providing feedback to the user. More detail will be found in respective Chapters 4 and 5. Consequently, a trial spans the period from when the user initiates a mental task until the feedback mechanism informs the user of its completion, such as when a feedback cursor reaches a threshold on the correct or erroneous side of a feedback bar. The participants performed an initial MI calibration session and subsequently proceeded with one or more closed-loop, "online" sessions with the best (in terms of classification accuracy) MI pair (for Chapter 5 it is right/left-hand extension motor attempt vs rest and for Chapter 4 MI 1 vs MI 2) and a classifier trained on the calibration data. During both the calibration and online experiments, every trial starts with a fixation cross lasting 2 to 3 s on a screen in front of the participants. Despite the various visualization and parametrization options, all the training and operation protocols presented in Chapters 4 and 5 adopt a largely common visual feedback representation (1D cursor in a feedback bar) and a corresponding trial structure based on the respective experiment. Fig 1.1 illustrates the general representation of the BCI trial with corresponding screen visualization. More specifically, each trial begins with a fixation cross appearing on the screen. During this phase, the user is required to focus on the centre of the screen, refraining from any activities that may produce artifacts, such as blinking or moving. Subsequently, the user experiences a brief cue period that provides a mental task indication. Following the

cue, there is a task-engagement period during which the user performs the mental task while receiving continuous feedback. Once the trial concludes and a decision threshold is reached, a short decision interval informs the user about the type of decision that has been reached. Trial timeout varies and it is different for Chapters 4 and 5. Additional details about the training protocol and accumulation framework are presented in the respective chapters (see Chapters 4 and 5).

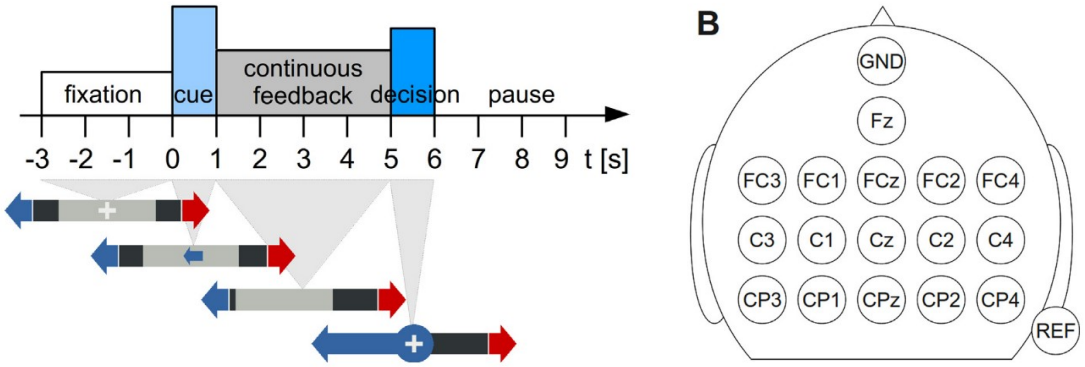


Fig. 1.1 (A) Timing of BCI trial with corresponding screen visualization. (B) EEG Electrode locations over motor cortex [1].

### Electroencephalography (EEG) processing and feature extraction

EEG channels are spatially filtered with a cross-Laplacian derivation, where the uniformly weighted sum of the orthogonal neighbouring channels is subtracted from each channel. The PSD of each Laplacian channel was estimated during the movement attempt or no-movement period for the frequency bands 4 to 48 Hz with 2 Hz resolution (23 bands) in sliding 1 s windows shifting by 62.5 ms with the Welch method and identical parameterization to [5].

### Individual experimental methods

The feature selection and classification modules differed substantially for the two studies in question. The necessary details can be found in the respective Chapters (4 and 5).

# Chapter 2

# State of the art

This chapter provides a thorough literature review of methods, practices, and algorithms designed to promote learning in BCI. It includes state-of-the-art methods for adaptive/co-adaptive training and other relevant challenges. I further delineate how expert knowledge embedding enhances conventional feature selection methods and promotes learning by integrating neurophysiological priors with data-driven knowledge. A short review of adaptive methods aimed at minimizing the amount of calibration sessions for BCI-based stroke rehabilitation follows. The chapter concludes with a comprehensive review of the EEG correlates of learning complex motor skills focusing in particular on acquiring and enhancing race-driving skills.

## 2.1 Co-adaptation in BCI

In general, learning is the dynamic process of acquiring a new skill through the processing and synthesis of diverse information. It involves a continuous optimization of various attributes essential to describing the desired skills and associated entities. Learning is a universal concept applicable to both humans and machines. It is closely associated with adaptation, which signifies the gradual, permanent changes in the

physical attributes of learning agents, such as the neuroplasticity observed in animal brains or the parameters of a learning machine. From a BCI point of view, subject learning involves the dexterous control of a neuroprosthesis actuated by the central nervous system. Mainly subject learning refers to the process through which a user or subject learns to effectively operate and interact with the BCI system. This learning process is crucial because it involves not only understanding how to use the device but also training the brain to generate clear and consistent signals that the BCI can recognize and interpret. A BCI user actively adapts or stabilizes their brain activity to either help the BCI better interpret their mental intentions or maintain control over the BCI. This user adaptation is essential for the BCI's feedback mechanism, which is central to learning in closed-loop BCI systems, mirroring general biofeedback learning approaches. This feedback acts as both a result of one learning process (BCI adaptation) and a stimulus for another (neuroplasticity and user learning), forming a key interactive link between these processes. Similarly, the BCI can recalibrate itself by adjusting its parameters, either continuously or periodically, to enhance its ability to interpret mental intents. This adaptation is supported by ongoing monitoring of the user's brain activity and any supplementary information about the user's actual intent, thereby creating a dynamic input-output relationship between the user and the machine learning processes. Therefore, a successful BCI lies not only in optimizing individual learning processes but also in accommodating their interactions.

From the perspective of a subject, learning objectives in the context of BCI systems can be defined through modulability, separability, and stability. Modulability reflects the capacity to differentiate one's brain activity during the execution of a mental task compared to the resting state or any other brain pattern. Separability is a closely related concept, focusing on the subject's ability to generate distinct brain patterns for all mental tasks involved in the BCI. Stability, on the other hand, emphasizes the subject's

proficiency in maintaining and recalling specific brain patterns during BCI operation. BCI adaptation plays a crucial role in aligning with and reinforcing the subject's learning efforts. This involves the implementation of optimal feature extraction, feature selection, and translation through classification or regression modules. Achieving these objectives not only ensures optimal BCI performance but also reinforces subject learning through the appropriate adaptation of BCI-driven feedback [20, 31].

Effective BCI training is integral to ensuring learning success, and it can be categorized into two main approaches: early BCI and recent BCI. Early BCI was predominantly characterized by feedback training and operant conditioning. In contrast, recent BCI developments heavily rely on signal processing and machine-learning protocols. Much of the contemporary research in BCI training revolves around co-adaptive training [32]. While co-adaptation is a natural evolution from conventional mutual learning [33] approaches, its emphasis has primarily been on addressing challenges related to online learning in the classification/regression and feature extraction/classification modules. BCI adaptation research has delved into the non-stationarity problem inherent in EEG. The inherent non-stationarity of EEG signals, characterized by their dynamic and evolving properties over time, necessitates the application of online ML techniques. Unlike stationary signals, where statistical properties remain constant, EEG signals exhibit variations due to factors such as changes in brain state, environmental conditions, and user fatigue. Consequently, traditional offline ML models, which assume stationarity and are trained on pre-collected datasets, often fail to capture the temporal dynamics and variability inherent in real-time EEG data. Online ML, by contrast, continuously updates its models in response to newly acquired data, thereby adapting to the signal's non-stationary nature. This adaptation is crucial for developing more accurate and reliable EEG-based applications, ensuring that the ML models remain effective as the characteristics of the EEG signals evolve. This has led to the recognition

of the necessity for online ML. Various adaptive classification methods, including Bayesian and/or Kalman Filter (KF)-based methods, different variations of adaptive (continuous or discontinuous) Linear Discriminant Analysis (LDA) and Quadratic Discriminant Analysis (QDA), or Gaussian Mixture Models (GMM) and generative or discriminative models with gradient-descent online learning, have been explored [34–37]. Machine learning-based methods have been extensively studied, eliminating non-stationarity during the transition from calibration to feedback sessions or within the latter. Non-invasive BCI research significantly benefits from online adaptation, addressing the supervision issue in learning and proposing that such protocols may assist individuals unable to gain control through conventional methods. Semi-supervised adaptive classification with SVM classifiers has been explored in various BCI (i.e., P300 and motor imagery BCI). Early co-adaptive training involved online recalibration of neuronal tuning curves based on different objective functions. Co-adaptive BCI studies are progressively embracing actual mutual learning principles [32, 33], transitioning from offline evaluations to online feedback experiments. Also, moving from supervised to unsupervised learning frameworks. There is an increasing emphasis on reporting the effects of co-adaptation in the subject's brain patterns. However, recent BCI-related methods are mostly giving the main focus on the technical ML and Deep Learning (DL) aspects [38, 39].

One of the major challenges in today's BCI landscape, especially with SMR-based BCI, is the presence of performance fluctuations within and across BCI sessions, coupled with a significant number of users struggling to gain control. Co-adaptive BCI show promise in addressing this issue by effectively mitigating performance instability through the tracking and adaptation to non-stationarity effects in brain signals. The literature suggests [22, 24, 32, 40] that decoder adaptation in online BCI control may also offer a solution to the problem of non-universal accessibility, where subjects fail to

exhibit the desired modulation of SMRs for exploitation by the BCI. Although the long-term impact of an evolving decoder on subject learning remains unclear, a transition to closed-loop training is seen as beneficial. Adaptive BCI provide a way to bypass open-loop calibration protocols entirely, a stage traditionally deemed necessary in modern BCI paradigms relying on ML. This necessity arises from algorithms requiring a supervised parameter estimation process, involving the synchronized collection of both brain signal data and actual mental task labels—a knowledge base not always readily available. However, the 'offline' data collection process is both time-consuming and demotivating, underscoring the importance of considering psychological factors in training protocol design. With compelling evidence on the significance of motivation, co-adaptive schemes are believed to play a significant role in enhancing BCI training protocols [21, 22, 24, 40]. This thesis tries to identify novel methods by taking into account adaptive and co-adaptive BCI, especially in the context of neurorehabilitation to avoid the celebration sessions (see Chapter 5).

## 2.2 Methods exploiting expert knowledge to promote learning

BCI systems have evolved from neurofeedback paradigms [41], where subjects learn to regulate their brain activity by observing direct feedback of it; this acquired skill is subsequently exploited for BCI by mapping the learned brain activity patterns onto commands to an external device [42]. These early BCI designs relied on expert neurophysiological knowledge to identify a few (often, a single one) salient and learnable brain features a subject may be able to get control of, as well as on lengthy feedback training. Subsequently, the introduction of elaborate ML and pattern recognition allowed to considerably minimize the training requirements while also boosting the BCI's

information transfer rates, by facilitating the decoding of complex, highly multidimensional and distributed brain activity associated with certain mental tasks (e.g., motor imagery) [43]. As a result of these developments, the basic Pattern Recognition (PR) processing pipeline is now the dominant BCI design model; its architecture thus consists of a series of standard modules conventionally including signal pre-processing, feature extraction, feature selection and decoding (classification/regression) [44].

Despite great benefits brought forward by the established "ML way to BCI", this approach has failed to deliver on its promise of zero-training interfaces, of universal accessibility to BCI for all prospective users, as well as of reliable and stable performance [45]. The BCI community gradually acknowledges these limitations [22] leading to a recent revival of interest in issues pertaining to the "human in the loop", like man-machine coadaptation [22, 24, 40], user training methods [20], subject learning [46] and its roots in brain plasticity mechanisms [47–49]. In this context, an important aspect that has been largely overlooked regards the tendency of the ML-oriented implementations to rely exclusively on purely data-driven methods; consequently, and in contrast to the field's aforementioned origins and interdisciplinary nature, significant insights derived by research in neuroscience and neuropsychology are often ignored, to the final BCI system's detriment. Similarly, the investment on ever more elaborate ML, including DL methods recently attracting considerable interest [50] in the field, renders the BCI a "black-box" system that lacks interpretability and obscures the neurophysiological basis of a BCI [51, 52]. This is particularly problematic in a field mostly targeting translational applications, where explainability is as critical as performance. There is thus a need to combine and enrich data-driven methods with prior knowledge in order to enjoy the best of both worlds in the form of both powerful and white-box models.

Feature selection is essential for any PR system; it helps remove redundant and irrelevant features that can degrade decoding performance and reduce the dimensionality of the feature space, which can attenuate or eliminate overfitting effects [43]. Despite the vast majority of published BCI work concerns methodology [53], research on feature selection tailored to BCI is scarce [54–57]. Furthermore, these works and, in general, most BCI systems presented so far, adopt one of the popular data-driven feature selection techniques derived by general PR literature [43, 53] irrespective of the particularities of brain signals. While the rise of DL lately shifts the focus towards embedded techniques (where feature extraction and selection are incorporated into, inseparable from and performed simultaneously with classifier estimation), "filter"-based methods are still the most popular in BCI [58]. Wrapper methods (including evolutionary approaches) have also been extensively tried [56, 59], but are not preferred in real-world settings because computational complexity and model training time are important considerations for realistic BCI application scenarios.

Filter feature selection regards ranking each candidate feature according to some fitness criterion which reflects their projected value for classification; the $N$-best, according to this criterion, features are then selected, where the dimensionality $N$ is determined taking into account the amount of available data for training and the number of emerging "good" features. The fitness criterion used is most often related to the separability of a feature with respect to the mental classes involved, either explicitly (e.g., Fisher Score [60], Canonical Variate Analysis [47, 61] and other [57]), or implicitly, e.g., based on correlation with class labels [62], mutual information [63], or on statistical methods assessing significant differences of feature values among classes, redundancy and consistency [64].

On the other hand, BCI systems that do take into account the outputs of basic neuroscience research in the design of the PR modules tend to ignore or only naively

fuse data evidence. A typical example is the category of adaptive interfaces that either fix [24, 40] or narrow down [65, 66] the brain features fed to the classifier to the EEG channels, time points and/or frequency bands that previous neurophysiological studies show will be modulated by an "average" user. In other works, data-driven and prior knowledge are combined through manual intervention [1, 61, 47], which requires the presence of a BCI expert, a pre-requisite that cannot be acceptable in clinical and home applications of BCI. There is thus a gap in the BCI literature with respect to feature selection methods capable of integrating neurophysiological priors with data-based knowledge in a fully-fledged, transparent and fully automatic manner.

Although exploiting expert information is possible with Bayesian techniques in the common probabilistic and statistical setting [67], it has been shown that FL [68] and Dempster-Shafer theory [69] allow far greater flexibility in managing this task. Here, in Chapter 4, I chooses to work within the FL framework to propose a feature selection module as a Mamdani fuzzy controller. My fuzzy controller generates a revised fitness ranking for all candidate features by taking into account both data-driven attributes (the separability of features) and BCI expert knowledge (anticipated feature suitability according to the relevant neuroscience literature). Fuzzy logic has demonstrated remarkable potential in managing uncertain and ambiguous information inherent in real-world scenarios by estimating and minimizing the impact of uncertainties. Moreover, it excels not only in addressing static imprecision in data but also in handling dynamic situations. As one of the widely accepted methodologies within soft computing paradigms, fuzzy logic finds widespread use in robotics and pattern recognition [70]. The interpretability and transparency of models derived from fuzzy logic, coupled with the abundance of fuzzy logic-based approaches for analyzing, interpreting, and classifying brain neurophysiologic data, particularly EEG data—make it an ideal choice

[71–73]. Fuzzy logic allows for the fusion of expert knowledge with a data-driven approach, contributing to a holistic understanding of complex systems.

FL-based feature selection has been previously attempted [74–77], however, the methods proposed there are fully data-driven, with no effort to exploit expert information. FL has been used in BCI also for feature extraction and classification with EEG signals [78–84]. However, none of them addresses the importance of combining the expert knowledge with the data-driven methods. Chapter 4, therefore, proposes a completely novel use of FL in the BCI context, by considering the main strengths of FL to address a corresponding identified need in this literature.

## 2.3 Adaptive methods to minimize the calibration sessions and to promote learning

BCI technology has been effectively used to restore motor function in patients with severe motor impairments caused by stroke [85]. It is hypothesized that BCI-based stroke therapies foster beneficial neuroplasticity promoting recovery by reinstating the intention-action-perception loop of natural motor control that has been broken due to the brain lesion. This is achieved as BCI-driven, rich afferent feedback is temporally coupled to the efferent motor commands decoded by the BCI sparking activity-dependent, associative plasticity [5]. In particular, motor rehabilitation for the upper limb has been largely grounded on "rewarding" sound ERD modulation of SMR through a wide range of feedback types and end-effectors [5, 86–91].

SMR-based BCI conventionally requires a calibration phase before it can decode motor intentions from raw EEG signals in real-time [5, 47]. This is due to the usual employment of supervised machine learning methods to learn the parameters of the BCI model, techniques that require labelled, ground truth data. During calibration,

the subject is asked to repeatedly rehearse the same motor tasks that will be later exercised and detected by the BCI in the therapeutic sessions, while the examples of the brain activity corresponding to these tasks are recorded and labelled by the experimental protocol. Furthermore, due to the non-stationary nature of brain activity, the performance of trained BCI models may soon degrade, and novel calibration procedures are necessary to reinstate decoding accuracy [22, 40]. Even if re-calibration is grounded on recent "online", closed-loop data derived from the therapeutic sessions, so that additional re-calibration sessions for data collection are not needed, the re-training process is likely to demand the presence of expert, technical personnel, increasing the regime's complexity.

Re-calibration sessions are time-consuming and demotivating for patients, as they do not involve closed-loop control [40]. The need for calibration reduces the therapy's intensity as therapeutic sessions need to be pushed back to interleave calibration ones or classifier re-training. Overall, the calibration stage and/or the re-calibration/re-training procedures pose a severe obstacle considering the stringent logistical and financial constraints in clinics. Therefore, the identification of calibration-free methods is essential for the technology transfer of BCI-based clinical interventions.

The issue of calibration-less ("zero-training") BCI has been studied as one of the main motivations behind the BCI adaptation literature [31]. However, most of these investigations are based on able-bodied users [92–95] and primarily regard assistive applications (e.g., there is a focus on unsupervised adaptation [24], largely unnecessary in the rehabilitation context where labels can be available). Very few works have addressed the problem specifically within the BCI-based rehabilitation context, employing either subject-specific adaptation [96] or various forms of transfer learning [97, 98]. Of note, although EEG markers of motor imagery/attempt in stroke patients tend to be similar to those of able-bodied individuals, they are likely to be

weaker and less consistent, leading to lower single-trial classification accuracy [5, 99]. Hence, SMR classification in stroke poses greater challenges than in general SMR BCI literature.

Identification of calibration-free BCI-based methods for stroke rehabilitation by taking into account the immediate launch of therapy without imposing any prerequisite is important. Very little literature addressed this need. Chapter 5 indicates that calibration-free BCI-based rehabilitation algorithms can be established, discarding calibration needs without compromising performance. Proposed methods not only lift a major barrier for stroke rehabilitation but also promote learning by escalating the calibration phase. By eliminating the need for a prolonged calibration phase, these methods enable algorithms to learn the parameters of the BCI model and promptly initiate feedback. Consequently, this not only streamlines the overall process but also enhances the learning at the machine end.

## 2.4 Learning and plasticity for complex motor skills acquisition

Learning different skills is a fundamental process in our everyday lives. The mechanism behind learning complex motor skills (i.e., race driving) remains poorly understood. Brain plasticity plays a pivotal role, from learning new motor skills to recovery from brain-related injury [100, 101]. A proper understanding of the mechanisms of neuroplasticity behind learning complex motor skills can help to develop tools and strategies to enhance or accelerate learning in healthy people and recovery from brain injury in patients, thus constituting an important clinical and scientific goal.

One of the main questions related to human brain plasticity revolves around understanding how sensory, motor, and cognitive functions undergo adaptation throughout

the protracted process of skill acquisition spanning many years [101]. A recent surge of interest in cognitive neuroscience is directed towards comprehending the distinct functional and structural characteristics inherent in the brains of athletes. Achieving professional performance in many fields like sports, arts, or music, is closely related to sensorimotor and cognitive capacities and can be examined to push to the very limits of human potential. A particular focus of numerous studies has been to address the question of whether the acquisition of expertise, obtained through many years of extensive, domain-specific training, leaves discernible traces of experience-dependent plasticity within specific, localized neural circuits [101, 102].

In recent years several works have studied neural signals like non-invasive electrophysiological (e.g., EEG) or metabolic (e.g., fMRI) brain imaging techniques to understand how domain-specific expertise builds up, especially for different sports [103]. Race driving particularly requires high-level domain-specific motor skills acquisition to effectively and efficiently command a multi-dimensional vehicle control system (i.e., steering, brakes, throttle and other controls). The functional and structural plasticity promoted by the rigorous practice of a race driver begs the question of whether the underlying plasticity mechanisms can be manipulated to give rise to faster and more effective motor training approaches.

Many studies also focused on EEG alpha and beta rhythms to link the expert performance and subsequent changes in those EEG rhythms [103]. Highly skilled race drivers, particularly those at the top levels of formula racing car competitions, undergo extensive psychophysical training and face extreme competitive conditions. The need for heightened concentration and precise sensory-motor control places a substantial demand on both their bodies and brains. Many of these drivers have engaged in high-speed activities, such as go-karting or motor racing, from a very young age, a period when brain plasticity is at its peak [104]. Consequently, it is anticipated that visuospatial

and motor processing in highly skilled individuals involves significantly more efficient use of brain activity compared to a matched group of untrained naïve drivers. A few articles [104–106]are based on functional magnetic resonance imaging fMRI to measure brain activity during motor reaction tasks and visuospatial tasks, examining the brain functional correlates associated with extreme training and competitive conditions faced by high-speed car racing drivers. In their study, Bernardi et al. [104, 105] conducted a comparison between skilled race drivers and regular car drivers, indicating that racing drivers exhibited more consistent recruitment of brain areas dedicated to motor control and spatial navigation compared to their regular counterparts. This finding suggests a distinct neurological pattern associated with the expertise of race drivers. However, an alternative perspective, presented in a different research study [106], hypothesizes that the observed differences in brain activity between racing drivers and regular drivers may be attributed to the task familiarity of the former. This viewpoint suggests that the variance in neural activation could be a result of the specialized cognitive demands and extensive practice associated with racing. Notably, a study [107] involving a Formula E Champion driving under extreme conditions demonstrated a relationship between brain activity in the delta, alpha, and beta frequency bands and hand movements. This manuscript [107] showcases the feasibility of using mobile brain and body imaging even in extreme conditions, such as race car driving, to explore sensory inputs, motor outputs, and brain states characterizing complex human skills.

However, limited research has focused on the perceptual and cognitive skills of race drivers. Based on papers [102, 108] a large amount of deliberate practice is required to obtain professional-level skills. On the contrary, a meta-analysis [109] suggested that deliberate practice contributes insignificant variance in sports performance, emphasizing the need to consider findings from cognitive ability, personality psychology, behavioural genetics, and sports sciences to comprehend the determinants of expertise. While many

studies have explored the effects of visual stimuli on steering control [110], very few have directly compared the brain activity of experienced racing drivers with that of normal drivers. One study indicated that exceptional driving abilities may involve the acquisition of a specific behavioural and functional motor repertoire distinct from everyday driving [105]. Another study aimed to highlight differences between racing drivers and naïve drivers, revealing superior driving performance in terms of faster lap times and fewer crashes [111].

Furthermore, complex motor learning involves two major aspects: the acquisition of motor skills, substantiated by performance improvements, and the ability to retain these skills after intervals or breaks. Recent studies consistently point to the pivotal roles played by the cerebellum and the primary motor cortex (M1) in both the acquisition and retention of complex motor tasks [112, 113].

Recently, non-invasive brain stimulation approaches have become popular and have been applied to focally change neuronal activation [114, 115]. One such promising approach involves non-invasive neuromodulation through tDCS, where DC currents are delivered to the brain tissue through electrodes placed on the user's scalp, increasing or suppressing cortical excitability depending on the mode of stimulation (anodal vs cathodal) [114, 115]. tDCS holds promise as a potential enhancer of motor skill learning in diverse populations, including neurotypical individuals and those with neurological disorders like stroke [116]. Meta-analysis evidence [117] suggests that individuals who undergo tDCS to the motor cortex during motor skill practice exhibit superior performance compared to those receiving sham tDCS. However, it remains unclear whether the combination of complex motor skill practice with tDCS results in faster skill acquisition than when sham tDCS is applied. tDCS enhancing motor skill learning involves the modulation of corticospinal excitability, leading to the induction of long-term potentiation a fundamental mechanism underlying learning.

The polarity-dependent effects of tDCS play an important role, with the anode electrode over the primary motor cortex (M1) resulting in a relative increase in corticospinal excitability [118–120]. It is hypothesized that anodal tDCS paired with practice can further enhance motor skill learning. Studies across various motor tasks support this hypothesis, showing that anodal tDCS to M1 during task practice improves motor performance more significantly than practice with sham tDCS [121, 122]. The identification of neuromarkers associated with motor learning has begged the question of whether the underlying brain plasticity mechanisms can be manipulated to give rise to faster and/or more effective training of race drivers using tDCS.

While various studies have provided insights into how racing drivers can focus on tasks, making their reactions and decisions vastly different from those of normal road car drivers [111], there remains a gap in understanding how this knowledge can be leveraged to extract even more performance on the track. The ability to measure brain activity using EEG is poised to become the next frontier in performance for race teams, offering a unique glimpse into how a driver's brain reacts to inputs on the track. This avenue holds significant promise for extracting additional performance from drivers. Additionally, exploring the role of tDCS in enhancing complex motor skills raises questions about how electrical stimulation can boost the brain's capacity to learn and retain new skills. The potential of tDCS extends beyond the average road car user to professional race drivers. Notably, there is a lack of studies clearly indicating differences between professional drivers and normal road car users, incorporating both neuro markers and behavioural analysis during driving.

Therefore, the identification of neuromarkers of race-driving proficiency and the exploration of tDCS to enhance race-driving training demand further research. Chapter 3 investigates by exploiting EEG signals the plasticity underpinning the effort of novice drivers to learn to master a racing simulator, the differences in the neural activity

between professional race drivers and novice drivers, and the effects of tDCS on learning. This research work seeks to identify EEG correlates of learning complex motor skills, aligning them with behavioural analysis. The scientific objective of this research is to lay the groundwork for the future design of innovative race-driving protocols using neurotechnology.

# Chapter 3

# EEG correlates of acquiring race driving skills

## 3.1 Introduction

Research over the last 30 years has demonstrated that motor skill acquisition is accompanied by plastic changes in the brain which can be revealed and studied with non-invasive electrophysiological (e.g., EEG) or metabolic (e.g., fMRI) brain imaging techniques. A recent study [123] has provided preliminary evidence that neuroimaging can be used to assess proficiency in complex motor skills such as race driving. Specifically, changes in the cerebellum have been identified through MRI imaging after driving training. Functional and structural differences have been also found between skilled and novice drivers by using fMRI scanning. Race driving is a complex motor task which engages multiple cognitive processes in different regions of the human brain in order to maintain and optimize speed and control throughout the racing track.

The acquisition of complex motor skills gradually unfolds across multiple training sessions, resulting in nearly asymptotic levels of performance. Regardless of the ex-

perimental paradigm employed, skill acquisition often follows a pattern where rapid improvements are observed in the initial stages, and subsequent gains occur more gradually over multiple practice sessions [124]. Recent advancements in neuroimaging technologies and noninvasive brain stimulation, such as tDCS, have significantly contributed to our understanding of the neural substrates involved in motor skill acquisition and retention [124]. Many studies [125, 126] have demonstrated that motor skill training induces brain plasticity. These changes encompass the optimization of the working patterns within local brain regions and alterations in global brain network connectivity [127]. Utilizing noninvasive neuroimaging techniques, like fMRI, allows us to detect both structural and functional brain plasticity following extensive motor skill training. Insight into the neural mechanisms driving this plasticity may serve as a foundation for identifying the most effective types of practice or training methods to enhance performance [128]. Consequently, the investigation of plastic changes associated with complex skill learning and expertise in the human brain stands as one of the most relevant areas in current neuroscience research.

Recently, the non-invasive brain stimulation approach tDCS has become popular and has been applied to focally change neuronal activation [114, 115]. Although tDCS seems to be a promising approach for enhancing motor training [116, 117], very few studies addressed the impact of tDCS on complex motor skills like race driving [129, 130]. The identification of neuromarkers of these learning processes has begged the question of whether the underlying plasticity mechanisms can be manipulated to give rise to faster and/or more effective motor training approaches(e.g., using the tDCS) for race driving. This work wishes to build upon these findings to further study brain plasticity accompanying race-driving training and to collect evidence on the potential role of tDCS in this context.

## 3.2 Motivations

The main motivations behind this work are to explore in large populations and with easy-to-deploy EEG signals the neural correlates of learning to drive a racing car, and the collection of evidence on the potential of tDCS as a tool to enhance race driving training. To achieve that, I have collected and analyzed multimodal experimental data consisting of drivers' EEG, telemetry from a driving simulator and meta-data towards the identification of neuromarkers of race driving proficiency and the assessment of the possibility to enhance race driving training through tDCS.

The objective of this work is to lay the foundation for the future design of innovative race-driving protocols exploiting neurotechnology, a perspective that is therefore regularly discussed here in light of the currently extracted results. To my best knowledge, this is the first investigation of the EEG correlates of learning to race.

## 3.3 Materials and Methods

### 3.3.1 Experimental setup

This research took place on the premises of the BCI-NE lab of the University of Essex campus in Colchester, UK. Each experimental session entailed EEG and Electrooculography (EOG) monitoring during driving in a racing simulator with active or sham tDCS taking place before the race driving task. The following main pieces of hardware equipment composed the experimental setup:

1. A complete racing simulator provided by GTA Global/Octane Junkies. The simulator replicated a Formula E car cockpit and consisted of a Playseat racing seat, Thrustmaster steering wheel and pedal inputs, and a single computer display monitor, all arranged and fixed on a metallic base. The monitor was connected

to a desktop PC running Windows 10 operation system, and placed next to the simulator. The simulator employed is shown in Fig 3.1a.

2. An ANT Neuro eego 64-channel EEG system (ANT Neuro b.v., Hengelo, Netherlands) extended with two bipolar EOG channels (Fig 3.1b).

3. A PlatoWork tDCS headset (PlatoScience ApS, Copenhagen, Denmark) (Fig 3.1c).

4. A laptop visualizing and recording the neurophysiological data. Telemetry data were recorded by the simulator desktop. The two separate data streams were synchronized with hardware triggers as described below.

5. A custom-made USB serial trigger box based on Arduino Micro microcontroller.

6. An anti-static wrist strap with a ground plug to equalize the body potential to the system ground and prevent electrical interference with the EEG from the simulator.

The employed software includes:

1. rFactor2 racing simulator on Steam. The race car model corresponds to that of the e.dams team car of the 2020-21 Formula E season, made available by GTA Global and NISSAN.

2. The open-source CNBIToolkit BCI platform used to acquire, store and annotate biosignal data.

3. A custom-made rFactor2 plugin shared library (dll) to export and record telemetry, as well as to deliver hardware triggers (short pulses) from the simulator desktop PC to the eego amplifier for syncing between telemetry and biosignals.

4. PlatoApp and PlatoLab smartphone applications for active and sham tDCS, respectively.


Fig. 3.1 Main hardware items of the experimental setup.(a) Driving simulator (b) ANT neuro eego EEG system (c) Platoscience Platowork tDCS system.

### 3.3.2 Data format

Each racing run outputs two types of data, each with its own format and file type:

1. The run's telemetry data are saved as a race log text file (TXT extension, which can be imported also as CSV). The content is a table where rows correspond to sampled timepoints/timeframes of telemetry during racing, and columns to the

various telemetry variables recorded. The sampling rate is 100 Hz. The telemetry variables saved are:

- Time elapsed from the previous frame (for sanity check, diagnosing lags and delays).
- Elapsed time since the racing session started.
- Current lap index.
- Elapsed time since the racing session started at the current lap start.
- Car position (x,y,z world coordinates in meters). The world coordinate system is left-handed with +y pointing up (towards the sky).
- Car rotation (x,y,z radians/sec in local vehicle coordinates). The local vehicle coordinate system is as follows: +x points out the left side of the car (from the driver's perspective). +y points out the roof. +z points out the back of the car. Rotations are as follows: +x pitches up. +y yaws to the right. +z rolls to the right.
- Car velocity (x,y,z meters/sec in local vehicle coordinates).
- Car acceleration (x,y,z meters/sec$^2$ in local vehicle coordinates).
- Car rotational acceleration (x,y,z radians/sec$^2$ in local vehicle coordinates).
- Car speed (meters/sec).
- Gear (since gear change in Formula E is automatic, this is of little interest).
- Throttle (in [0, +100], corresponding to no pedal press and full pedal press, respectively).
- Brake (in [0, +100], corresponding to no pedal press and full pedal press, respectively).

- Steering wheel (in [-100, +100], corresponding to full left turn and full right turn, respectively. Middle steering wheel position corresponds to 0.).
- Elapsed time of last car impact (with barriers, etc.).

Date and time stamps ensured that the correspondence between the racing log file and the EEG GDF file of each racing run could be established after the experiment.

2. The biosignal (EEG, EOG) data are saved in GDF format and were sampled at 512 Hz. GDF files can be loaded as a data matrix, columns correspond to biosignal channels and rows to sampled entries over time. The first 64 channels correspond to EEG electrodes (10-20 system positions in Fig 3.2a) referenced to position CPz (position AFz is ground), except for the channel at position 32 which is an EOG channel placed on the nasion. Another two bipolar EOG channels (horizontal in channel index 65, vertical in 66) are recorded by means of eego's bipolar box extension; the corresponding electrode positioning for the two EOG components are shown in Fig 3.2b. The last recorded channel (index 67) corresponds to the trigger/status channel (see below).

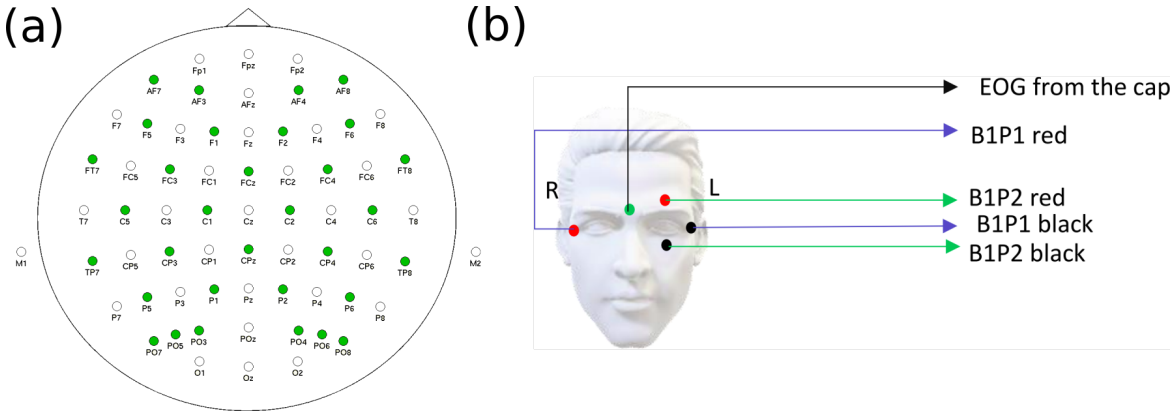


Fig. 3.2 Biosignal electrode configuration.(a) EEG channel positions in the 10-20 system (b) EOG bipolar channel placement.

### 3.3.3 Data synchronization

Telemetry and biosignal data are synced through hardware triggers that link the two separate data streams.

### 3.3.4 rFactor2 racing environment and settings

The racing task is accomplished with the rFactor2 simulator platform. All experimental racing runs were executed with the same settings (including the professional driver sessions) to exclude those as confounding factors. All racing runs were implemented as rFactor2 "Practice sessions". There are no opponents on the track, the driver is racing on their own so that no overtaking skills are to be learned and evaluated. Importantly, although all driving aids are disabled (traction control, automatic brake/throttle/steering assistance, etc.), the tyre wear and, especially, the car vulnerability were also disabled; this has some important implications for my results, as explained below. Overall, the learning task only involves learning to minimise lap time and impacts. Of note, a practice session in rFactor2 begins at the pit lane, so that the first lap of each training run starts counting after the car crosses the starting line. The Diriyah track of the Saudi Arabia Formula E e-Prix has been selected for the experiment. This is a demanding track encompassing 21 turns, as shown in Fig 3.3. The car model replicated the Formula E e.dams car of season 2020-21.

### 3.3.5 Experimental protocol

The study comprised two separate legs: longitudinal training of novice race drivers and single-session evaluation of professional/experienced race drivers.

In the first leg, each novice participant was asked to undergo 10 experimental race driving sessions, with a (non-binding) commitment to accomplish at least 5 of those in order for their data to be deemed usable. All participants finished their training

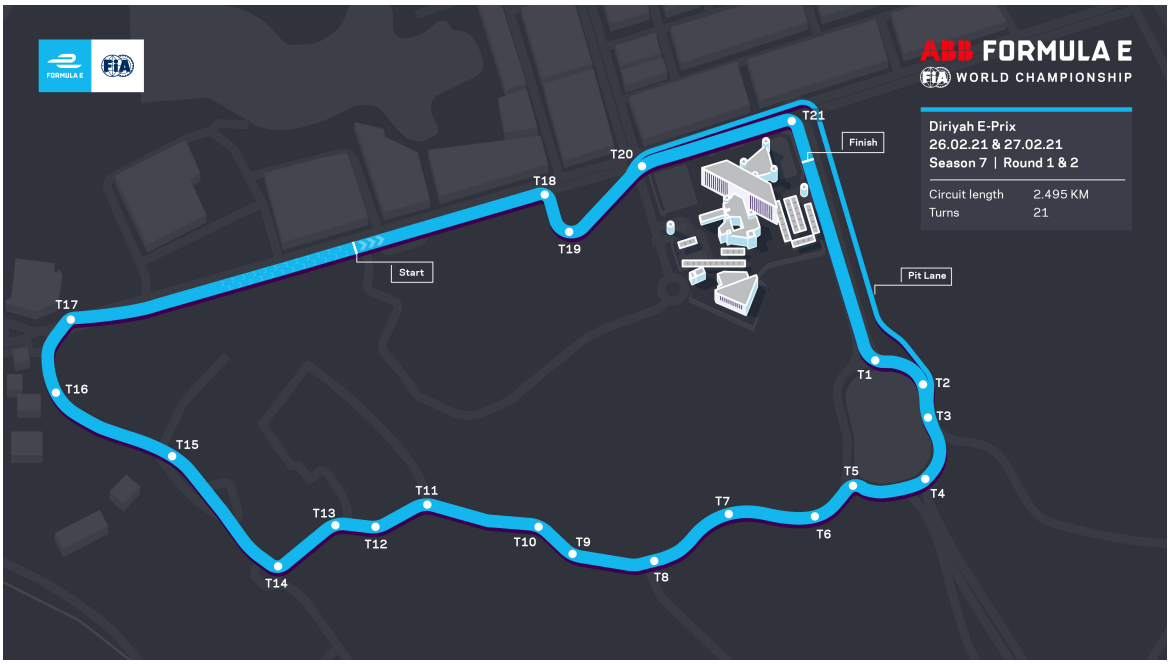


Fig. 3.3 Map of the Diriyah track with all turns labelled.

sessions within a period of two weeks so that the maximum logistically possible training intensity was achieved.

An experimental session comprised, first, 20' of (active or sham) tDCS stimulation with PlatoWork, followed by approximately 45' of simulated race driving. 11 novice participants were recruited. All subjects were randomly assigned to one of two tDCS groups (6 active + 5 shams). The active tDCS group received anodal stimulation with PlatoWork's fixed electrode positioning designed and parameterized to assist learning by increasing neural excitability over prefrontal brain regions associated with learning. The second group received "active sham" stimulation (i.e., stimulation that generates the same feeling without giving rise to cortical excitability). Novice subjects remained blind to their group allocation. Active tDCS was achieved with the PlatoApp of PlatoScience running on an Android smartphone and operating in "Learning" mode. Sham stimulation was accomplished with the PlatoLab app in the mode instructed by the PlatoScience collaborators.

The driving task targeted 20 laps per session. Participants were asked to complete the racing tasks in 5 blocks of 4 laps each. These blocks are defined here as "racing runs". Each racing run has a race log file and a biosignal GDF file associated with it, as described above. The instructions given to the subjects were simple and focused on three objectives: participants should try, to the best of their ability, to i) minimize lap time (visual feedback on lap time was delivered at the end of each lap by enabling the corresponding rFactor2 setting), ii) minimize the number of crashes (i.e., impact with barriers) and iii) avoid, as much as possible, movements and actions that generate EEG artifacts (speaking, excess blinking, intense neck movements). It has been taken for granted that, given the realistic scenario, complete avoidance of EEG artifacts is not possible.

In the second leg, three professional race drivers were recruited on two separate days. The two professional drivers of the e.dams Formula E team 2021-22, Sebastian Buemi and Maximilian Günther, executed a single session identical to those of the novice participants (i.e. 5 racing runs of 4 laps each while wearing the eego EEG system). The sessions of the two professional drivers were executed consecutively and included no tDCS. The racing sessions were implemented with the exact same specifications as for the novice drivers so that the EEG data acquired can be used for comparisons to neurophysiological data. Furthermore, an extra session was done with a 12-year-old volunteer who has won several junior national karting competitions and is the raining champion in his category.

### 3.3.6 Participants

Eleven (11) participants with no known neurological conditions were recruited. Table 3.1 illustrates the demographics, tDCS group allocation and driving proficiency of all novice drivers recruited. Frane's allocation algorithm (runs multiple t-tests to more accurately

identify unbalanced groups) was used to ensure that the two groups were balanced across all these possible confounding factors (see Table 3.2). Prior driving proficiency was assessed taking into account whether a subject had any previous driving and, especially, racing experience (karting, etc.). This work considered subjects with a driving license but no recent driving experience as NaÏ've. At the same time, I also consider the participants' video game experience, mainly related to car racing. Apart from two participants (EF06HE and RE03AN), none report any experience with karting or car racing video games. Since both groups are properly balanced, it is very unlikely that the performance of any specific participant is correlated with age or any other confounding factors.

### 3.3.7 Ethics and safety

The study was approved by the ethical committee of the University of Essex (UoE) (number ETH2021-1785 and amendment ETH2122-0411 for inclusion of a minor participant). All participants were informed about the tasks to be accomplished prior to the experiments, the protocol, the evaluation methods, the use of their data and any rare potential annoyances (e.g., obtrusive tDCS sensation, itching from EEG placement, headaches). All subjects were explicitly made aware of the possibility to withdraw from the study at any moment without a need to provide a reason. The experimental protocol fully complied with the Declaration of Helsinki.

### 3.3.8 Evaluation methods

#### Behavioural driving proficiency metrics

It is critical for the study's goals to identify metrics of race-driving proficiency upon which the concept of "learning to race" can be grounded (as the optimization of these metrics over time). The obvious learning outcome used throughout the study is the lap

time (i.e., the time needed to complete one lap). As a secondary measure of proficiency, this research work also counts the number of impacts per lap, since the ability to avoid crashes also reflects driving proficiency and there was explicit instruction to subjects to avoid impacts to the extent possible (in spite of the fact that the car's vulnerability was disabled in order to avoid large numbers of runs that would have to be restarted because of fatal crashes).

Table 3.1 Novice participant information

| SubjectID | Age | Gender | Corrected Vision | Handedness | Driving Proficiency | tDCS Group | Sessions | Laps |
|---|---|---|---|---|---|---|---|---|
| TE03ES | 32 | Male | Yes | Right | Naïve | Active | 10 | 195 |
| MA23GI | 25 | Female | Yes | Right | Naïve | Active | 8 | 159 |
| YA25AI | 22 | Male | No | Right | Naïve | Sham | 10 | 190 |
| MA16TE | 33 | Female | Yes | Right | Proficient | Sham | 8 | 170 |
| SA03UR | 34 | Male | Yes | Right | Naïve | Sham | 10 | 207 |
| EF06HE | 33 | Male | No | Right | Naïve | Active | 10 | 198 |
| LO30KI | 37 | Male | Yes | Right | Proficient | Sham | 10 | 193 |
| NI28LD | 18 | Male | No | Left | Proficient | Active | 9 | 179 |
| JA07NA | 30 | Male | No | Right | Naïve | Sham | 9 | 180 |
| MA14LY | 32 | Male | Yes | Right | Proficient | Active | 10 | 200 |
| RE03AN | 22 | Male | No | Right | Proficient | Active | 10 | 196 |

Table 3.2 Balance and influence of confounding factors. Proportions are noted for Male in Gender, Proficient in Driving Proficiency and Yes in Corrected Vision.

| | Age | | | Gender | | | Driving proficiency (Proficient) | | | Corrected Vision (Yes) | | |
|---|---|---|---|---|---|---|---|---|---|---|---|---|
| | Active | Sham | p-value | Active | Sham | p-value | Active | Sham | p-value | Active | Sham | p-value |
| Balance | 27.0±6.3 | 31.2±5.7 | 0.23 | 5/6 | 4/5 | 0.85 | 3/6 | 2/5 | 0.78 | 3/6 | 3/5 | 0.78 |
| | Correlation | | | Male | Female | p-value | Proficient | Naïve | p-value | Yes | No | p-value |
| Lap time gain | r=0.61, p=0.78 | | | 12.0±5.7 | 10.1±1.0 | 0.63 | 9.9±6.2 | 12.8±3.4 | 0.25 | 12.6±5.6 | 10.2±3.9 | 0.54 |

This study further defines a "penalized lap time" (actual lap time) metric which attempts to combine both aspects of racing (i.e., both fast and "accident-free") by augmenting the actually achieved lap time with 250 ms for each impact (the last column of the race file indicates the elapsed time since the last car impact). All these metrics are straightforward to compute based on the information stored in the race log files.

With respect to behavioural metrics, this work further analyzes the use of the throttle, brake, and steering wheel, based on the assumption that learning to race could probably lead to the milder, smoother and more precise use of some or all of these inputs. To do so, the number of brake and throttle push/release and turning left/right events per lap must be extracted. This is made possible through suitable processing of the corresponding columns in the race log files. Specifically, for brake and throttle press/release events, the raw input is first filtered with a Savitzky-Golay smoothing filter. The position and number of major peaks/sinks are then found by thresholding the derivative of the signal, and merging events that are too close in time (less than 0.5 s difference) together. Further identification of the peaks of the signals is done (using the peakfinder function of MATLAB Central which finds minima and maxima of an arbitrary signal) and compute, for each event, its slope/derivative $|S_{min/max} - S_{onset}|/(t_{min/max} - t_{onset})$ so that events corresponding to abrupt/clear movements can be distinguished from those that are smoother and less clear to the segment from the general activity. Finally, left/right turns are identified by using, again, peakfinder to locate the time points with maximum left/right steering wheel turning, signifying the offset of a left/right turn movement. The corresponding onset is found either as the offset of the immediately previous turning movement (e.g., for the cases where a left/right turn succeeds a right/left one, respectively), or, by extracting the offset of the latest period of inactivity (zero-derivative of steering wheel signal), whichever happens last. The slope of steering events is then found in the same manner

as for braking/accelerating. The analysis scripts also spot and store periods of complete inactivity (with no movement at all) in the lap, to be potentially used as "control" (e.g., for the Movement-related Cortical Potentials (MRCP) analysis). Based on the extraction of braking, accelerating and steering events in this fashion, the amount of extracted events can serve as an index of race driving proficiency as hypothesized. Fig 3.4 illustrates this process for the best lap of Max Günther.

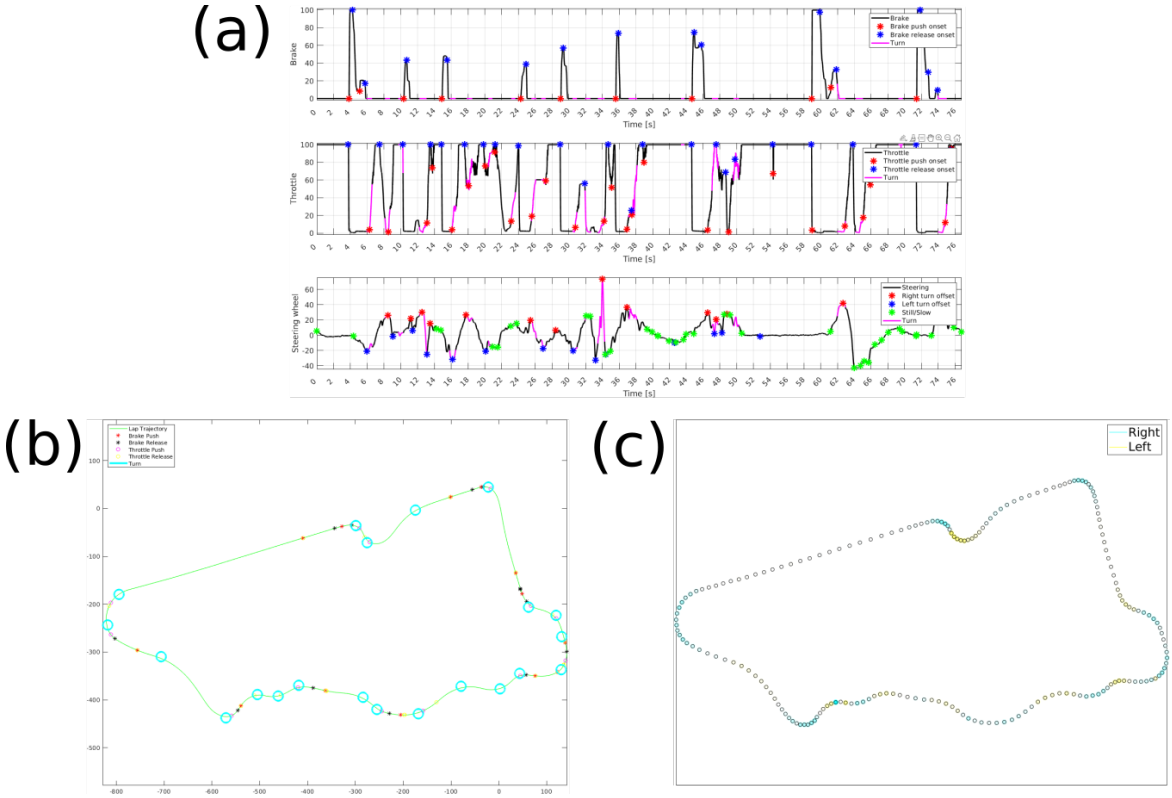


Fig. 3.4 Extraction of brake, throttle and steering wheel events for the best lap of Max Günther. (a) Identification of events in the signal input streams (b) Position of events on the car's trajectory (c) Steering events color-coded on the car trajectory.

Similarly, proficient racing also prerequisites knowledge and ability to follow the ideal race line. This aspect is evaluated by computing the deviation of each lap from an optimal trajectory. The best lap of Max Günther (achieved at his 17th /20 lap) and the best lap overall in the study are taken as references. The race line deviation is then calculated as the area between the curves of a given lap and the optimal lap trajectory.

The area between the curve is ideally computed as the integral $|\int_{x_{min}}^{x_{max}} f(x) - g(x)|$, where $f(x), g(x)$ the curves of the optimal and the current lap trajectory. Since the track defines closed trajectories, for any given interval along the horizontal axis the integral is evaluated separately for the upper and lower parts of the trajectory. Furthermore, the integral is not exactly computed, but only approximated by sampling evenly the x-axis with a step of 0.5 m and computing the average of the differences of the two trajectories on each of the $N$ x-points: $\frac{1}{N}\sum_{x_i}|f(x_i) - g(x_i)|$. Fig 3.5 illustrates by example this metric (area between the curves highlighted in red). It is clear that the first lap of Max Günther (when he was still getting accustomed to the track and the virtual car) has only marginal deviations from the race line of his best lap, which is not surprising given his professional racing skills. On the contrary, the deviation of the first lap of subject EF06CH from the optimal race line is substantial. This investigation assumes that improvements across time on this metric suggest that part of the learning process entails learning to follow the best trajectory.

### EEG signal pre-processing

Pre-processing operations applied to the raw EEG signal include:

1. Linear detrending of each channel, to remove slow fluctuations (the eego amplifier does not apply any hardware filters).

2. DC removal (baseline correction).

3. CAR spatial filtering to remove common noise sources. Fig 3.6 shows a visual representation of CAR. CAR spatial filtering involves re-referencing each EEG channel to the average of all or a subset of the available EEG channels. The assumption behind CAR is that any global noise components—such as electrical line noise, environmental noise, or biological artifacts not localized to specific areas

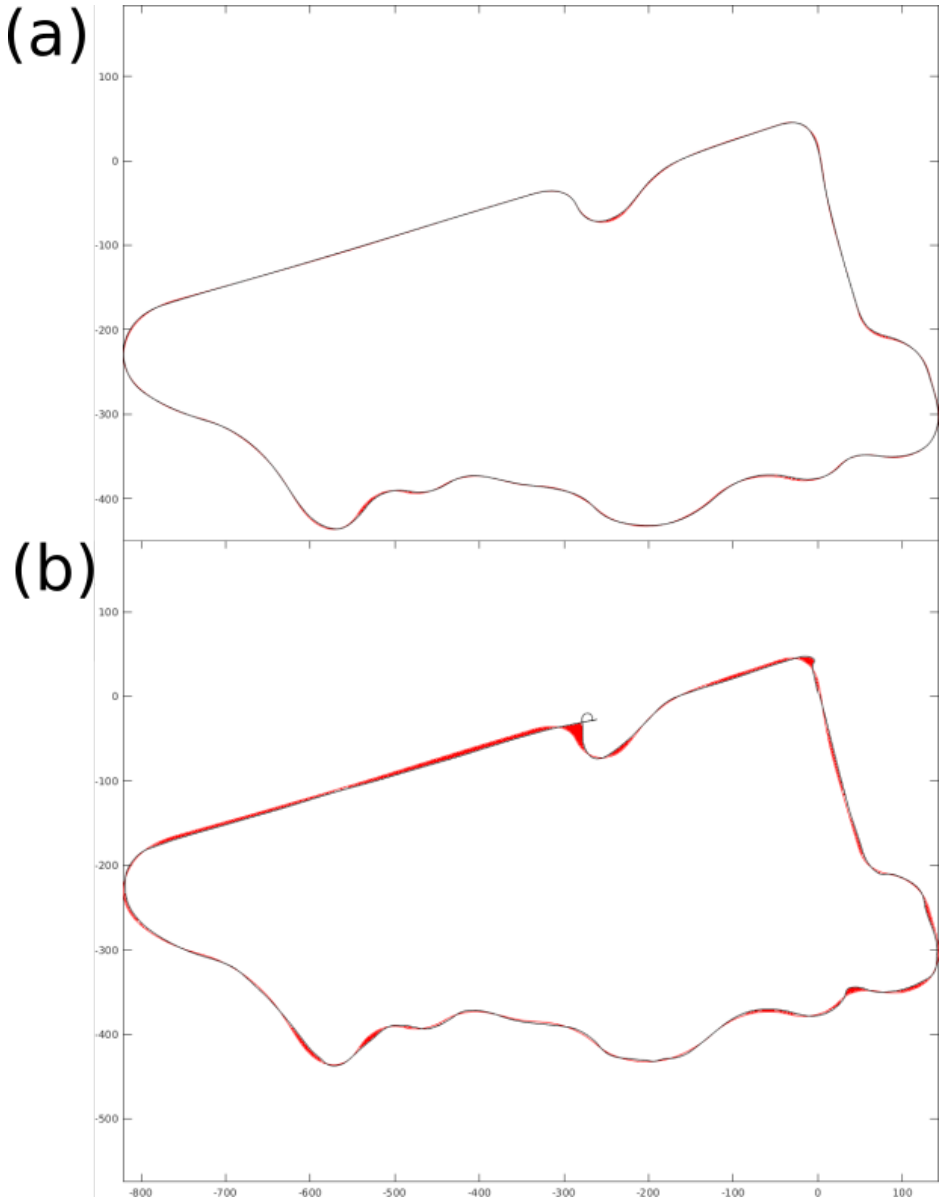


Fig. 3.5 Extraction of race line deviation. The area between the curve for (a) best lap against the first lap of Max Günther (b) best lap against the first lap of EF06CH highlighted in red

(like eye blinks or heartbeats)—are present equally in all channels. By subtracting the average of all channels from each individual channel, these common noises are attenuated.

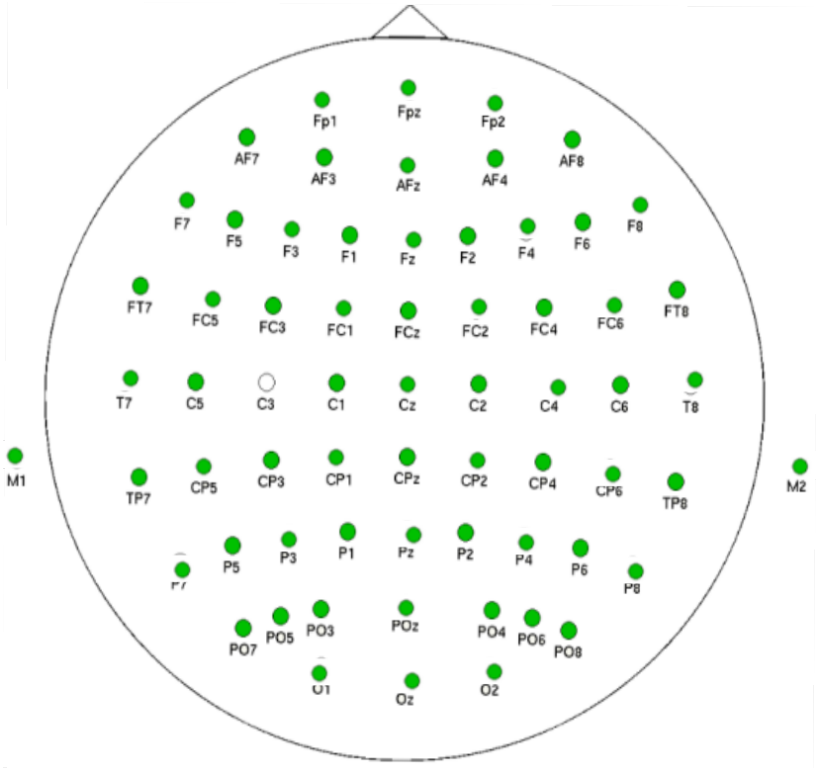


Fig. 3.6 CAR spatial filtering

4. Surface Laplacian (for PSD and effective connectivity analysis) or anti-Laplacian (for MRCP analysis) spatial filtering. The available four cross neighbours are used. Anti-Laplacian refers to adding, rather than subtracting, the potential average of a channel's neighbours, thus enhancing, rather than removing, the local EEG activity.

5. Artifact removal by using FORCe [131].

For all EEG-based analysis, channels M1, M2 (mastoids0 and PO5/PO6 (which are usually not included in the 10-20 system) are completely excluded. Depending on the particular analysis domain, this analysis further limits the investigation to specific cortical regions and channels, as specified below.

### EEG rhythms

My analysis attempts to identify changes across time in various neurophysiological variables, which could thus suggest or subserve cortical plasticity related to learning to race, as well as to correlate these with the learning outcome (i.e., race-driving performances). A first such candidate regards EEG rhythms. Oscillatory cortical activity has been associated with numerous cognitive processes, especially in the theta and alpha band including learning in general, and learning of motor skills, specifically. Hence, I aimed to explore whether any combinations of frequency bands and regions of cortical EEG exhibit such modulation over time and correlation to behavioural outcomes.

EEG PSD is extracted for each channel with the Welch method for each lap (i.e., the whole EEG segment corresponding to a lap is fed to the corresponding function). This analysis employs 2 s internal Welch windows with 125 ms overlapping resulting in 0.5 Hz PSD resolution on 59 EEG channels. I then average the lap PSD within 5 broad bands: delta [1,4] Hz, theta [4,8] Hz, alpha [8,12] Hz, beta [13,30] Hz and (low) gamma [30,40] Hz and 9 Regions of Interest (ROIs) (channels included after semicolon):

1. Frontocentral Left: F1, F3, F5, FC1, FC3, FC5, AF3
2. Frontocentral Medial: Fz, FCz (note that AFz is unavailable as it is the ground channel)
3. Frontocentral Right: F2, F4, F6, FC2, FC4, FC6, AF4
4. Central Left: C1, C3, C5
5. Central Medial: Cz
6. Central Right: C2, C4, C6
7. Centro-parieto-occipital Left: P1, P3, P5, CP1, CP3, CP5, PO3

8. Parieto-occipital Medial: Pz, POz (note that CPz is unavailable as it is used as reference channel)

9. Centro-parieto-occipital Right: P2, P4, P6, CP2, CP4, CP6, PO4

Hence, this ends up with 5 bands $\times$ 9 ROIs = 45 candidate spatiospectral EEG rhythms that must be investigated for involvement in learning to race. The following criteria are imposed to accept any of these candidates as an index of functional brain plasticity:

- The rhythm in question must correlate significantly with lap time.
- It must correlate significantly with the chronological lap index (i.e., consistently change over time).
- The correlation with the lap index must be positive (i.e., the bandpower must increase over time, as reported in relevant literature)
- The correlation with lap time must be negative (since increased power should be associated with lower lap time–better performance thanks to learning)
- It must differ significantly when comparing the onset of training (first two sessions) and the learned outcome (last two sessions).

Importantly, given the exploratory (rather than hypothesis-driven) nature of this analysis leading to many comparisons, this investigation employs everywhere strict Bonferroni correction to avoid false positives. Statistical testing for correlations is performed with Student's corresponding test based on the chi distribution. For pre- vs post-training comparisons, non-parametric, Wilcoxon, unpaired, two-sided tests are used. For novice users, all 10 sessions (i.e., approximately 200 laps) are included in the analysis. For professional users that executed a single session (20 laps), the same

criteria apply, but the pre- vs post-training comparison involves the first and the last 7 laps.

### Effective functional connectivity

Functional plasticity with respect to brain connectivity has also been implicated in learning. Here, Directed Transfer Function (DTF) effective connectivity is employed, which provides information not only for the strength of the association between two brain regions but also for the direction of this association (i.e., relies on Granger causality). Here the study employs a version of the DTF algorithm of the eConnectome toolbox, with order 10 for the autoregressive model. DTF connectivity is computed for all pairs of channels (in both directions) with 1 Hz frequency band resolution and is then averaged within the same bands as for the PSD analysis and within 3 wider regions:

1. Frontocentral: F1, F3, F5, F7, FC1, FC3, FC5, Fz, FCz, F2, F4, F6, F8, FC2, FC4, FC6, AF3, AF4, AF7, AF8, FT7, FT8
2. Central: C1, C3, C5, Cz, C2, C4, C6, T7, T8
3. Centro-parieto-occipital: P1, P3, P5, P7, CP1, CP3, CP5, PZ, P2, P4, P6, P8, CP2, CP4, CP6, POz, PO3, PO4, PO7, PO8, O1, O2, Oz, TP7, TP8

There are thus again $5 \times 3 \times 3 = 45$ candidate connectivity features that are examined in the same manner as the EEG rhythms described above.

### Motor-related Cortical and anticipatory Potentials

This analysis further hypothesizes that the MRCP Contingent Negative Variation (CNV) signals associated with race-driving actions (braking, accelerating, steering) may also provide information on plastic changes accompanying race-driving learning.

I, therefore, filter the pre-processed EEG signal (after anti-laplacian spatial filtering) with an Infinite Impulse Response (IIR) bandpass filer with pass-band in [0.4, 3] Hz. Then isolate the interval [-1, 1] s around each brake/throttle push/release and turning left/right event as described above, where $t = 0$ is the event onset. The filtered signals are then averaged separately for each event type within each session to output a final MRCP curve. The analysis then seeks to relate the amplitude of the negativity peak, its time gap from the movement onset and the slope of the negativity to the learning outcomes.

Finally, this work extracts the same kind of curves for each participant's lap on the ideal action positions, using again Max Günther's best lap as reference. In other words, the necessary examination has been done to trace the existence of potential MRCPs around potential onsets of ideal events as shown in Fig 3.4b. The idea behind this analysis is that this metric should reveal to what extent a novice driver starts placing better his actions so as to improve his lap time, and whether this information can be extracted from the brain through MRCP-like anticipatory potentials.

## 3.4 Results and Discussion

### 3.4.1 Data collection

Data collection has approached the maximum of the set targets. As shown in Table 3.1, 7 out of 11 participants completed all (designated maximum of) 10 sessions. Two subjects completed 8 sessions and another two 9. Participants completed on average 187±14 laps (out of the maximum target of 200). The table shows that all subjects almost always completed 20 laps/session, as desired, with a few laps missing in most cases due to wrong counting (4 laps per run were planned).

### 3.4.2 Balance of confounds

One major goal of the study has been the investigation of any tDCS effects on race-driving learning. It is thus critical to eliminate the influence of any other factors that may affect performance and learning. Elimination is done by balancing suspected confounding factors between the two tDCS groups with Frane's methodology at recruitment. Frane's method is an adaptive minimization method for randomized allocation which monitors the statistical differences of each confounding factor for each possible allocation and selects the one that minimizes the greatest current imbalance across all confounds. The confounding factors considered were: Age, Gender, Driving proficiency/experience and Corrected Vision. It must be noted that all recruits but one (NI28LD) were right-handed. For numerical confounds (e.g. Age) I report averages and standard deviations between the two groups and the p-value of an unpaired, two-sided Wilcoxon ranksum test. For categorical variables, I report the p-value of a chi-squared test for proportions.

This investigation further checks whether any of these confounds explain the gains in terms of lap time exhibited by subjects. Lap time is computed as the difference of the average lap time between the first two and the last two sessions. For Age, I correlate the lap time gain to each participant's age and seek for significant correlation. For categorical variables (Gender, Driving Proficiency, Corrected Vision) I calculate the average gain per category (e.g., Male vs Female for Gender) and perform an unpaired, two-sided Wilcoxon ranksum test.

Table 3.2 shows that all confounding factors were appropriately balanced, as no p-value is significant. The same table illustrates that none of these confounds seem to explain the learning outcome (in terms of lap time gain). It has to be noted, though, that, as elaborated later on in this analysis, neither the tDCS treatment seems to significantly influence the overall lap time gain as measured here. Still, as will be

argued, further analysis demonstrates that, in fact, tDCS does seem to have an effect on the learning process, in contrast to any of these other variables.

### 3.4.3 Behavioural results on learning to race

Obviously, it is pointless to search for neural correlates of learning and effects of tDCS on the learning process if learning effects cannot be established in the first place. However, it can safely be concluded that in this study obvious learning effects have taken place with regard to most metrics implicated. In the following figures, this analysis shows, for each of the examined metrics and for each user category (novice vs professional users), a composite figure consisting of:

- Individual learning curves per lap, with linear and exponential fits (to examine whether a learning curve reaches the consolidation/convergence stage by the training offset)
- Learning curves averaged within sessions either with mean or with median (to attenuate the effects of outliers) for each subject and grand-averaged across all subjects.
- Pre-training vs post-training comparisons with statistical testing (unpaired, two-sided Wilcoxon ranksum tests). For novice users, the first two sessions are compared to the last two. For professional users, the first 6 laps are compared to the last 6.
- Grand averages of lap times within each session with linear fits and Pearson correlation. This is to evaluate learning taking place within each session (20 laps) at the different stages of training.
- For Novice users that underwent active or sham tDCS, I also show the average and standard deviation within each group and overall with statistical significance.

For novice users, one-way repeated measures ANOVA is reported with the single factor session to substantiate the significance of learning across the variable in question. Furthermore, I perform mixed-design ANOVA with within-subject factor session/time and between-subject factor tDCS and look for significant session × tDCS interaction to test whether tDCS treatment significantly influences learning.

The final, high-level goal in racing under the specified conditions is to minimize the lap time. The other metrics identified should be viewed as components of the overall racing skill which is best evaluated through lap time. Hence, learning in terms of lap time is of the utmost interest. Fig 3.7 and 3.8 illustrate the concentrated results for this metric for novice and professional users, respectively.

For Novice users, a significant group learning effect is found through repeated measures ANOVA with single factor time/session $F = 19.81, p < 10^{-13}$. Significant learning effects are also apparent by inspecting the individual subject curves and the grand averages. All users have significant pre- (first two sessions) vs post-training (last two sessions) improvement, and the difference is also significant at the group level (i.e., comparing the eleven pre-training averages to the equivalent post-training ones). More than 10 s gain in lap time completion is found on average. Most novice users exhibit exponential learning curves (i.e., there is an intense learning period followed by consolidation of the racing skill to a certain level). A few novice drivers seem to have further improvement potential (linear curves). Specifically, 6 out of 11 subjects show significantly smaller root mean square error of residuals of the exponential compared to the linear fit. Within-session learning takes place, especially in Sessions 1-3, followed by another breakthrough around sessions 7-8 (on average), as shown on the per-session grand averages of lap time (with a significant, negative correlation of lap time vs lap index).

Overall the existence of strong group learning effects in terms of lap time is beyond any doubt; the effect is found for all subjects individually and not only on average.

Professional drivers (including the 12-year-old local champion in this group) also show significant group learning effects within the single session executed, although in this case, it should probably reflect the familiarization process with the simulator, the virtual car and the track, rather than "learning to race". Specifically, repeated measures ANOVA with single factor time/session shows a significant effect of time on lap time $F = 2.4, p = 0.01$. The individual subject curves and grand average corroborate that professional drivers were able to minimize their lap time throughout the session. All professional users exhibit significant pre- (first six laps) vs post-training (last six laps) improvement, the gain in lap time approaching on average 3 s. Individual curves seem to be rather a line, meaning that professional drivers could probably further improve with time.

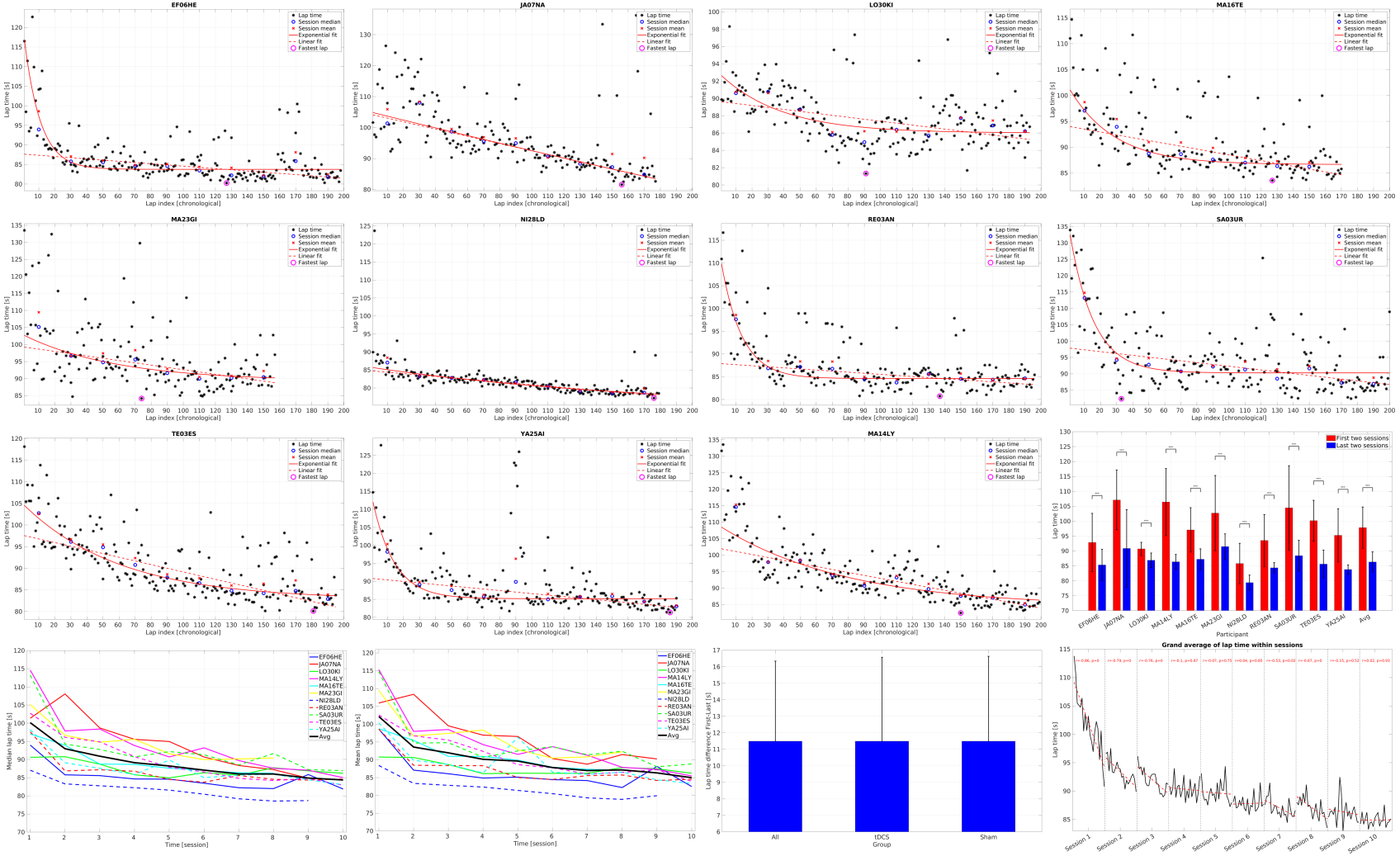


Fig. 3.7 Lap time learning for novice users

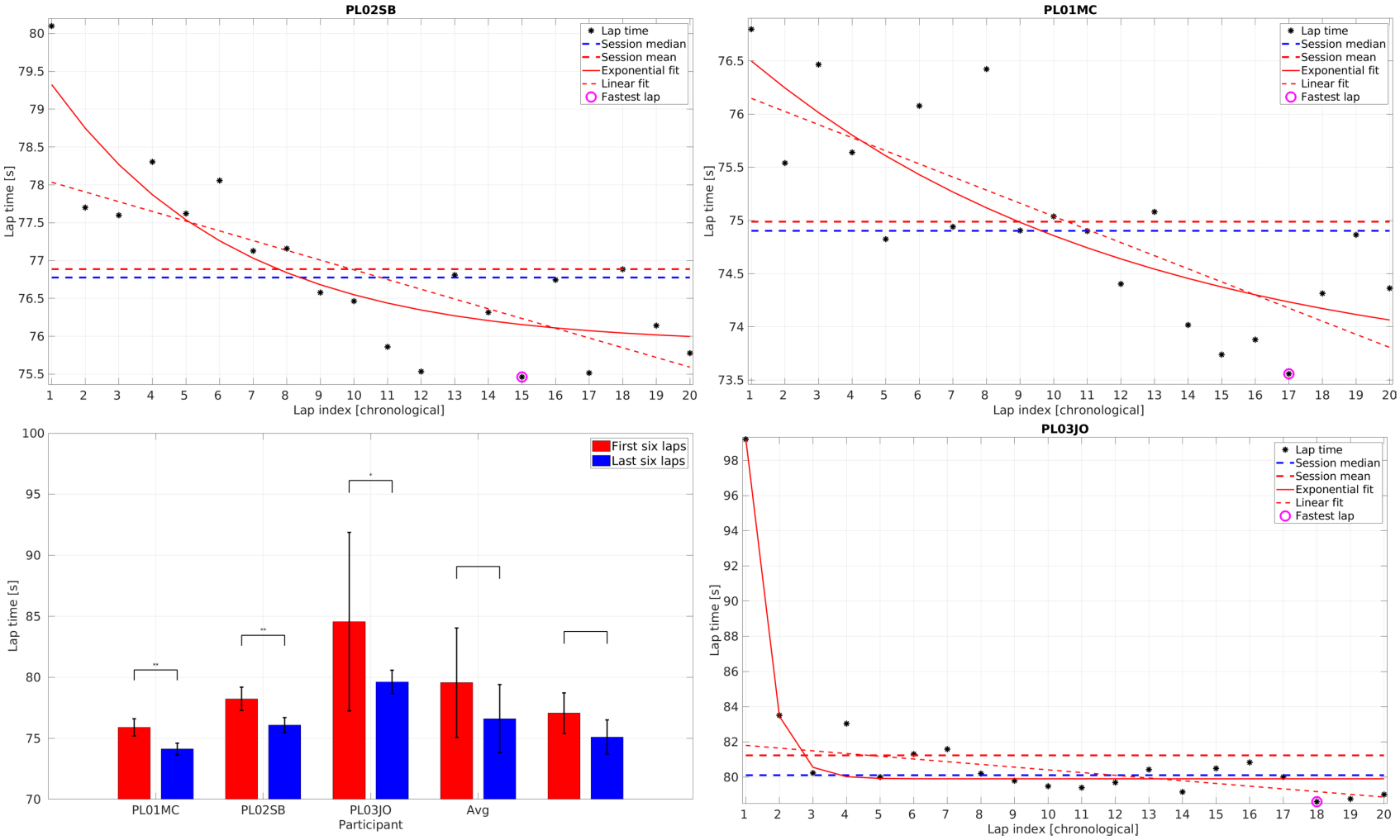


Fig. 3.8 Lap time learning for professional users

The comparison between novice and professional users in Fig 3.9 shows that pro drivers converged towards 73-75 s lap time, with the 12-year old "professional" driver achieving 78-79 s. Novice drivers converged on average to 84-85 s. Interestingly, one novice subject (NI28LD) performed markedly better than the others, with the fastest lap at 77.2 s and the best session average at 78.9 s. These performances are very close to those of the professional drivers, well ahead of the second-best novice driver (EF06CH with 80.3 s fastest lap and best session average of 82.2 s) and also surpass the achievements of the 12-year-old experienced race driver (fastest lap 78.6 s and session average 81.2 s; of course, it has to be taken into account that the young professional only trained for a single session).

Of the remaining metrics of race driving performance this study has identified, the impact number is the only one that is not simply a component metric of the overall lap time, but rather "antagonistic" to lap time. This is because I reasonably assume that all drivers, in their effort to go as fast as possible, may risk impacts; hence, lap time and impact number minimization should be, in general, two independent skills that need to be mastered. Of course, it is also correct that too many impacts should influence lap time in a real setting, however, in the particular simulated task where the car vulnerability was disabled, impacts did not have a devastating effect on lap time; on the contrary, many subjects realized that slight impact in specific turns would even result in time saved, and followed actively this strategy despite the instruction to avoid crashes.

Novice users show no group learning effect (repeated measures ANOVA with single factor time/session $F = 1.27, p = 0.27$) with regard to the number of impacts. In Fig 3.10 the grand averages are mostly flat. Inspecting the individual subject curves and pre- vs post-training comparison, it is interesting to note that there seem to be different/adversary driving styles. Some (about half) users followed the instructions

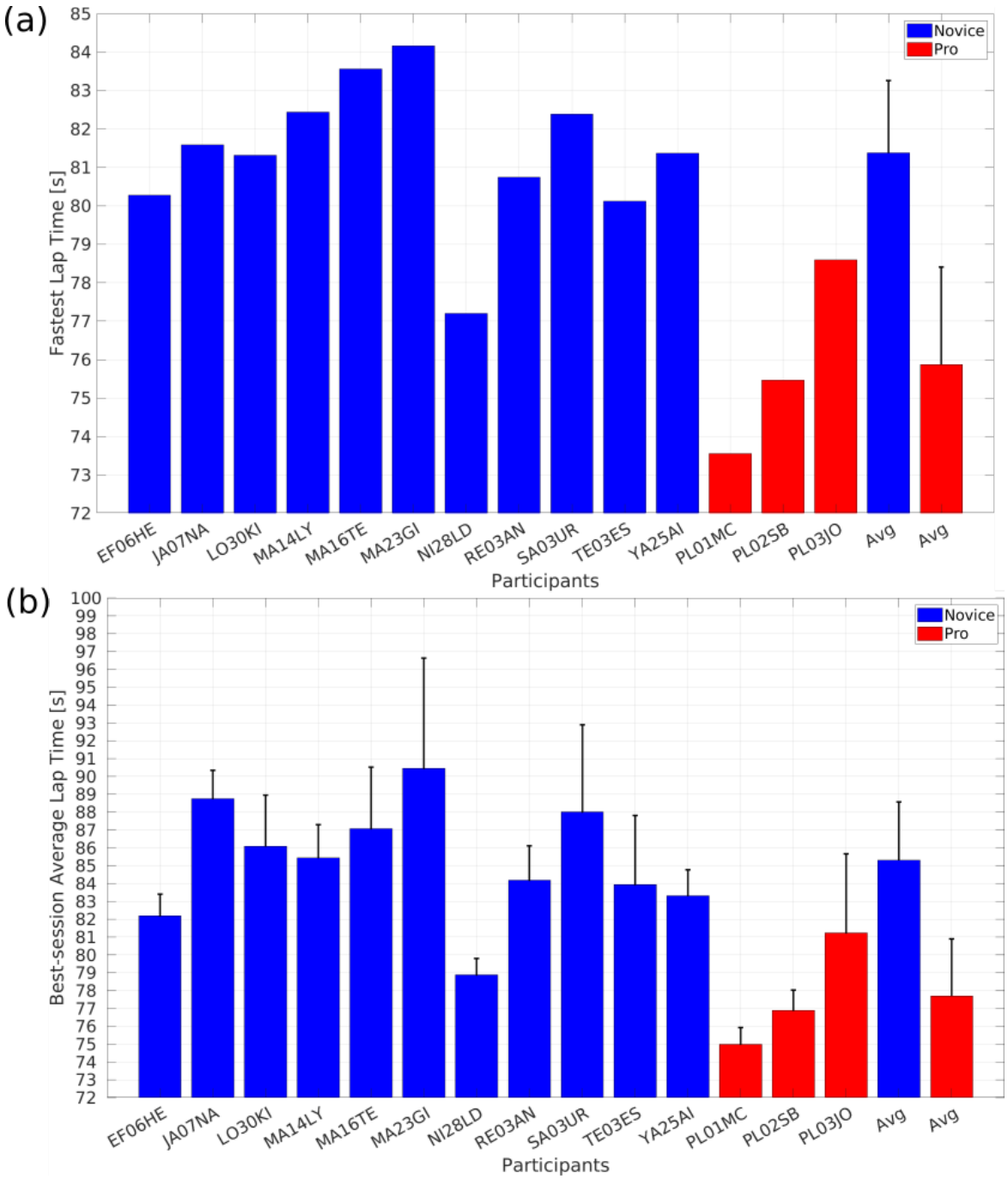


Fig. 3.9 Lap time comparison novice vs professional users. (a) The fastest single lap of each user (b) The best session average of lap time for each user with standard deviation.

and reduced impacts significantly over time (although even these drivers increased a bit in the end, probably a sign of their effort to further push down lap times). Other

users, though, constantly increased impacts throughout. As said, it seems that many subjects, overriding the instructions, ignored impacts by exploiting the invulnerability of the virtual car in order to push the lap times as much as possible. Here, the fact that there was only feedback on lap time and none on impacts must have been crucial to "bias" users towards this behaviour. Still, inspecting the per session grand averages, there is a significant reduction on average in the first two sessions (significant, large correlation lap index vs impact). It seems that the subjects that do improve, mostly do it in the first two sessions.

Professional drivers (Fig 3.11) had no significant effect either (ANOVA is degenerate due to few points, no pre- vs post-training differences found). This is due to the fact that professionals collide very rarely to begin with so no learning effect can be extracted in this aspect (i.e., there is a ceiling effect where performance is already too good at the training onset and cannot further improve).

Given the absence of group learning effects in terms of impacts the composite penalized lap time metric I have come up with is only driven by lap time, and thus has no extra value compared to it.

In terms of race line improvement, novice users (Fig 3.12) do show a significant group learning effect (repeated measures ANOVA with single factor time/session $F = 4.37, p = 0.0002$). The individual subject curves, grand averages and pre- vs post-training comparisons show that all, but one, novice driver learned to better follow the optimal race line over time, and 9 out of 11 novice drivers significantly so.

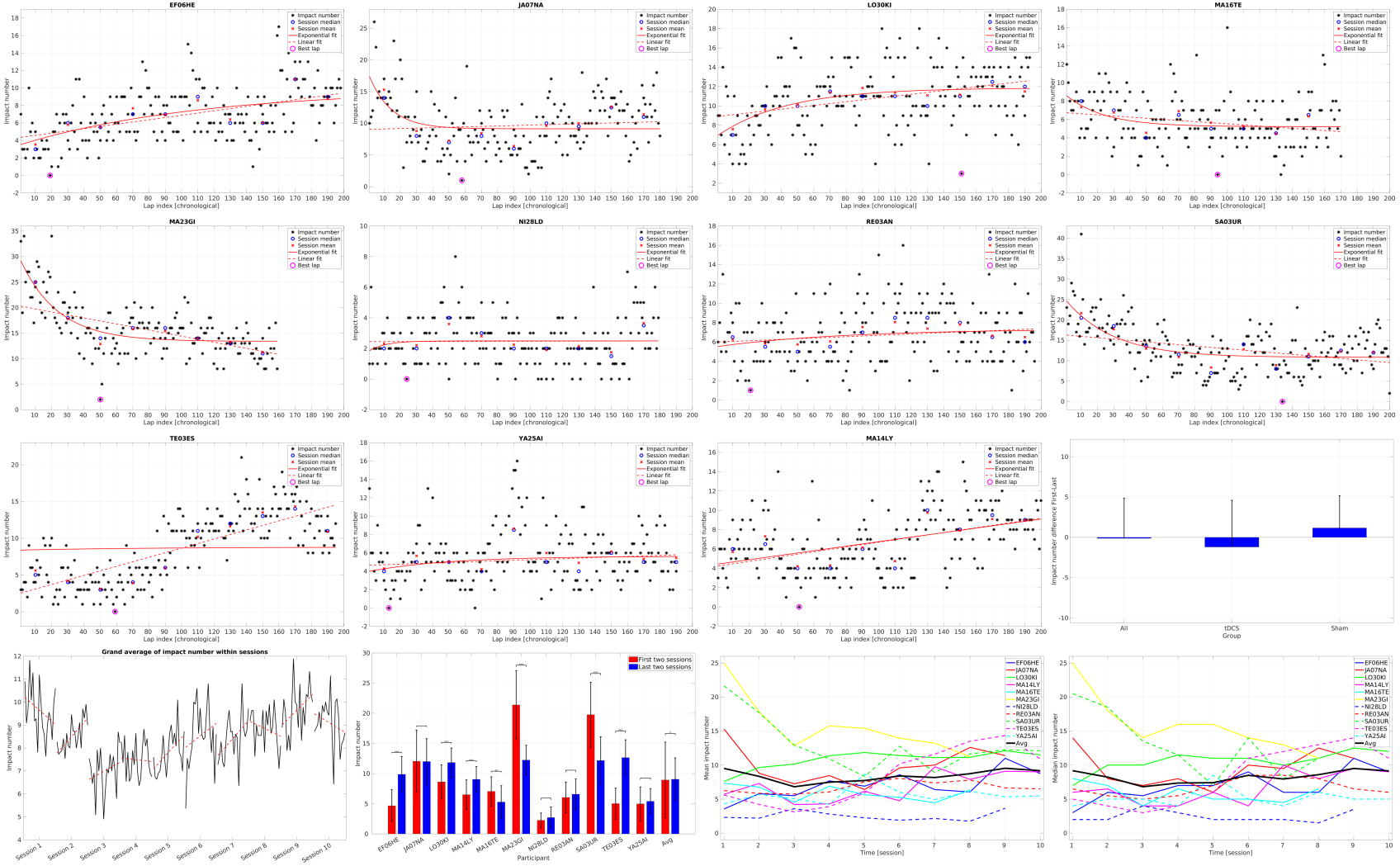


Fig. 3.10 Impact number learning for novice users

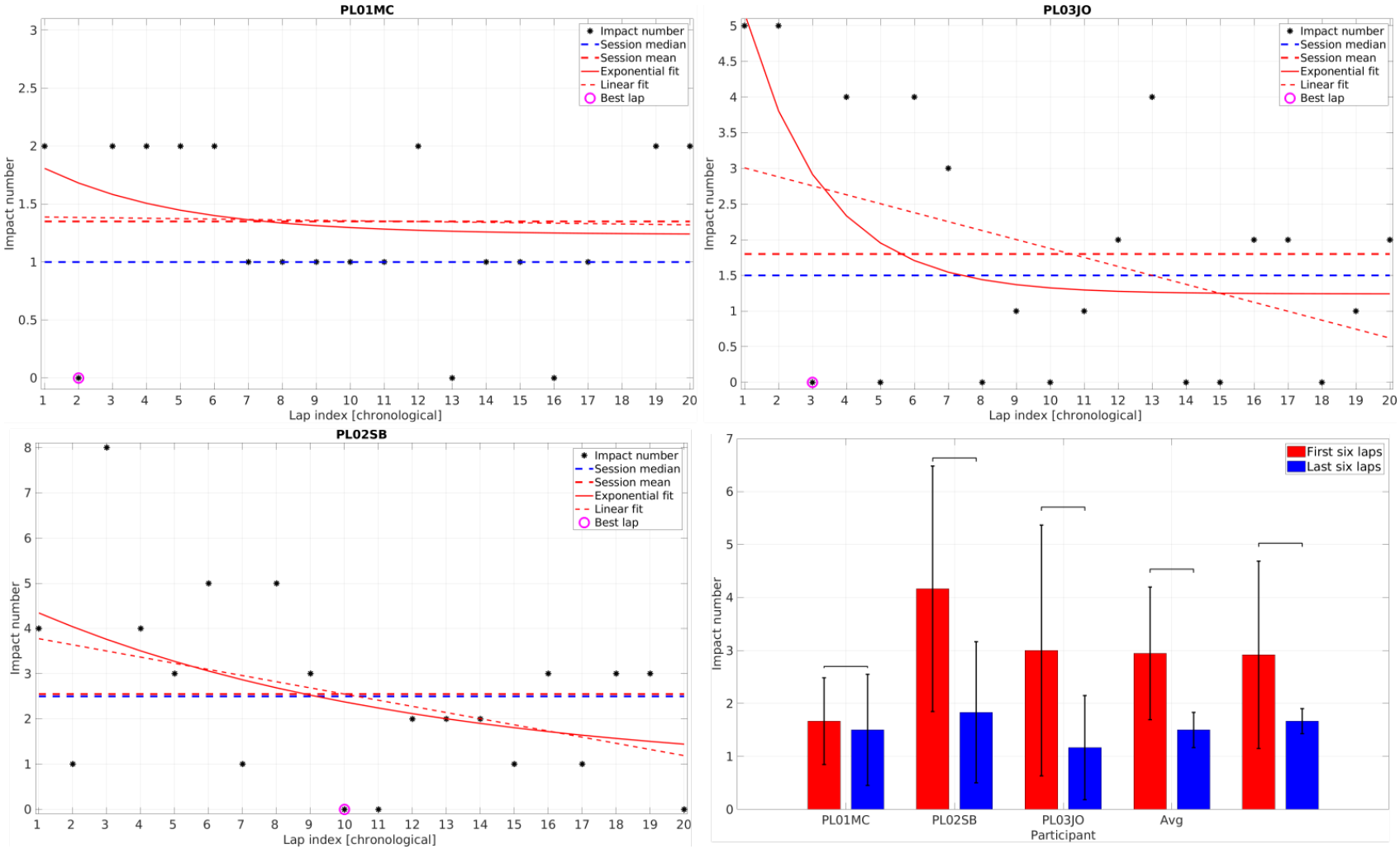


Fig. 3.11 Impact number learning for professional users

There exist users with exponential and others with linear learning in this aspect Professional drivers (Fig 3.13) also improve (see Pre vs Post bars, but not significantly (repeated measures ANOVA $F = 1.7, p = 0.13$, no pre- vs post-training significance), which should be attributed again to a ceiling effect, as these drivers can be assumed to already know how to follow the correct race line and they merely need to slightly adapt to and remember the particular track.

The analysis has finally assumed that learning to race should also be related to reduced "redundancy" in driving actions (braking, accelerating, turning); in other words, reaching a state where all these actions only happen at specific, optimal positions on the track, with no (or only a few) corrections needed. If this assumption is correct, learning should also show with the reduced number of these events, as described above.

However, this assumption is only partially supported by the data. No significant group effect is found when considering the sum of all types of events (ANOVA $F = 0.52, p = 0.85$), although most novice drivers do show significant improvements, evident in pre- vs post-training bar graphs, individual learning curves and grand averages (not shown here). It thus seems that, although not a significant and generic effect, in principle, most subjects learned not to “over-use” the brake, throttle and steering wheel.

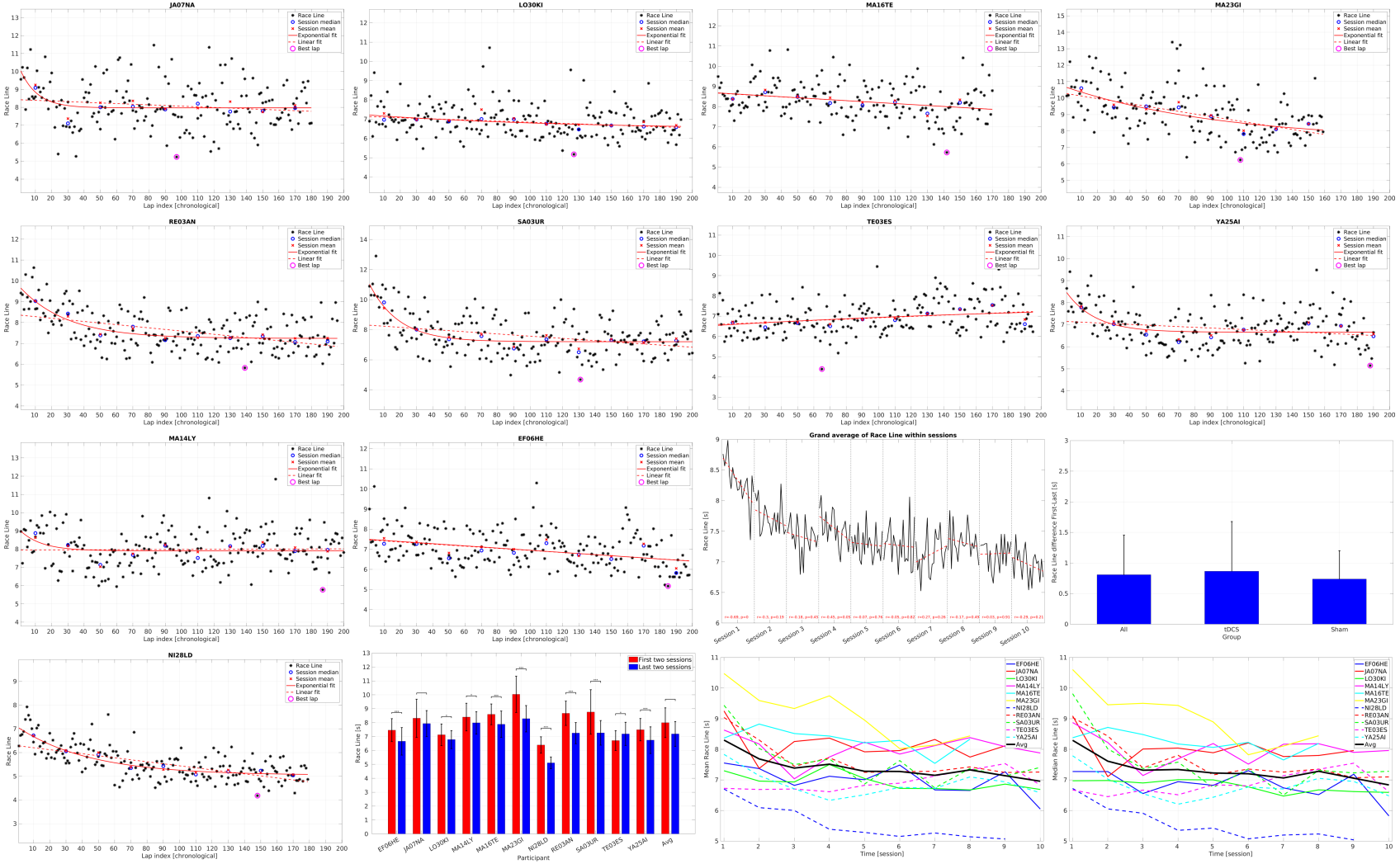


Fig. 3.12 Race line learning for novice users

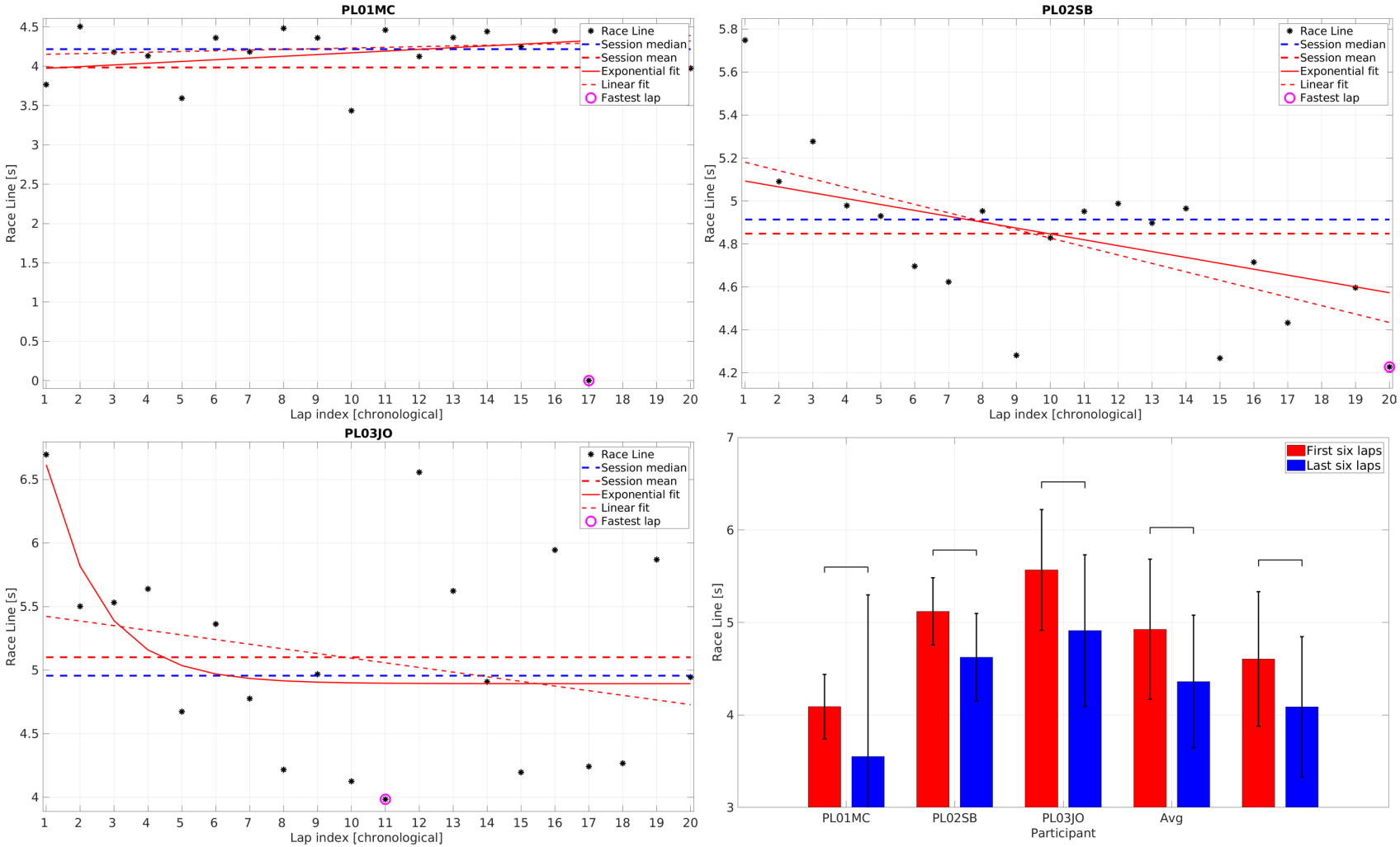


Fig. 3.13 Race line learning for professional users

It must be underlined that, as steering events are much higher in number than Brake and Throttle push/release, the total event metric mostly reflects the steering performance.

The Brake and Throttle use learning curves and pre vs post-tests are rather erratic (not really resembling learning curves at all, there exist irregular fluctuations for many users, and pre- vs post-training performance is not consistent across the population). The ANOVA result for Brake use is significant, but this only shows that session means are not equal, not that they are converging to a consistent learning outcome (this is evident by the grand averages, which are flat, and the individual subject curves which are irregular). The same holds for Throttle use (except for the first two sessions where there seems to be a fairly consistent reduction across the sample).

Hence, it turns out that the overall assumption is fully verified only with regard to the use of the steering wheel. As shown in Fig 3.14, all subjects, but two, reduced their use, and most of these significantly so; so that on, average, the pre- vs post-training reduction is significant (although the ANOVA main effect is not: $F = 1.45, p = 0.19$). The absence of ANOVA significance at the session level must be attributed to the fact that this effect takes place within the first two sessions only, as shown by significant event number vs lap index correlations in the per-session grand average plot. Improved, smoother use of steering is consistent with the racing line improvement found above. No significant effects are found for professional drivers (again, the ceiling effect is a reasonable explanation).

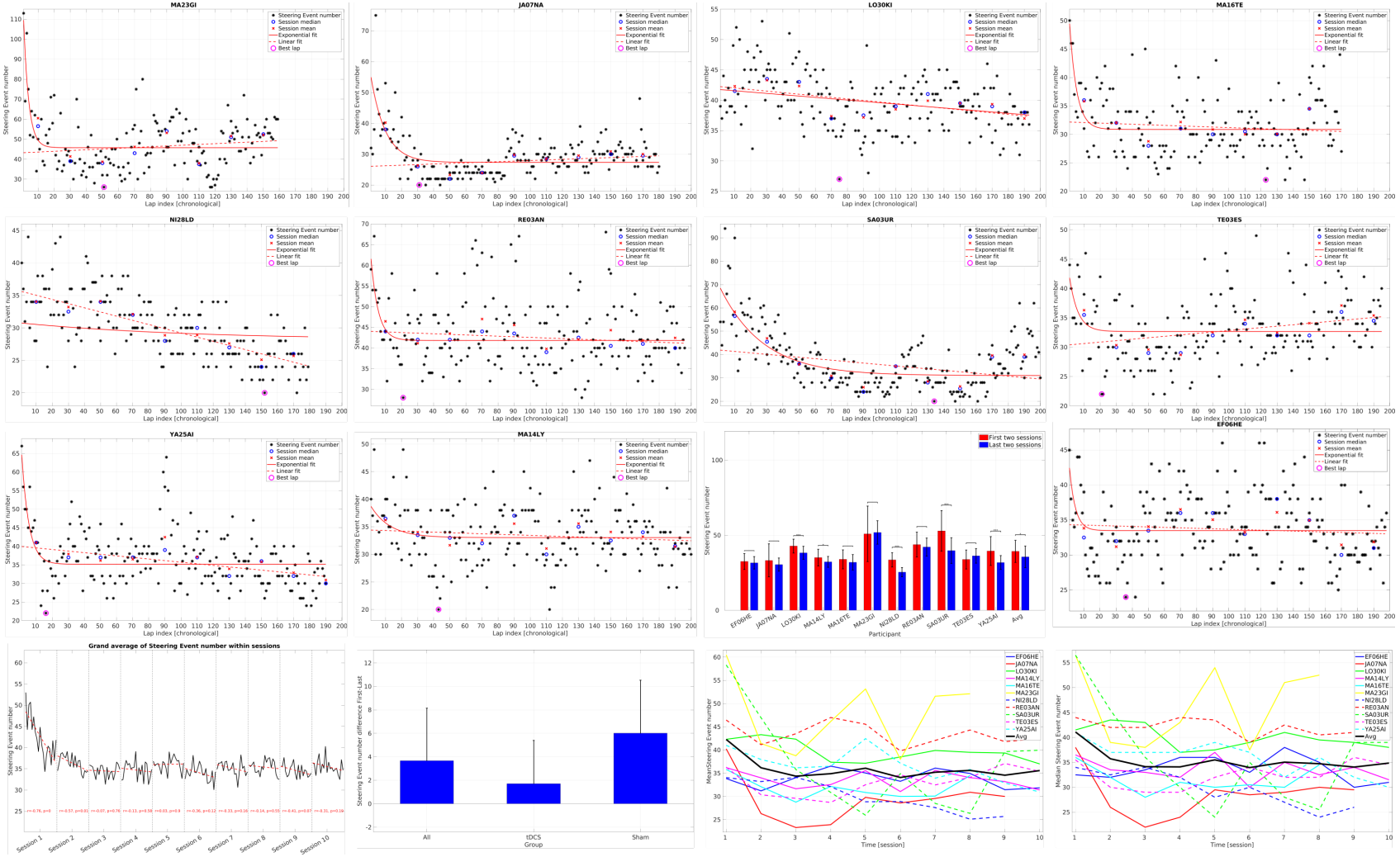


Fig. 3.14 Steering learning for novice users

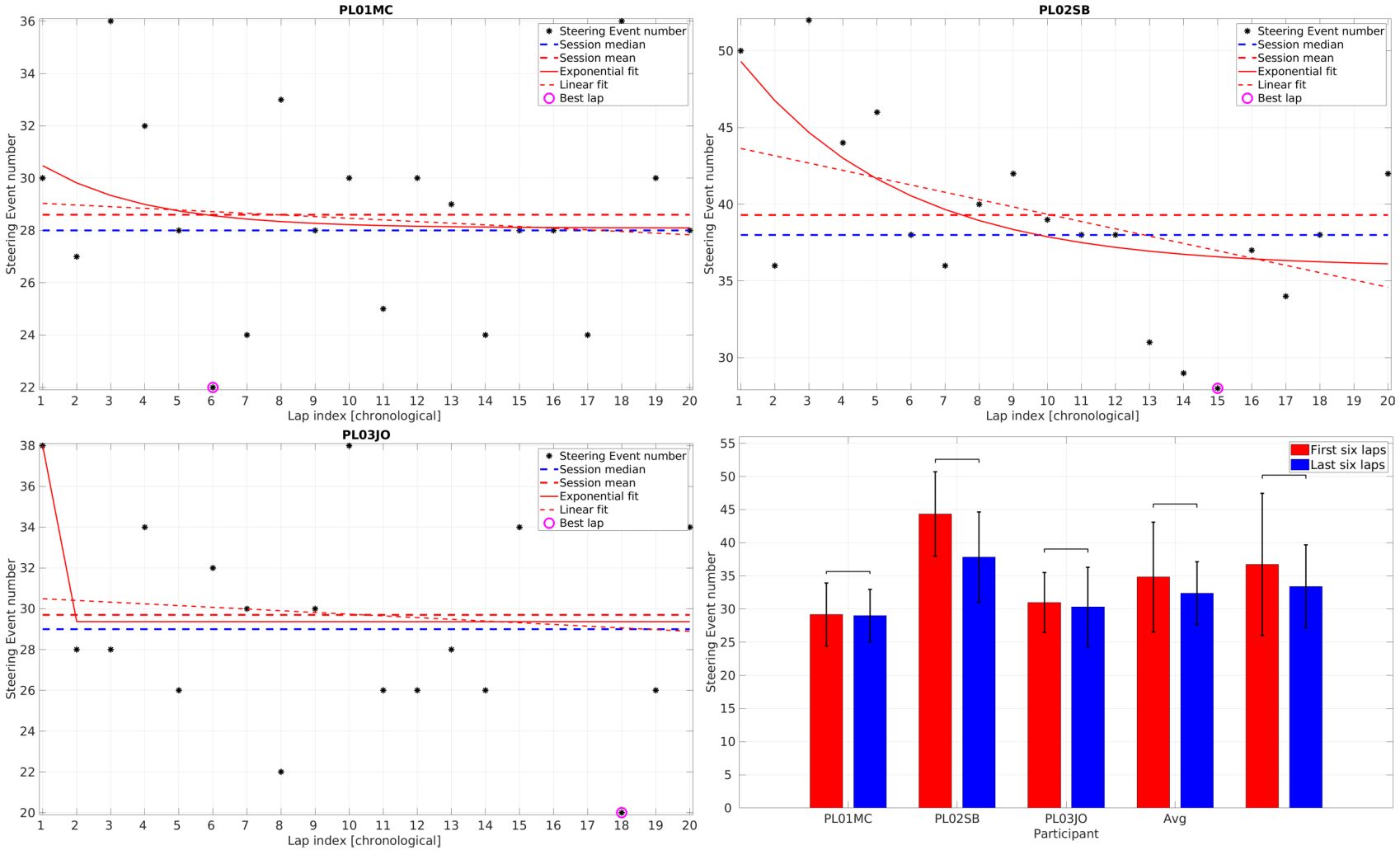


Fig. 3.15 Steering learning for professional users

The study shows that parsimonious use of brake and throttle is essential; however, it seems that novice users follow different driving styles so it is not always the case that frequent use improves to a more parsimonious one during training. On the contrary, comparing the average Braking events between novice and professional drivers and the individual pre- vs post-training bars, it looks like many novice drivers started with very low use of Brake and converged closer to the optimal number of Brake push/release. These are probably subjects that initially did not use the Brake at all, and tried to decelerate by merely releasing the throttle. Hence, it must be noted that a different metric reflecting better the fitness of using Brake/Throttle (e.g, deviation from the optimal number, which could be taken from the fastest lap of a professional user, similar to the race line metric) may have shown clearer signs of learning. Such metrics can be attempted in future analysis.

### 3.4.4 tDCS effect on learning

The novice driver study has been designed specifically to investigate the potential role of tDCS in learning to race. The first conclusion is that there does not seem to be a strong, clear effect of tDCS on the learning outcome measured as the number of improvements participants were able to achieve through the learning process. This has been evaluated by means of mixed-design ANOVAs where the response variable is the gains on the corresponding behavioural metric (as the average of the last two sessions subtracted from that of the first two sessions), and the between-subject factor is tDCS treatment (with levels Active and Sham) and the within-subject factor is time (in sessions, with 10 levels S1-S10). The analysis also checks the average, standard deviation and significance with unpaired, two-sided Wilcoxon ranksum tests of the gains in the two groups for each metric.

Almost all ANOVAs for the metrics considered do not result in significant tDCS × session interaction that is the prerequisite for a significant role of tDCS on learning outcomes. Specifically, for each metric, the result is as follows:

- Lap time: $F = 0.63, p = 0.76$
- Penalized lap time: $F = 0.34, p = 0.96$
- Impact number: $F = 1.81, p = 0.09$
- Race line: $F = 0.65, p = 0.74$
- Total events: $F = 2.25, p = 0.04$
- Brake events: $F = 0.69, p = 0.71$
- Throttle events: $F = 2.22, p = 0.04$
- Steering events: $F = 2.05, p = 0.06$

Therefore, only the Brake, Throttle and Total events show a (marginally) significant interaction, while for Steering events the equivalent result is only marginally non-significant at the 95% confidence interval. Still, even in these cases, the trends are either unimportant (i.e., for Brake push/release where the use only differs by one event between Active and Sham and it is an increase, rather than reduction) or even opposite to what was hoped (active tDCS novice drivers improved far less than Sham for Throttle, Steering and overall events). Hence, a strong effect of tDCS on performance gains at the session level cannot be established.

However, further analysis reveals that pulling all the lap times of all participants in the Active tDCS group together and comparing it to the equivalent Sham group, results in significantly better performance for the Active group: 89.4±9.5 vs 92.0±10.5, $p < 10^{-17}$, i.e., Active tDCS subjects performed on average better than the Sham

tDCS subjects by almost 3 s throughout the training regime. Of course, this does not necessarily imply a role of tDCS on learning; this difference could be attributed to inherently better, more "talented" drivers and/or better learners recruited by chance in the Active tDCS group. However, it motivates the analysis to examine this comparison per session, as well as with other variables that are reasonable to assume may be implicated with racing performance, but for which the analysis has no reason to believe that is associated with learning: prior proficiency and eyesight.

Fig 3.16 shows that the Active tDCS group did not perform better than the Sham group in the first session, which was anticipated since this study deliberately balanced the prior driving proficiency between the two groups so as to acquire approximately equal performance between them at training onset. The slight, non-significant difference in favour of the Active group may be attributed to increased learning effects taking place in this group within the 20 laps of the first session. The difference in favour of Active tDCS becomes significant in session 2, and again in sessions 5-10 (and, especially strong in sessions 5 and 8, as seen in Fig 3.7 (per session grand averages) a second learning breakthrough takes place. In sessions 3 and 4m, there is no significant difference and the two groups are also very close to each other. In other words, it seems that the Active tDCS group demonstrates better outcomes only during and after the training stages where intense learning takes place, while in the beginning, the two groups are balanced, as desired. On the contrary, both of the other two factors examined, the prior proficiency and the eyesight sharpness, although both seem to affect performance as anticipated, they do so in a uniform manner that seems irrelevant to learning. Specifically, prior driving and/or racing experience indeed affects the initial performance (this is precisely why I balanced this factor across the two tDCS groups) where, predictably, experienced drivers do better than naïve ones.

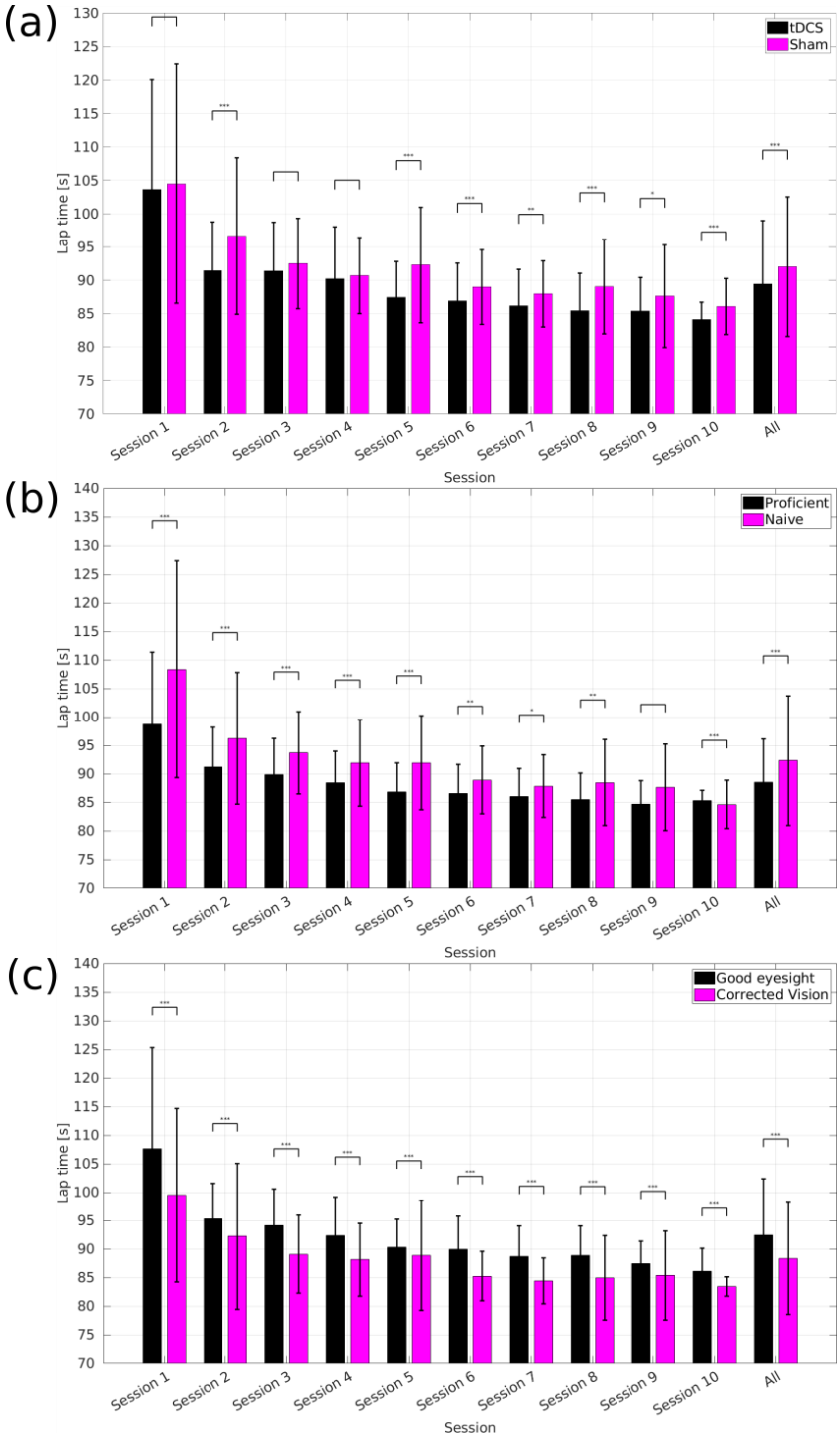


Fig. 3.16 Pooled lap time per session compared between two groups across different factors: (a) tDCS: Active vs Sham (b) Prior proficiency: proficient vs Naïve (c) Eyesight (Corrected Vision): Good eyesight vs Corrected Vision

The effect persists throughout the training sessions, although it diminishes with time (which is also reasonable: naïve users tend to "catch" up as time goes by since their margin of improvement through training is probably larger). Regarding the two groups with respect to eyesight (people with/without lenses or glasses), I observe that novice drivers with corrected vision did significantly better throughout; the conclusion that can be drawn from this is not, of course, that glasses help one to race faster, but, rather, that this factor did not affect learning and performance in any way: it simply happened that better drivers in this study were, on average, those with the need of corrected vision (since prior proficiency was balanced for the tDCS factor, not for the corrected vision factor). Hence, tDCS seems to be the only factor that is balanced at training onset and gives an advantage to the active group by influencing learning. It can thus be claimed that tDCS had a positive effect on race driving learning, but not so strong as to appear also in the per session ANOVA analysis.

### 3.4.5 Relation between EEG rhythms and learning to race

Only for the theta EEG band, following the analysis and criteria outlined in Section 3.3 there exist ROIs that satisfy all conditions for 7 out of 11 subjects. Relaxing the definition of ROIs this work can also identify single or smaller groups of channels that also satisfy the criteria (always with Bonferroni correction). Effectively, apart from novice driver LO30KI, there exist cortical areas with significantly desynchronized theta PSD as training progresses (Fig 3.17), which also positively and significantly correlates with lap time. The same holds for the single session of all three experienced drivers (Fig 3.18). Of note, there is a large body of literature associating theta EEG rhythms and their modulation with the learning of motor or other tasks [107].

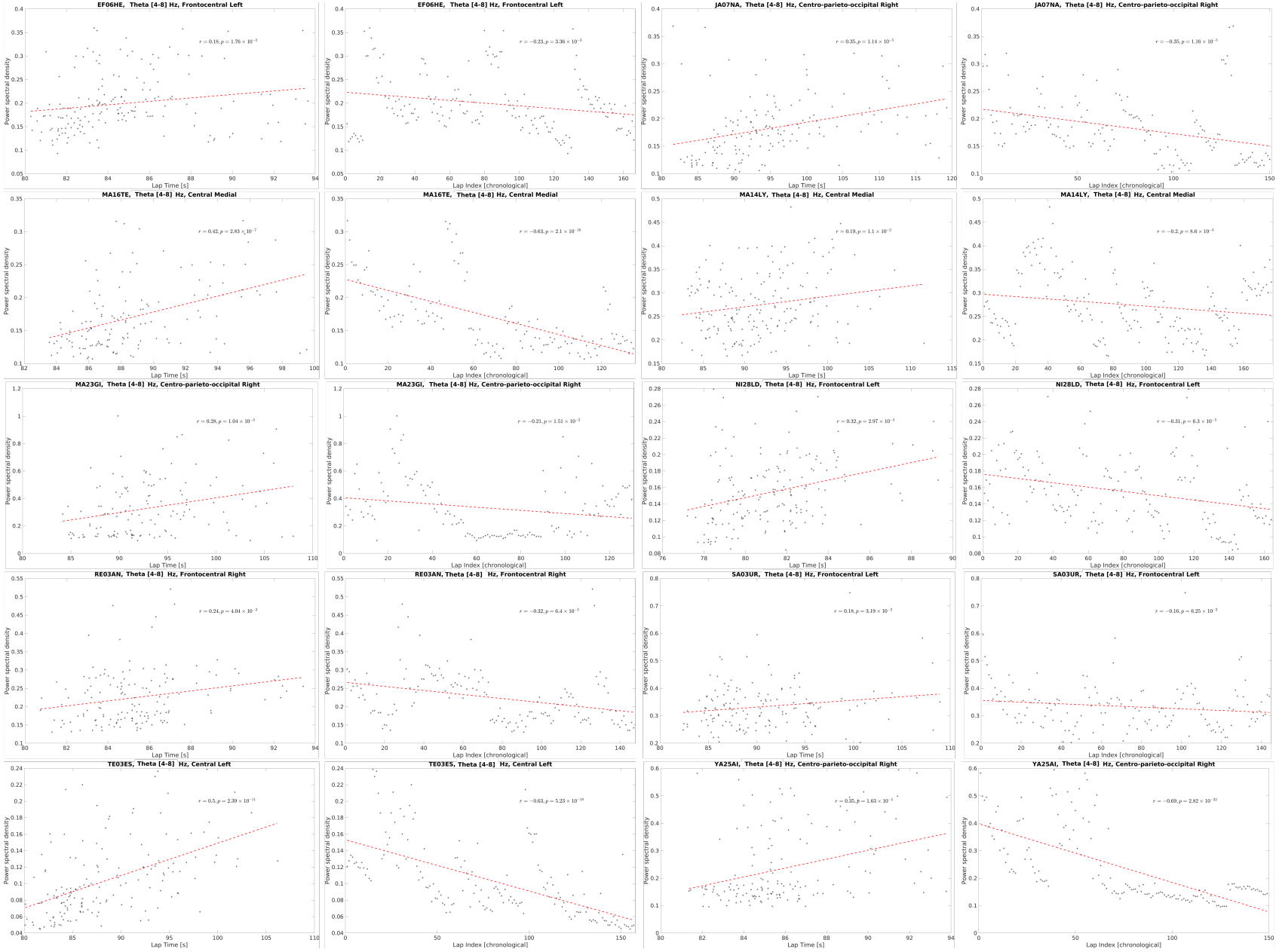


Fig. 3.17 EEG Theta rhythms for novice users

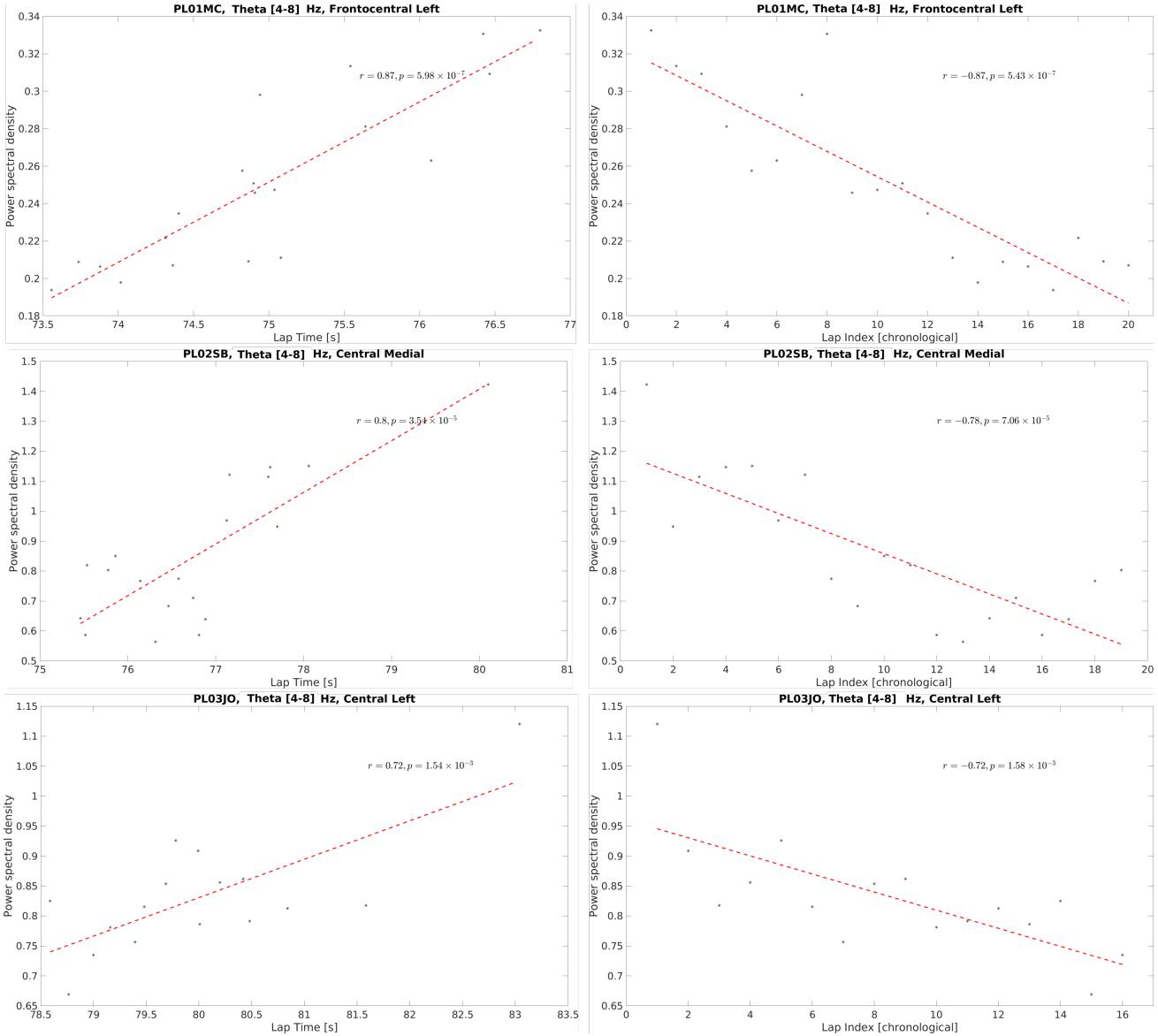


Fig. 3.18 EEG Theta rhythms for professional users

### 3.4.6 Relationship between functional connectivity and learning to race

Similarly to the theta EEG rhythms, this work was able to find significantly increasing DTF effective alpha-band connectivity pre- vs post-training for all but 3 novice drivers (MA16TE, MA23GI, SA03UR) and all professional drivers (Fig 3.19). Of note, in this case, connectivity is computed and tested for significance for each channel pair (with Bonferroni correction for novice users; correction is relaxed for professional drivers who have much less data) and the connectivity of significant channel pairs is then selected for each subject and averaged to produce the final connectivity index in the broadest region possible for each participant. Increasing alpha functional connectivity has also been heavily associated with learning in the literature, especially for motor learning.

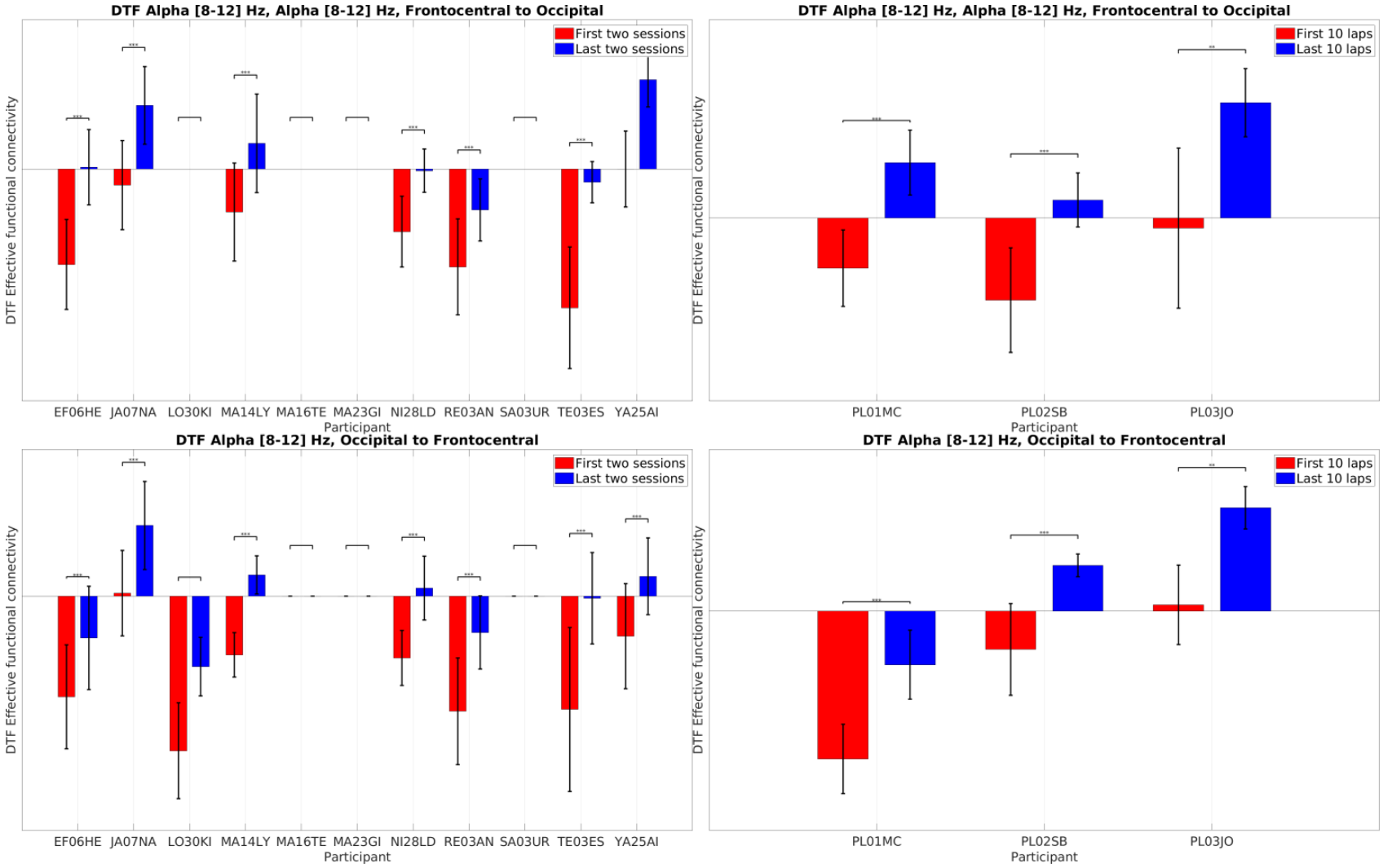


Fig. 3.19 DTF effective connectivity from frontocentral to occipital regions (first row) and vice versa (second row) for novice (first column) and professional (second column) drivers.

### 3.4.7 MRCPs in a realistic driving scenario

MRCPs can be identified for both novice and professional drivers (examples in Fig 3.20 and Fig 3.21) and are most prominent for the Brake push movement. It is noted that, in most cases, the MRCPs seem to be "smaller" (i.e., with swallow maximum negativity) than what is reported in the literature: The negative peak is usually around -2.5 to -4 uV, while down to -10 or -15 uV has been reported. Every other aspect of the grand average MRCP extracted resembles a textbook case: the shape, the timing of the negativity, the rebound, etc.

A first reasonable explanation for the swallow depth is that the realistic scenario followed here creates greater misalignment, imposes great cognitive workload and, importantly, creates overlapping MRCPs due to movements happening too close in time to one another, resulting in lower average depths (which, anyway are not far from -5uV reported elsewhere for break push movements in a less realistic protocol). In addition to this, the MRCPs extracted here are filtered in the band [0.4 3 Hz] instead of the ideal [0.01 1] or [0.1 1]Hz pass-band, in order to avoid instability (given the comparatively low sampling rate used here). Rejecting the high-energy 0-0.4 Hz band may explain the small depths of the MRCPs. Lastly, it must be underlined that in certain cases (e.g., novice driver JA07NA) the MRCP depth reaches the range of -10 uV.

The results do not seem to get clear MRCPs for steering wheel turning, and not so much for throttle push/release actions, either. A possible reason is that these movements are not as "clear-cut" as the Brake action (especially the brake push). They are usually smoother and not so abrupt, which must have a negative impact on the associated MRCP. There are still visible CNVs for these movements, but they are not as consistent as for the Brake Push action.

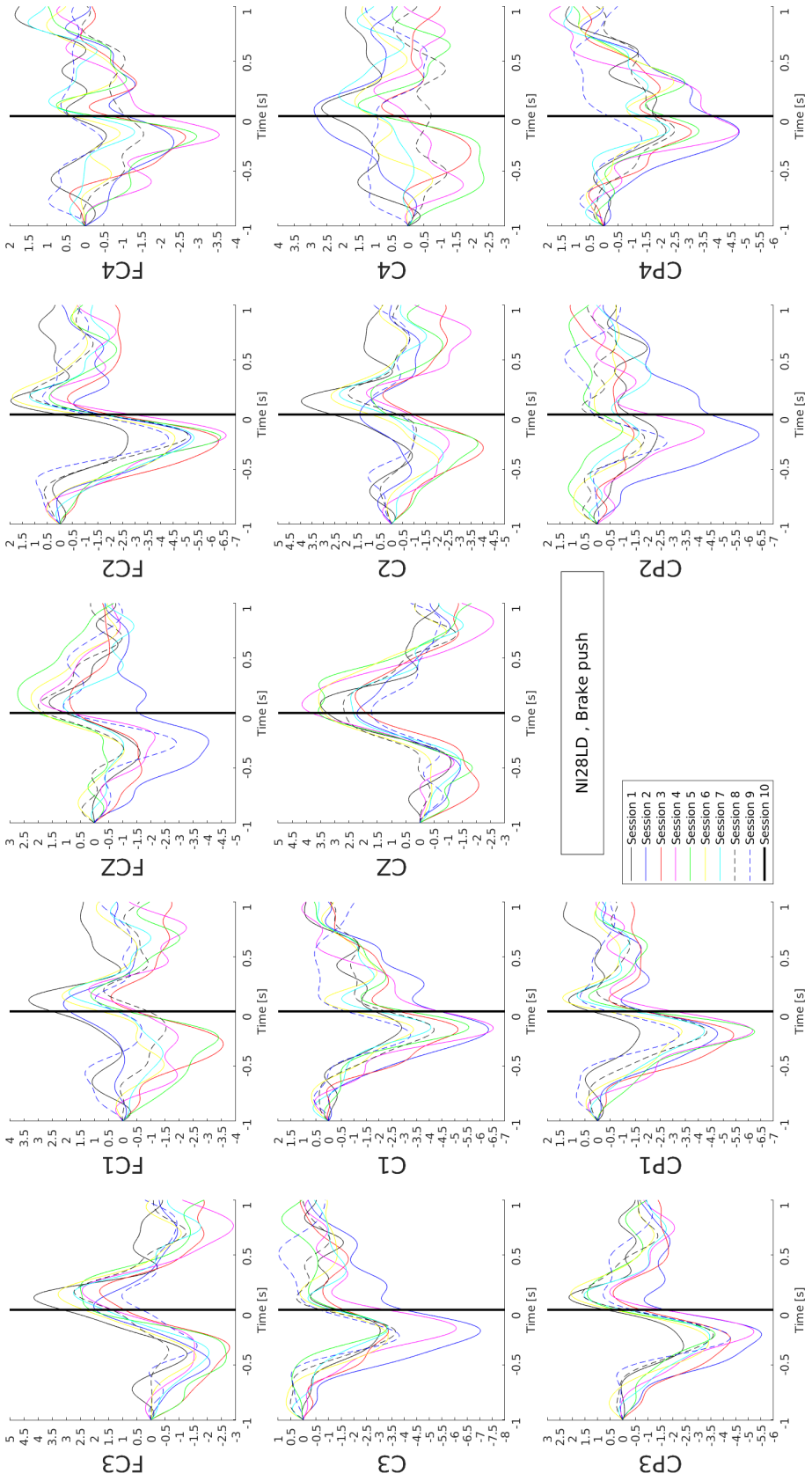


Fig. 3.20 MRCPs of NI28LD for Brake push

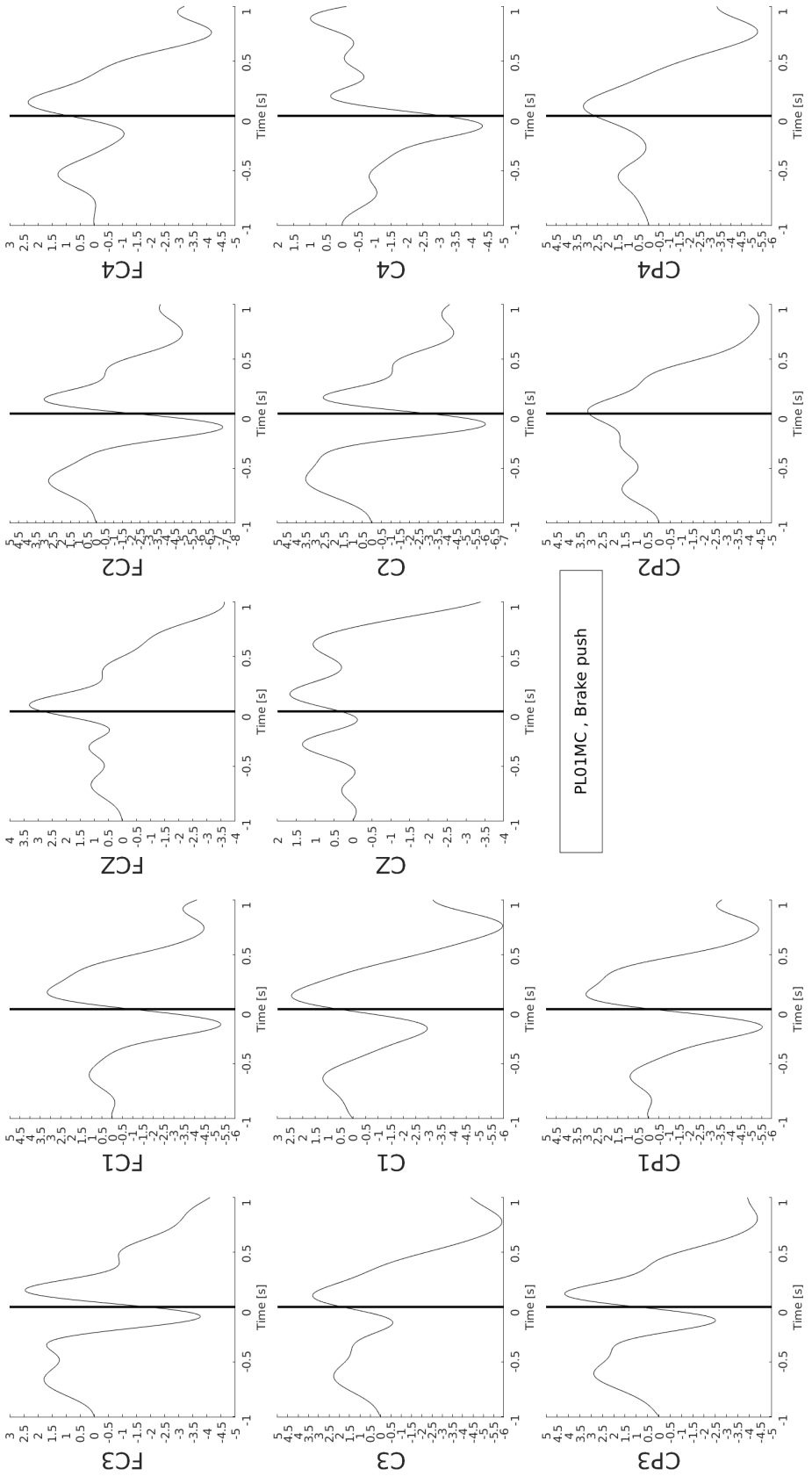


Fig. 3.21 MRCPs of Max Günther for Brake push

Despite successfully extracting MRCP signals, it has not been possible to relate features of these like their depth, or the timing of the negative peak to the learning and performance metrics at the session level. There are no significant correlations with the lap time or with the lap index (i.e., there is no chronological improvement), neither for the depth nor for the time gap to the movement onset. A per-lap analysis, as done here for the PSD and connectivity results, may reveal significant associations to learning, however, the quality of lap-wise MRCP averages may be compromised because, within a lap, one only gets a small amount of each MRCP type.

### 3.4.8 Anticipatory MRCPs associated with racing proficiency

Exemplary Fig 3.22 and 3.23 demonstrate that only the professional drivers and the novice driver NI28LD who achieved near-professional performances exhibit MRCP at the ideal positions, verifying my assumption. Anticipatory MRCP figures for all participants and movement types (not shown here) confirm that for all other drivers, the driving actions are not placed timely and consistently enough to allow the formation of an MRCP. Hence, this index may have some use in a closed-loop training protocol, where the CNV negativity is used to assess on-the-fly whether drivers will be able to proceed with the next needed action in a timely fashion.

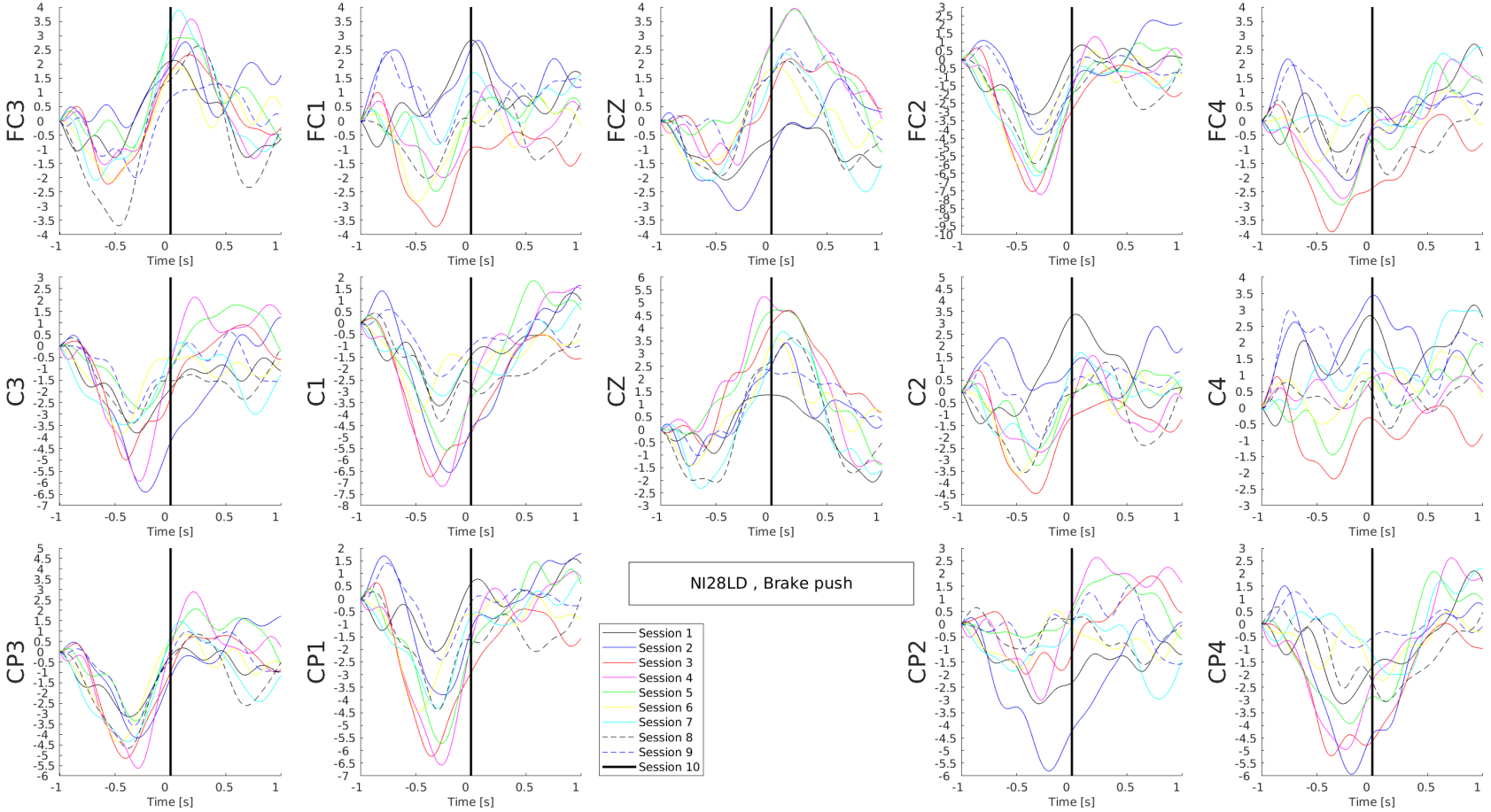


Fig. 3.22 Anticipation MRCPs of NI28LD for Brake push

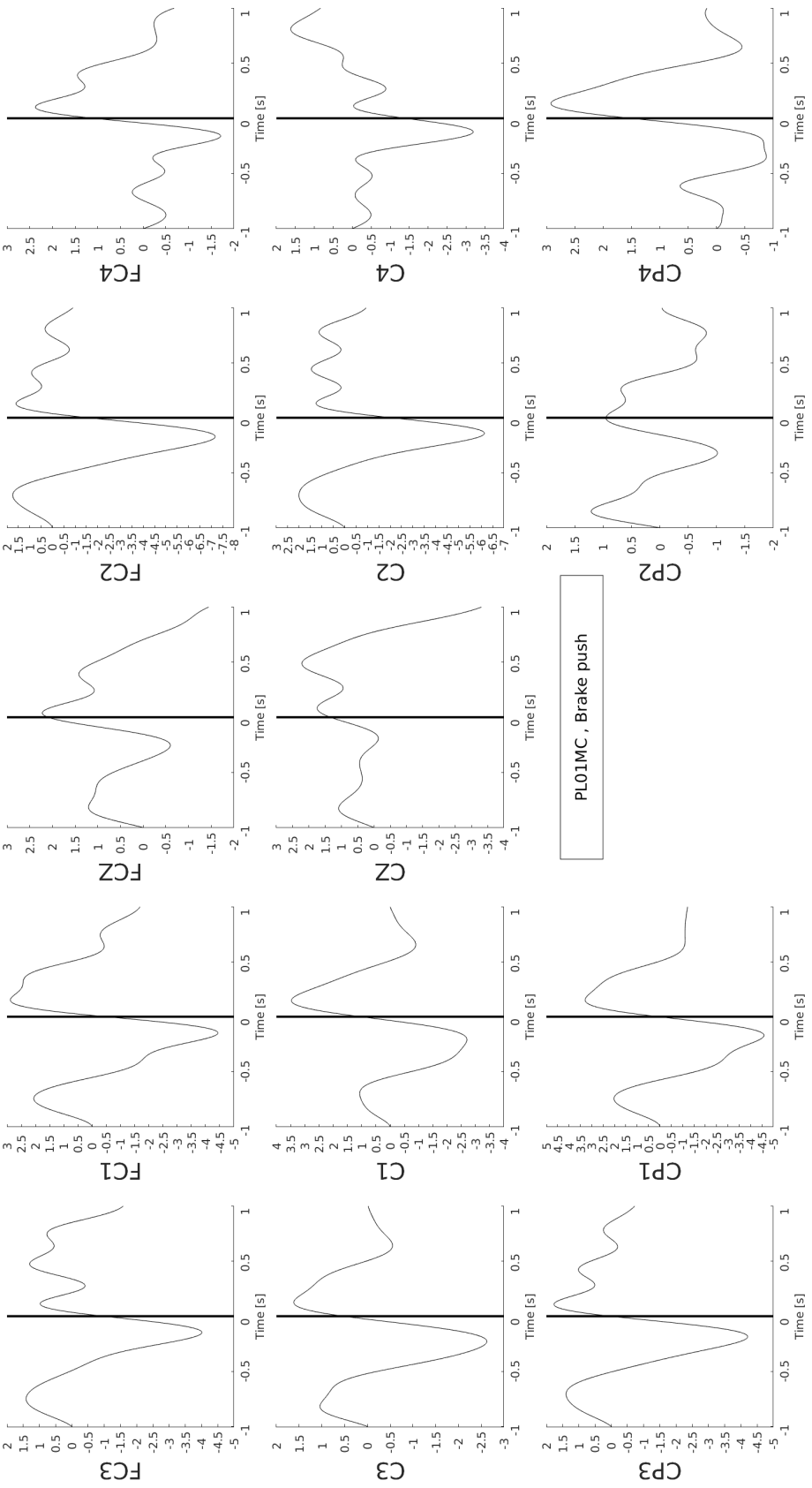


Fig. 3.23 Anticipation MRCPs of Max Günther for Brake push

## 3.5 Conclusions

The main conclusions of this analysis can be summarized as follows:

1. Novice drivers exhibited clear learning effects in terms of lap time, following the optimal race line and using the steering wheel. There were less clear learning outcomes in terms of impact management and usage of brake and throttle, which is related to the feedback given and the different strategies adopted by each individual.

2. Professional drivers also showed clear improvements along all these metrics within a single session, suggesting they were able to get accustomed to the virtual car, track and simulator controls.

3. I observe the anticipated difference in performance between novice and professional drivers, which remained at training offset despite, as also expected, novice drivers improved much more on average than the professional drivers did.

4. One of the novice drivers was able to perform markedly better than the others and approximate the performance of professional drivers.

5. tDCS seems to support the learning of race driving, although the effect is not so strong as to demonstrate on a session-wise, mixed-design ANOVA. Note though that the sample is small (11 participants), which justifies the absence of a strong effect.

6. Learning for all subjects but one was accompanied by progressively lower theta-band power in subject-specific cortical areas.

7. Learning for all subjects but three was accompanied by progressively stronger alpha-band functional connectivity between frontocentral and occipital cortical areas.

8. Clear MRCPs could be extracted for all subjects, especially for the Brake push movement. No feature of these MRCPs could be associated with learning through, checking at the session level.

9. Clear "anticipatory" MRCPs, as defined here, could be extracted for professional drivers and for the best novice driver NI28LD, especially for the Brake push movement. Again, no feature of these MRCPs could be associated with learning through, checking at the session level. However, it looks like these MRCPs can be used to infer early on whether a driver will take an action at the appropriate time.

This work assessed the neurobehavioural signatures and brain plasticity to learn complex motor skills like race driving. Simultaneously, it tries to understand the potential role of tDCS to enhance the learning process. The results show clear changes in the power of theta-band EEG rhythms correlated with lap time for both professional and novice participants. Alpha-band functional connectivity also seems to be a neuromarker of learning to race. At the same time, neurobehaviour between the professional driver and novice driver differs. I further conclude that tDCS can support the learning of race driving for Novice users, although the effect was not strong and would require replication in future studies. Future work will seek to delineate and confirm these effects in experimentation with larger populations.

# Chapter 4

# Embedding prior neurophysiological knowledge into feature selection for brain-computer interface through fuzzy logic

## 4.1 Introduction

By using a BCI system providing the user with direct feedback on their mental activity in closed-loop, it has been shown that users can learn to self-regulate their brain signals and optimize the operation of external devices through the BCI [22, 42, 47]. Initial BCI systems were mainly based on expert neurophysiological knowledge coupled with lengthy feedback training. On the contrary, the vast majority of recent BCI systems are based on data-driven and ML-oriented methods [44], shifting the focus of learning from the human to the machine. Despite the wide use of ML-oriented BCI nowadays, the efficiency and effectiveness of BCI systems are still not up to the mark, posing a

major barrier to universal access to BCI systems [45]. Therefore, I postulate that the combination of data-driven methods and expert knowledge may be able to bring about wider accessibility of BCI systems by exploiting the best of these two worlds [22].

It is well-known that FL theory, along with Bayesian and Dempster-Schafer methodologies [67], are ideal for fusing information from multiple independent sources in order to improve decision-making. Furthermore, FL is also suitable for specifically incorporating human expertise and knowledge, as the latter can be easily and effectively modelled through fuzzy rules within the FL framework. Previous studies [70–73] have employed FL-based approaches for the analysis, interpretation, and classification of EEG data. However, these works are still fully data-driven and do not take into account the rich expert neuroscience knowledge that forms the basis of all modern BCI paradigms.

This chapter proposes a novel feature selection method for BCI able to exploit both data-driven and expert neuroscience knowledge thanks to a fuzzy controller [68, 132]. This algorithm constitutes a completely novel use of FL in the BCI context, leveraging one of the main strengths of FL, its ability to perform decision-making that fuses heterogeneous information channels, in order to address an identified need in the field of BCI, namely, the possibility to inject expert knowledge into feature selection in an automatic manner. The automaticity is a critical contribution of my method since, although expert knowledge has regularly been exploited in conventional BCI model training [47], this required the physical presence of a BCI engineer. This is an impractical and expensive prerequisite, hindering the transition of BCIs to real-world scenarios.

The presented method follows a FL framework formalization for its suitability to handle uncertain information. I implement the proposed feature selection module as a Mamdani fuzzy controller that produces a modified fitness ranking of all candidate

features, taking into account both their separability and their anticipated suitability according to the relevant neuroscience literature and BCI expert experience.

## 4.2 Motivations

The motivation of this work is to fuse neurophysiological priors with data-driven separability information for feature selection with a fuzzy inference system so that expert knowledge on the neuroscientific relevance of candidate features can be exploited, as often done in conventional decoder training [22, 61], without an actual expert having to be present and perform it themselves. Embedding prior neurophysiological knowledge into feature selection for BCI through FL ensures that features are not blindly selected solely according to their separability, which is often greatly influenced by noise and thus may be misleading, but comply with the neurophysiology of the underlying tasks. As a result, my method helps so that the selected features remain inside the known "learnable" manifold [133], thus promoting subject learning and the overall effectiveness of BCI-based training.

Additionally, this chapter shows that the gains in accuracy are larger the more noisy the underlying data are. These benefits seem to arise because purely data-driven methods are unable to distinguish between physiological and noise-induced feature separability; embedding expert knowledge addresses to a great extent this shortcoming by attenuating the influence of separability emerging in physiologically unlikely locations and/or frequency bands (i.e., features that are most probably popping up as separable due to temporary noise effects), thus delivering a more consistent, informed and parsimonious feature selection outcome. This study is further distinguished for assessing the proposed method on a large MI BCI dataset comprising one or more sessions of 65 users, including several sessions of 21 patients with motor disabilities due to a variety of

different pathologies (stroke, spinal cord injury, muscular dystrophy, etc.), thus solidly grounding the reliability of the findings.

## 4.3 Materials and Methods

This section describes the dataset used for the analysis and the signal pre-processing and feature extraction methods applied prior to the novel FL-based feature selection algorithm. To clearly demonstrate the added value of the proposed approach, the MI data is deliberately further contaminated with varying amounts of eye and "teeth clenching" EEG artifacts derived by another EEG study [134]. The noise addition process is described in detail below. Finally, the proposed automatic feature selection method is elaborated.

### 4.3.1 MI BCI dataset of 65 subjects

The dataset comprises MI-based EEG recordings from 65 participants. Among these, 44 subjects are able-bodied volunteers (aged 41.0 ± 8.5 years, 10 female and 34 male) and 21 subjects are end-users (aged 55.5 ± 25.5 years, 3 female and 18 male). The end-users are affected by different levels of myopathy, tetraglegia, spinal cord injury, amputation, spinocerebellar ataxia or multiple sclerosis, but were without any mental deficits.

### 4.3.2 Data acquisition protocol

The EEG and overall experimental setup for this study are those described in Chapter 1, Section 1.5. The dataset is composed of, both calibration/open-loop and online/closed-loop runs. Each run contains by default 15 trials for each of the MI tasks attempted by the user. The MI tasks present in the database are right hand, left hand, both hands,

both feet MI and "resting" (idling). Calibration runs typically contain 2-4 MI tasks, while online runs always contain exactly two MI tasks (2-class MI BCI), which is the pair emerging as optimal for the particular user during training.

Each run begins with a 3-second display of a fixation cross on a screen facing the participants (Chapter 1, Figure 1.5). Following this, a cue appears for 5 seconds, represented by an arrow pointing left, right, upward or downward, depending on the number of tasks included in the training. Each direction is associated with a particular MI and the subjects are informed of this mapping before the experiment. Participants are then required to mentally simulate repetitive kinaesthetic movements of either their left hand, right hand, both hands or feet, based on the direction of the arrow. The BCI translates its output into movements of the feedback bar, which provides real-time brain status updates to participants in online experiments. When the feedback bar hits the decision threshold, a decision is displayed, signifying the chosen command that would be transmitted to the prototype for application control. In the initial calibration stage, where online feedback is not available, spurious (mostly "positive") feedback is used where the bar is pushed towards the ground truth side reaching the decision threshold in exactly 4 s. A random break (inter-trial interval) lasting randomly 3.0 to 4.5 seconds is imposed between trials.

Each participant undergoes a single calibration session at the onset of training, containing 3-4 offline runs. On rare occasions, when a good classifier could not be obtained from this data, the offline session was repeated. For online experiments, only two MI categories are used (selected based on the highest accuracy during classifier training), with each run consisting of 15 trials for each class/MI task. There are 4 to 8 closed-loop runs per online session. Participants transitioned to online training as soon as possible (i.e., as soon as a decoder yielding above-chance classification could be obtained), since it is known that only closed-loop control engages the subject's learning

capacity [22]. Most able-bodied users in the database have performed one calibration and one online session. However, several users have performed more than one online session (up to 10 sessions). Patients typically performed one calibration session and up to 10 closed-loop sessions.

### 4.3.3 Feature Extraction

This experiment follows the same feature extraction method mentioned in Chapter 1. The feature extraction procedure produces the initial dimensionality of the feature vector $N = 15$ channels $\times$ 23 frequency bands $= 368$ features, where individual feature reflects the estimated power of a specific cortical location (channel) and frequency band. For the subsequent processing steps, the information of which time-point within the trial the PSD reflects is disregarded and all PSD samples of all runs within a session are pooled together to form the final subject dataset (i.e., essentially, PSD samples are assumed to be independent and identically distributed).

### 4.3.4 Adding noise to extracted PSD

To highlight the added value of the proposed method in the presence of various noise sources inflicting the EEG signal with artifacts [134], various levels of noise are artificially superimposed on the PSD features. Importantly, the impact of artifacts on PSD features may not be particularly serious in controlled experiments taking place in the lab such as the one generating the dataset used here, but it is known to be much more pervasive and harmful under real-world BCI conditions) [47]. I have used the independent dataset containing artifact-contaminated EEG described in Jin et al. [134]. The PSD of each artifact trial for each EEG channel was extracted with the same parameters as for the MI trials. Subsequently, each original MI trial in my data may be contaminated by a randomly picked artifact trial with a probability of $p_{nl}$.

The parameter $p_{nl}$ defines the "noise level" added and is varied across repetitions of my analysis in $[0,1]$ with a step of 0.1. Hence, $p_{nl} = 0$ indicates no artificial noise interference at all, and $p_{nl} = 1.0$ that noise is superimposed on all of the MI trials. When some MI trial is selected for contamination, this is carried out through a weighted average $\mathbf{x'^f_t} = (0.5\mathbf{x^f_t} + 0.5\hat{\mathbf{x}}^\mathbf{f}_\mathbf{t})$, where $\mathbf{x'^f_t}$ the artificially contaminated PSD value for feature $f$ at time $t$, $\mathbf{x^f_t}$ the corresponding feature value extracted naturally from each subject's MI data and $\hat{\mathbf{x}}^\mathbf{f}_\mathbf{t}$ the PSD value of the selected artifact trial. Of note, only the "frowning" and "teeth clenching" artifacts are used from the data in [134]. The samples of each MI trial are randomly contaminated with one or the other artifact type with a probability of 0.5 (uniform distribution). The PSD of each channel in my configuration is contaminated with the same channel from the artifact data. Since the two EEG setups are highly overlapping but not identical, a channel that is missing in the artifact dataset is replaced by the nearest one available.

Lastly, in order to better simulate the vulnerability of peripheral channels to artifacts under real-world conditions, channel Fz of the MI setup is specifically contaminated, not with the equivalent Fz channel of the artifact trial, but with the most affected peripheral channel, instead; this is a channel among those in the following channel set: Fz, F2, AF4, FP2, FP1, P2, PO4, P6, O2, P5, O1, PO3, P1, AF3, F1, Oz, POz, and Pz. This special treatment of Fz is meant to compensate for the fact that, in the low-density EEG channel configuration used in the MI study, Fz may be the most peripheral channel but is still not "peripheral enough" to reflect well the amount of noise interference that can occur in a real BCI application with denser and more widely spread EEG locations.

I strongly believe that this algorithm for artificially contaminating the EEG data models well the real artifact generation process during BCI operation in out-of-lab, uncontrolled environments.

### 4.3.5 Feature selection through FL

To facilitate BCI control it is necessary to identify participant-specific spatio-spectral PSD patterns that maximize the separability between mental tasks, but, as I have argued here, also respect known neuroscientific principles. To automatically select the N-best features compromising separability with neurophysiological relevance, I propose a FL-based automatic feature selection method by combining the expert knowledge concerning the cortical areas and frequency bands that are expected to be activated by the employed MI tasks [135, 2] with the features' data-driven discriminant power ranking.

### 4.3.6 Fuzzy logic controller design

I devised a Mamdani-type fuzzy controller for automatically selecting $N$ features that reflect both adequate separability and compliance with background knowledge. This section details how fuzzy logic theory is applied to deliver the desired outcome and the various choices made with regard to the system's design.

#### Fuzzy sets and membership functions

My fuzzy controller operates independently for each feature to output a modified (with respect to a conventional, data-driven separability/discriminant power metric) feature fitness. This fitness value is used to rank the candidate features and allow selection of the $N$ best ones. The Mamdani-type fuzzy controller receives three inputs for each candidate feature: location (channel), frequency band and discriminant power indexed by $r^2$ feature separability (coefficient of determination between the feature values and the MI class label). Note that the choice of separability metric is of no particular importance (i.e., Fisher Score [24], Canonical Variate Analysis [1] or other similar metrics and filter-based feature selection approaches can be used without detriment)

because it is normalized by dividing the discriminant power of each feature with the total discriminant power of the candidate feature set (i.e., division is with the sum of the discriminant power values of all candidate features).

A single fuzzy set is defined for each of the three inputs whose membership function specifies what truth values can be considered "good" (and to what degree) for the input in question (i.e., which channels and which bands are good–for a particular taskset; and which $r^2$ values are good, in general). In this binary (good/bad) modelling for the controller's input variables the explicit definition of a fuzzy set for "bad" is not necessary, as the fuzzy operator NOT is later used in the fuzzy rules, thus implicitly defining the "bad" fuzzy set with the complimentary membership function $f_{bad} = (1.0 - f_{good})$.

Custom composite membership functions are created for all three inputs so as to accurately reflect the relevant neurophysiological knowledge from the literature [2, 135, 136] (see Fig. 4.1). In summary, it is known that subjects performing right or left hand MI exhibit strong contralateral SMR in the $\mu$ (8-12 Hz) band and/or the $\beta$ band (13-30 Hz). If feet imagery is part of the mental exercises, the topographic SMR distribution maps typically reveal central cortical activation in the $\beta$ band. During hand imagery tasks, ipsilateral activation may also be observed, although most often less pronounced than the contralateral one. The contralateral activations are more pronounced and stronger in the $\mu$ band, especially when performing left-hand/feet imagery tasks [2]. Notably, in the right-hand/feet imagery pair, subjects on average display equally strong ipsilateral and contralateral activation.

Based on such "rules of thumb" that can be derived from the literature as well as my own and my group's expertise with MI BCI, regarding the location input variable, a different membership function is created for each MI taskset (i.e., pair of MI tasks used for closed-loop BCI control) included in my analysis: right hand and left hand (RHLH), right hand and feet (RHBF), or left hand and feet (LHBF). These membership

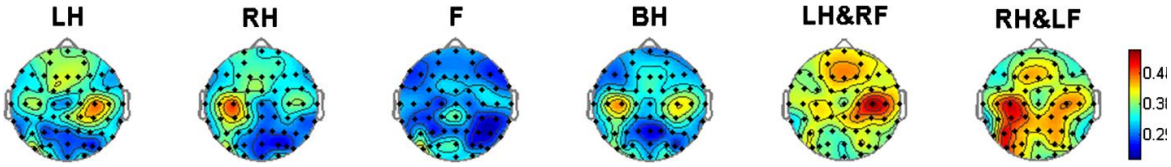


Fig. 4.1 Topographical SMR distribution plots for six mental tasks (from left to right: Left hand (LH), Right hand (RH), Feet (F), Both hands (BH), Left hand versus Right feet (LH&RF), and Right hand versus Left Foot (RH&LF)) for an arbitrary subject (adapted from [2]). Red color indicates strong activation (deep ERD/ERS).

functions are constructed as follows: the highest membership degree is assigned to contralateral (with respect to the right/left hand) channels (i.e., the maximum weight of 1.0 for C1 and C2, Fig. 4.2a) when the respective MI is part of the taskset employed. Slightly lower membership values are assigned to ipsilateral channels and electrodes that are more peripheral (than C1/C2, e.g. C3/C4) or vertically displaced with respect to the central zone (i.e., centro-parietal and fronto-central channels). Medial channels are given no membership whatsoever in the "good" fuzzy set for the RHLH taskset (Fig. 4.2a).

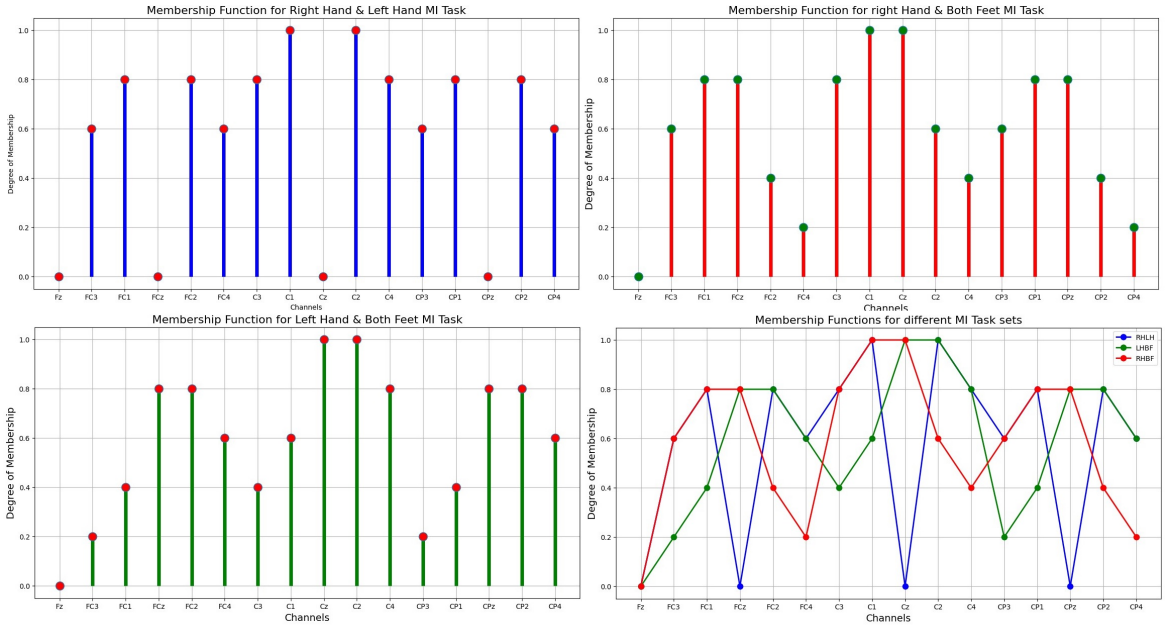


Fig. 4.2 Membership functions associated with the "good" fuzzy set of the location input for taskset (a) RHLH, (b) RHBF and (c) BFLH (d) all tasksets.

For tasksets containing feet MI (Fig. 4.2b-c), a high membership value is assigned to the medial channels (1.0 for Cz, 0.80 for CPz and FCz) and less weight is given to the lateral ones (0.40 for FC1, CP1 concerning LHBF; 0.40 for FC2, CP2 with respect to RHBF).

When a certain channel falls in two of these categories (e.g., for the RHLH taskset, channel C1 is both contralateral to the right hand and ipsilateral to the left hand) the maximum of the possible membership values is taken. Fig. 4.2 illustrates the membership functions designed in this manner for each of the aforementioned three tasksets examined in my analysis.

The membership function for the "good" fuzzy set of the frequency band input (Fig. 4.3a) is built by superimposing suitable trapezoidal function templates in such a way so that high membership is given to the $\mu$ and $\beta$ bands, in accordance with the literature.

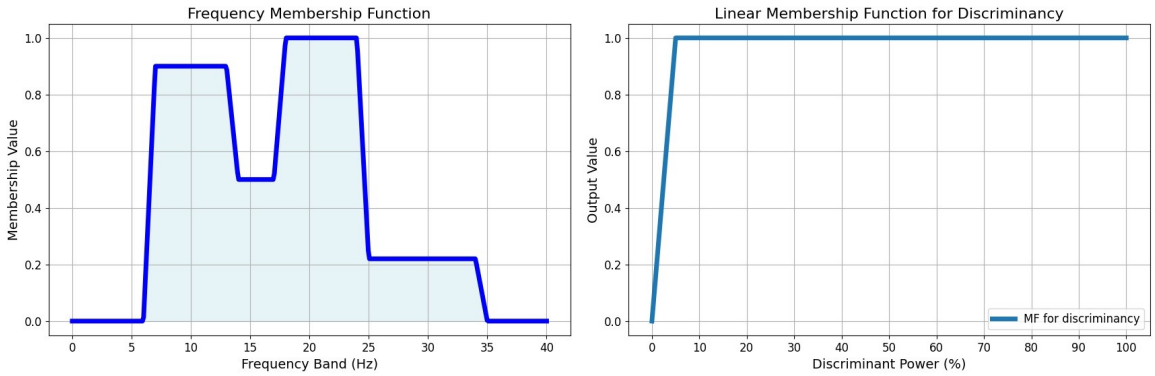


Fig. 4.3 Membership function of the "good" fuzzy set for the (a) frequency band input and (b) the discriminant power input.

The membership function for separability, which serves to fuse also the data-derived information into feature selection, is based on a linear function where the membership value starts at 0.0 and increases to 1.0 linearly. Since, as underlined above, the discriminant power is normalized, the truth value of separability for each feature in fact corresponds to the percentage (%) of the total separability accounted for by the feature

in question. Based on experience, and in particular, by inspecting the discriminant power % values achieved for the best features in the runs yielding high classification accuracy for the highest-performing subjects in the database, I conclude that 5% of the total discriminant power reveals a very separable feature. Accordingly, the "good" separability membership function of my controller will reach the maximum membership of 1.0 at 5% of discriminant power (Fig. 4.3b).

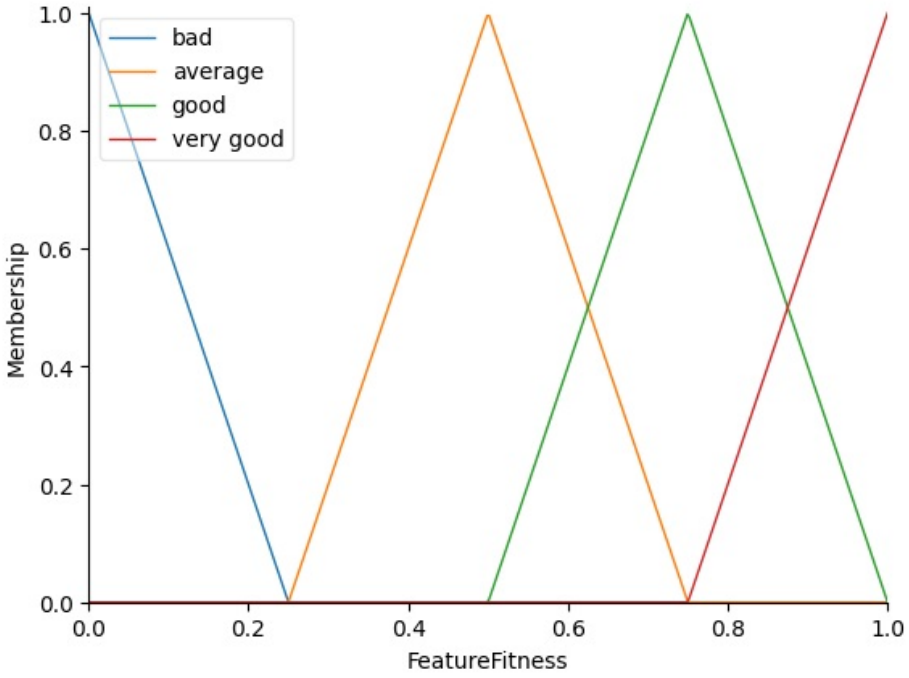


Fig. 4.4 Membership functions of the 4 fuzzy sets defined for the fuzzy controller's "Feature Fitness" output variable. Blue for the "bad" fitness fuzzy set, orange for the "average" fitness fuzzy set, green for the "good" fitness fuzzy set, and red for the "very good" fitness fuzzy set.

Finally, 4 fuzzy sets are defined for the output "feature fitness" variable, associated with "bad", "average", "good" and "very good" feature fitness. The respective membership functions, based solely on triangular function templates, are depicted in Fig. 4.4.

Table 4.1 Fuzzy rules of the proposed controller.

| Rule | Location | Frequency Band | Discriminant Power | Feature Fitness |
|---|---|---|---|---|
| 1 | good | good | good | very good |
| 2 | not good | good | good | bad |
| 3 | good | not good | good | bad |
| 4 | good | good | not good | bad |
| 5 | not good | not good | good | bad |
| 6 | not good | good | not good | bad |
| 7 | good | not good | not good | bad |
| 8 | not good | not good | not good | bad |

### Fuzzy rules and fuzzification

I defined 8 conventional IF-THEN-statement rules shown in Table 4.1. Each rule regards one of the $8 = 2^3$ possible combinations of our 3 binary (bad/good) inputs. For example, the first rule is described by the statement:

> R1: IF Location IS good AND Frequency Band IS good AND Discriminant Power IS good THEN Feature Fitness IS very good

Fuzzification in my controller proceeds as follows for each candidate feature: First, for each rule, the membership values corresponding to the three truth values (channel, band and discriminant power of the said feature) are extracted. These are then combined with the AND operator to form the rule's antecedent value. Operator AND is given its most common interpretation as the "min" membership value among the 3 inputs. Subsequently, in the rule's implication process, the fuzzy set of the consequent for this rule is computed with the "min" operator; effectively, this truncates the membership function of the output variable's fuzzy set that appears in this rule's consequent, as typically done in Mamdani-type fuzzy controllers. Fuzzification is concluded by applying this procedure with all 8 rules present in my system and aggregating the outputs of all rules through the "max" operator. All rules exercise the same effect on the output (i.e., all rule weights are set to 1.0). The final outcome of the fuzzification

process is the membership function of a final output (feature fitness) fuzzy set. Fig. 4.6-4.13 visualize graphically this process for 8 different exemplary sets of input truth values. Each example is selected to target the activation of a specific rule among the 8 rules defined.

### Defuzzification and final output

The defuzzification process extracts the controller's final, "crisp" feature fitness value. Among the different defuzzification methods proposed in the literature [137, 138], I have selected the most popular one, namely, the "centroid" method. In this defuzzification approach, the crisp output is the output value which corresponds to the output membership function's centre of mass. Fig. 4.5 summarizes the overall architecture of the proposed fuzzy controller.

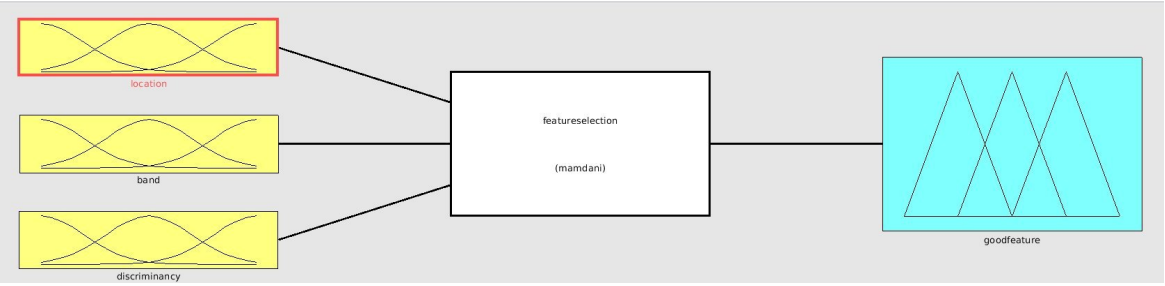


Fig. 4.5 Fuzzy controller architecture.

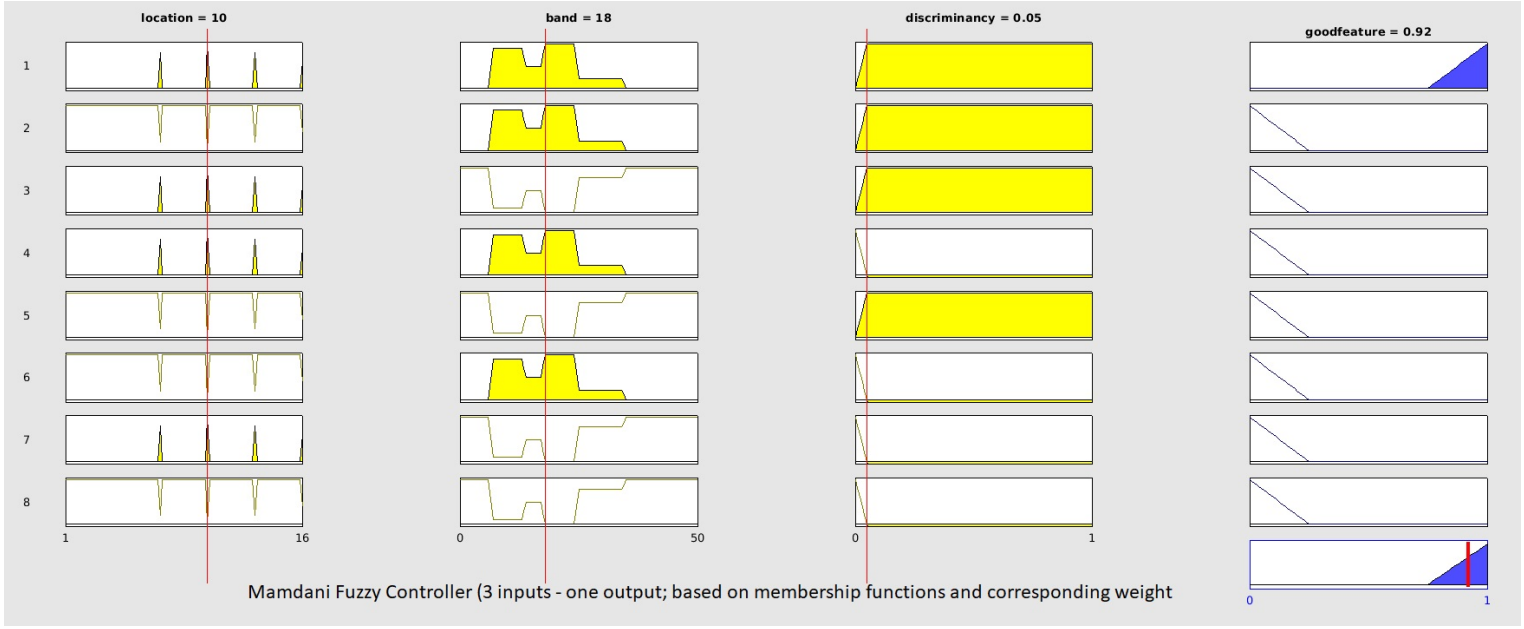


Fig. 4.6 Feature fitness for Rule 1: Good Location, Good Frequency Band, Good Discriminant Power

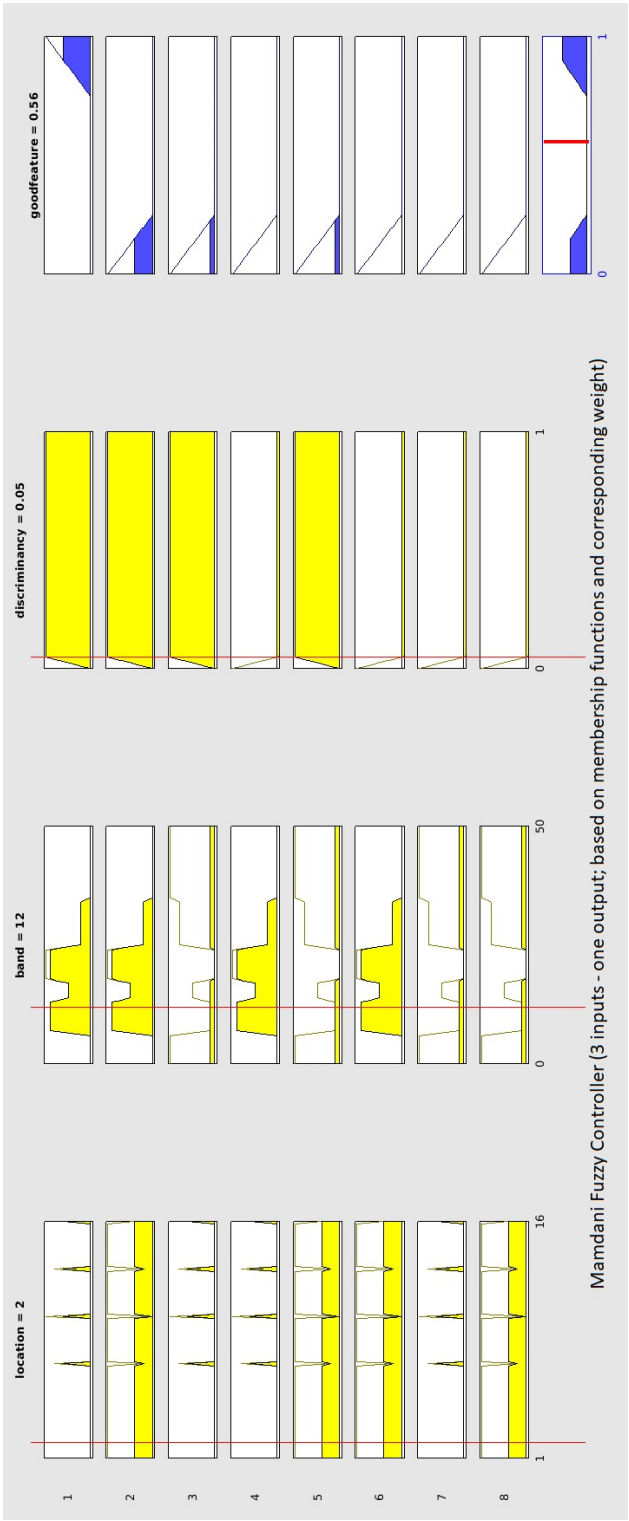


Fig. 4.7 Feature fitness for Rule 2: Not Good Location, Good Frequency Band, Good Discriminant Power

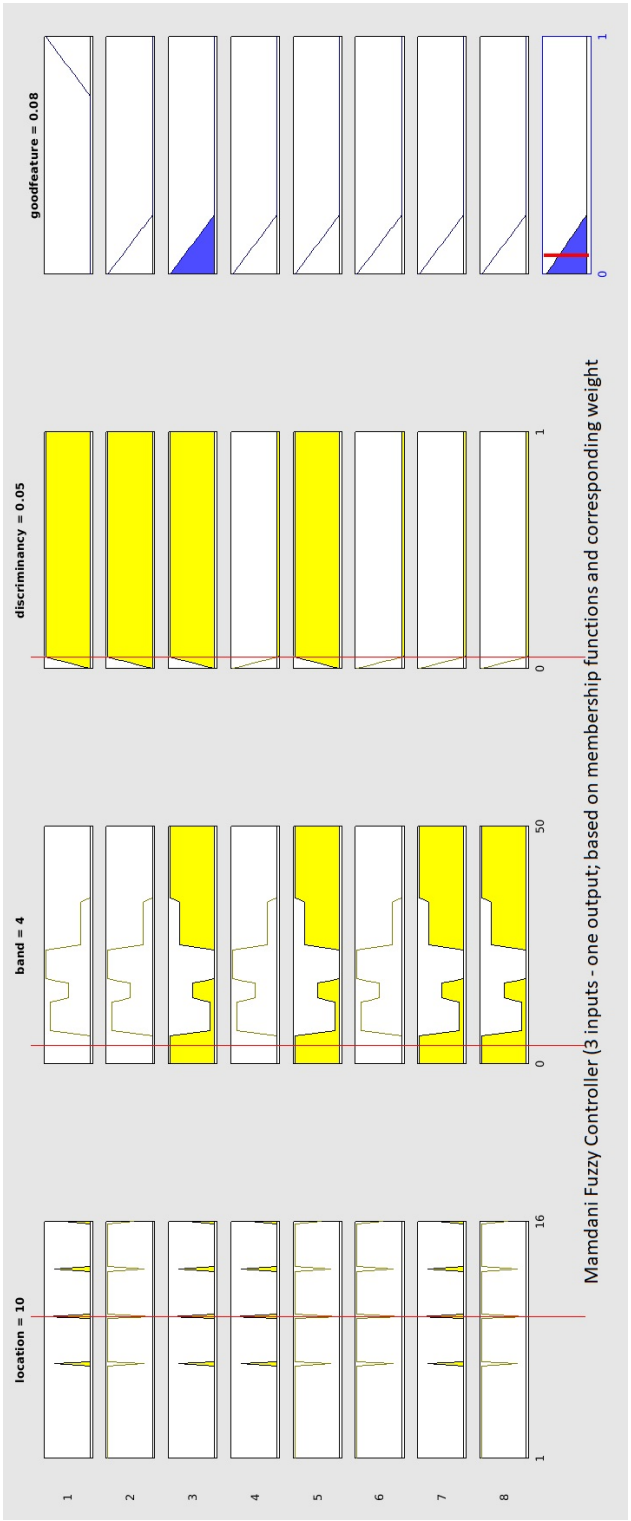


Fig. 4.8 Feature fitness for Rule 3: Good Location, Not Good Frequency Band, Good Discriminant Power

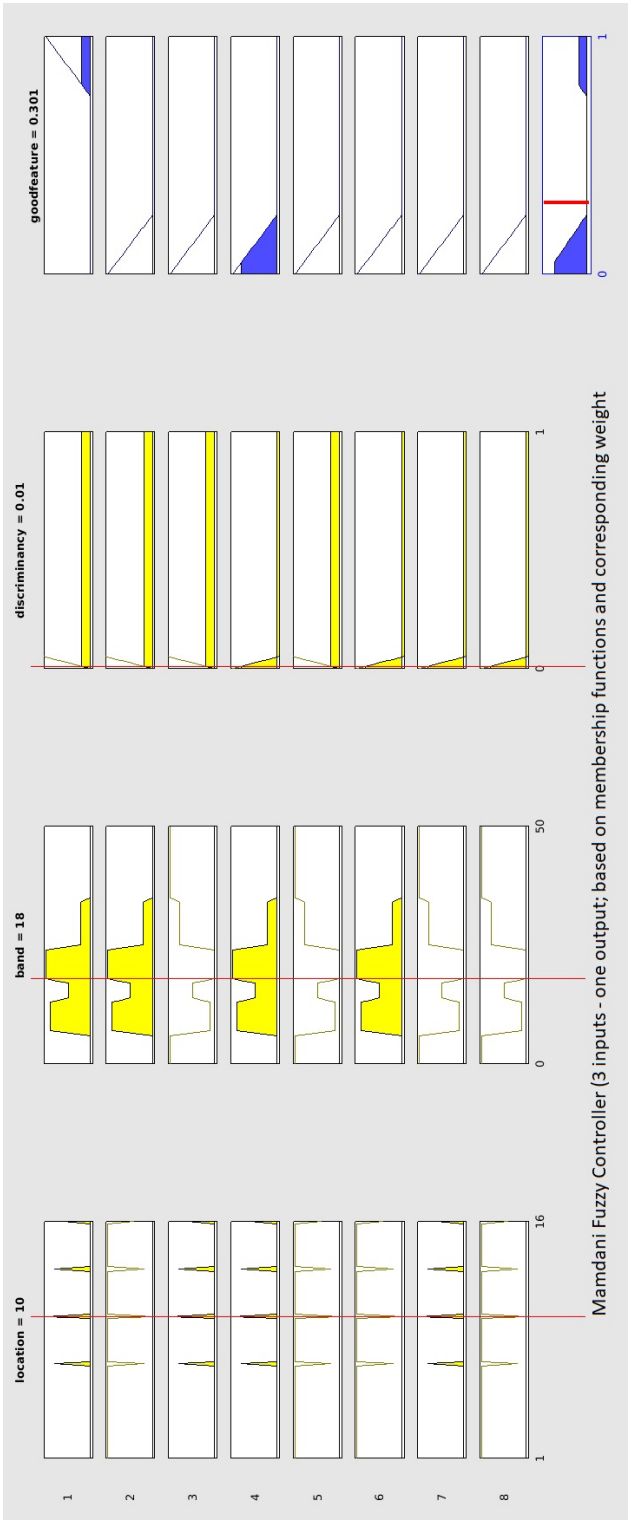


Fig. 4.9 Feature fitness for Rule 4: Good Location, Good Frequency Band, Not Good Discriminant Power

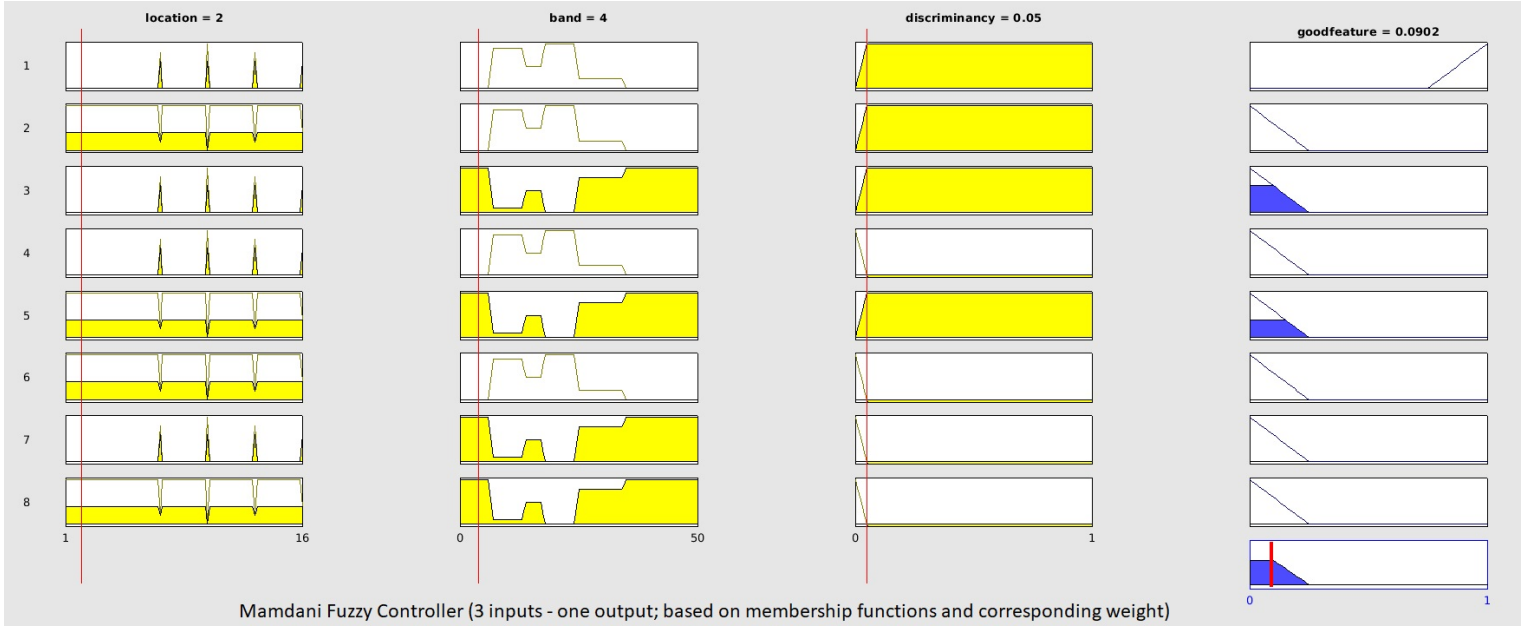


Fig. 4.10 Feature fitness for Rule 5: Not Good Location, Not Good Frequency Band, Good Discriminant Power

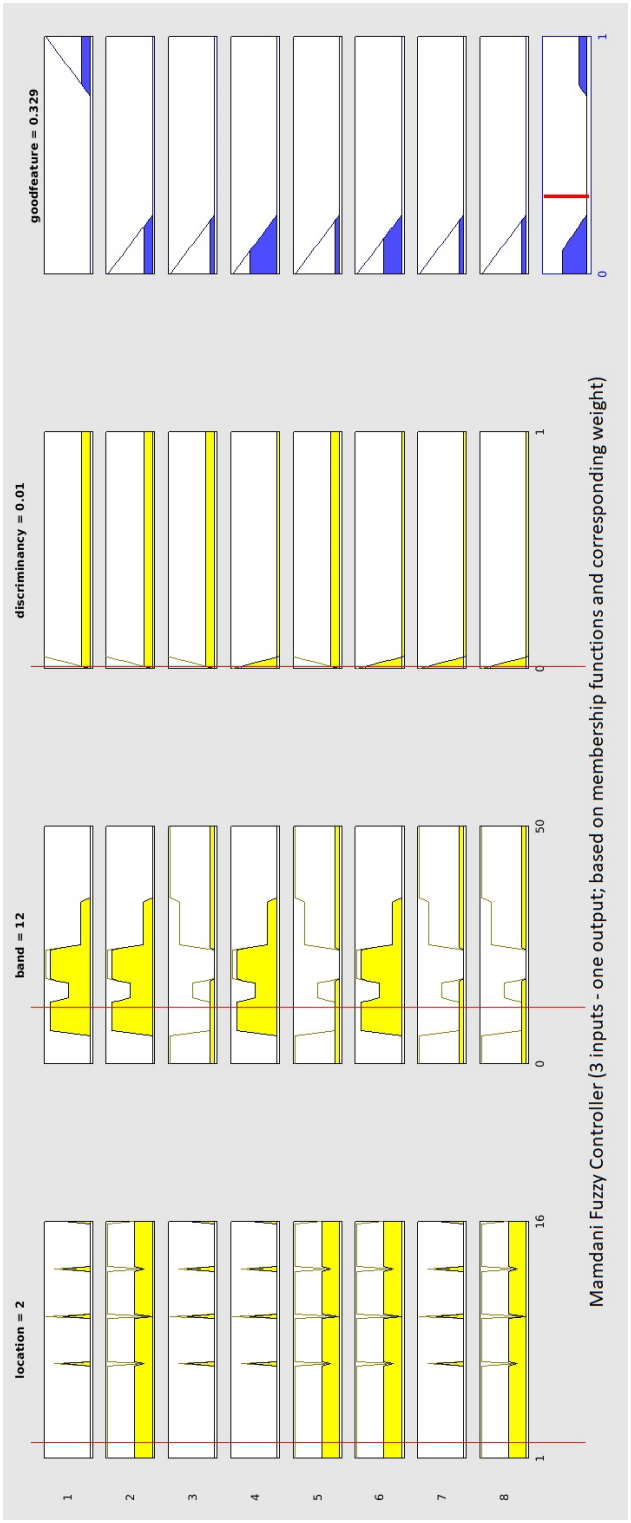


Fig. 4.11 Feature fitness for Rule 6: Not Good Location, Good Frequency Band, Not Good Discriminant Power

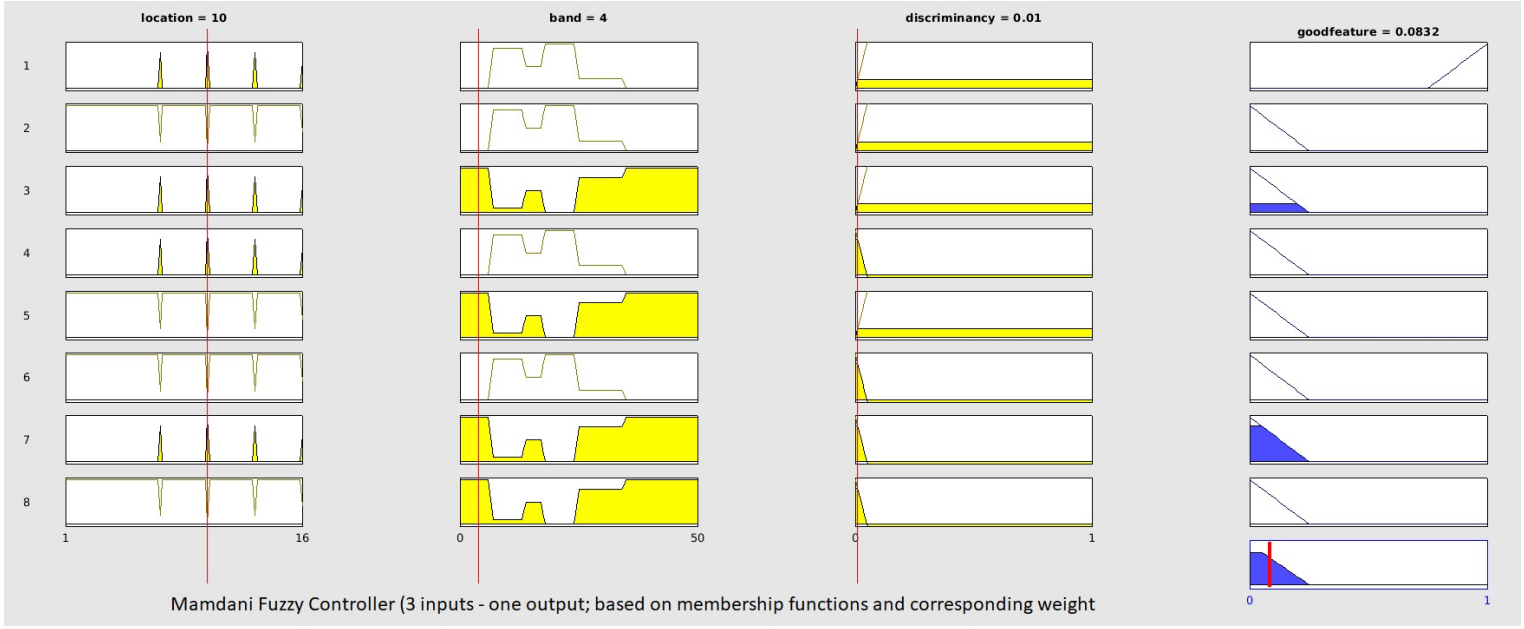


Fig. 4.12 Feature fitness for Rule 7: Good Location, Not Good Frequency Band, Not Good Discriminant Power

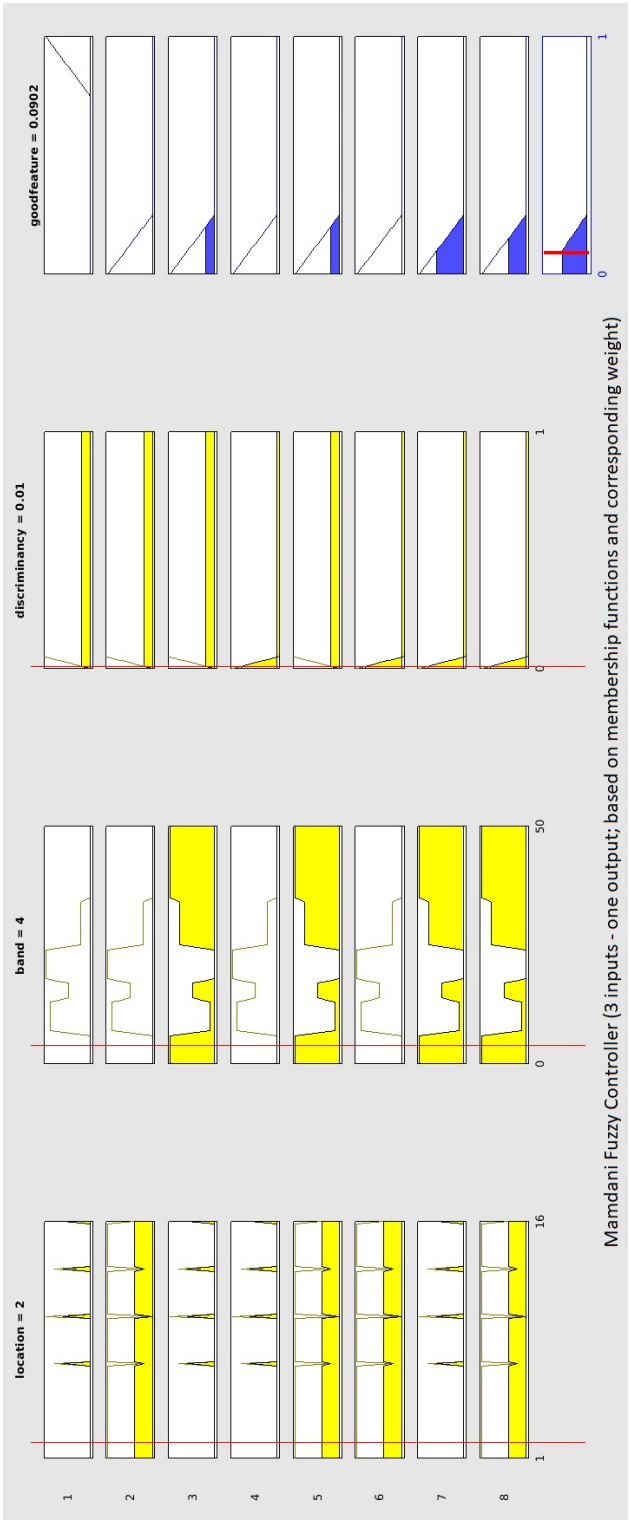


Fig. 4.13 Feature fitness for Rule 8: Not Good Location, Not Good Frequency Band, Not Good Discriminant Power

### 4.3.7 Controller design rationale and effects

The FL controller design described above targets two main interventions on the regular, solely data-driven feature fitness output. Primarily, I intend to suppress "false positive" discriminant power that often arises as a result of the presence of EEG artifacts. Two typical, but by no means unique, cases are shown in Fig. 4.14 and Fig. 4.15. Ocular and muscular artifacts may occur arbitrarily during the execution of one or more trials of some MI task. Given that the amplitude of these signals is at least one order of magnitude greater than pure EEG activity, the EEG signature these signals generate by propagating on the scalp is mistaken by the feature ranking/separability monitoring method as a strong EEG correlate of the underlying MI task. Much greater discriminant power than what the actual MI correlates yield is therefore inferred for at least some of the candidate features. There is no easy and efficient data-driven way to discriminate between "spurious" and "authentic" discriminant power. There do exist artifact detection and removal methods [134], however, no method guarantees absolute success in removing artifacts and all methods are still computationally expensive. Therefore, the best, and probably simplest, way to identify "spurious good" features is to challenge the origin of their high fitness on the grounds of prior neurophysiological knowledge. Indeed, artifact-induced separability will very often be found on EEG features that cannot be justified by neuroscience studies. In the context of MI BCI, where spatio-spectral features are commonly used due to their ability to capture all aspects of the ERD/ERS phenomenon, this practically means that spurious separability will most likely be found in channels and frequency bands not justified by MI studies.

Fig. 4.14 shows an example of spurious DP on channel Fz, the most frontal electrode of the EEG layout employed here, which makes it vulnerable to the eye and facial muscle artifacts (eye movements, blinking, frowning, eyebrow-raising, etc.). Hence, high discriminant power on the location of channel Fz is much more likely to be due

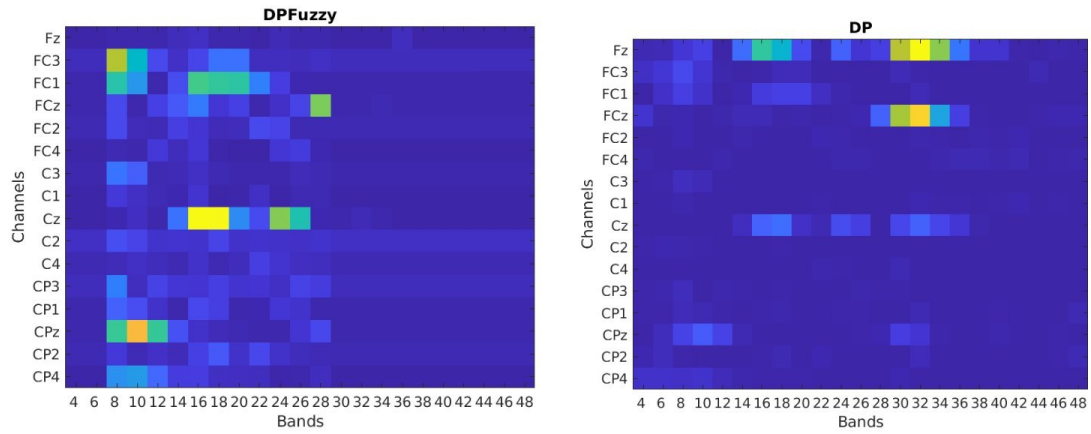


Fig. 4.14 Feature fitness heatmaps with the data-driven discriminant power method (right) and my fuzzy controller method (left). Blue indicates low fitness and yellow indicates good fitness. In this example, the fuzzy method successfully suppresses artifact-induced discriminant power on frontal channel Fz.

to noise, rather than related to the subject's MI. Furthermore, in this case, but, even more, in case of strong muscular artifacts such as those produced by teeth clenching and, in general, jaw movements, researchers often observe high separability in high-$\beta$ and $\gamma$ frequency bands (i.e., greater than 30 Hz, see the example of Fig. 4.15), usually evident in many neighbouring channels. Again, this separability cannot be possibly attributed to MI, yet, an exclusively data-driven automatic feature selection method will be bound to select these features as optimal, thus resulting in a classifier model unable to detect actual MI patterns. Fig. 4.14 and Fig. 4.15 show how my fuzzy controller design is effective in suppressing false-positive discriminant power that is not physiologically sound.

Furthermore, it is not necessary for all features to be simultaneously modulated (i.e., possess high fitness). Critically, the proposed method extracts a modified FL-based fitness for each individual feature. It then re-ranks these features according to their modified fitness scores. An interesting aspect of the proposed method relates to the frequency band input. The membership function for these inputs tends to assign similar

membership grades to neighboring or adjacent bands. This similarity arises from the choice to use a feature resolution of 2 Hz,—a resolution previous studies have found effective. For example, a 12 Hz, feature might be useful, while a 14 Hz, feature might not. If we were to use a lower resolution—such as grouping entire delta, theta, mu, and beta bands—the membership functions would encounter fewer input values and less overlap in membership grades. However, the fundamental approach remains the same and is adaptable to various types of features. For instance, if we were analyzing the P300 wave, there would be no frequency band input; instead, we would use a "time period" input.

The proposed method inherently produces an output for each feature independently and does not aggregate feature sets. However, if there were indications that certain patterns, such as C3/12 Hz and CZ/20 Hz, frequently co-occur, the method is flexible enough to incorporate additional inputs (i.e., co-incidence) and corresponding membership functions that favour these co-occurring patterns. Yet, there is currently insufficient evidence to suggest this extension is necessary for MI BCI used in this research. This is due to the high variability of spatio-spectral components, which tend to be highly specific to individual subjects and sessions. Nonetheless, the concept of including inputs related to feature sets and membership functions is significant. It opens the door to numerous methodological extensions, such as inputs that enhance consistency across different runs or sessions, or those that select features relevant to multiple (or all) classes, rather than just one.

As a secondary goal, the method proposed here is also designed to resolve cases of subjects with low MI aptitude. As shown in Fig. 4.16, in such cases, all candidate features have very low discriminant power, but due to the small differences in separability, the $N$-best features are again very likely to be in locations and bands unnatural for SMRs. Consequently, my fuzzy controller is designed to boost the fitness of the

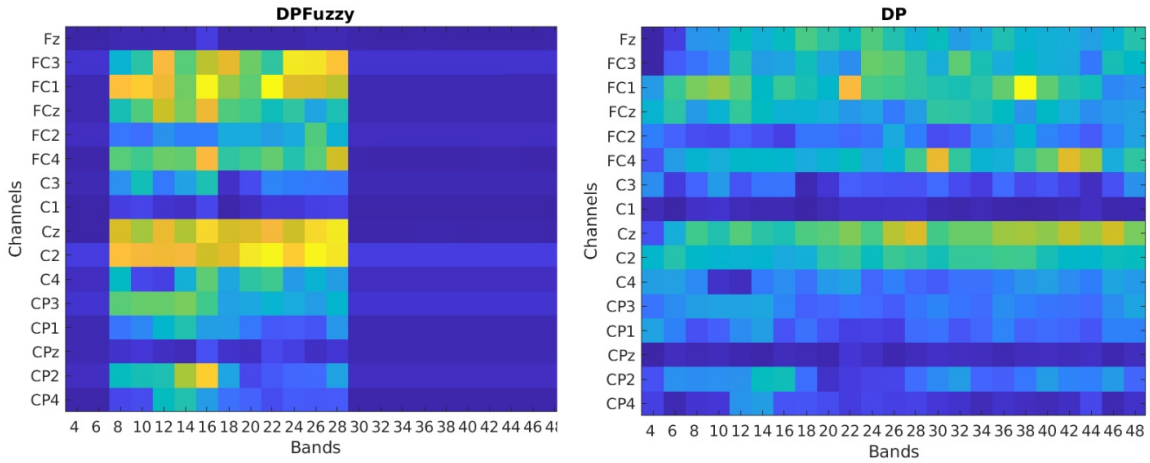


Fig. 4.15 Feature fitness heatmaps with the data-driven discriminant power method (right) and my fuzzy controller method (left). Blue indicates low fitness and yellow/orange indicates good fitness. In this example, the fuzzy method successfully suppresses artifact-induced discriminant power in abnormally high-frequency bands.

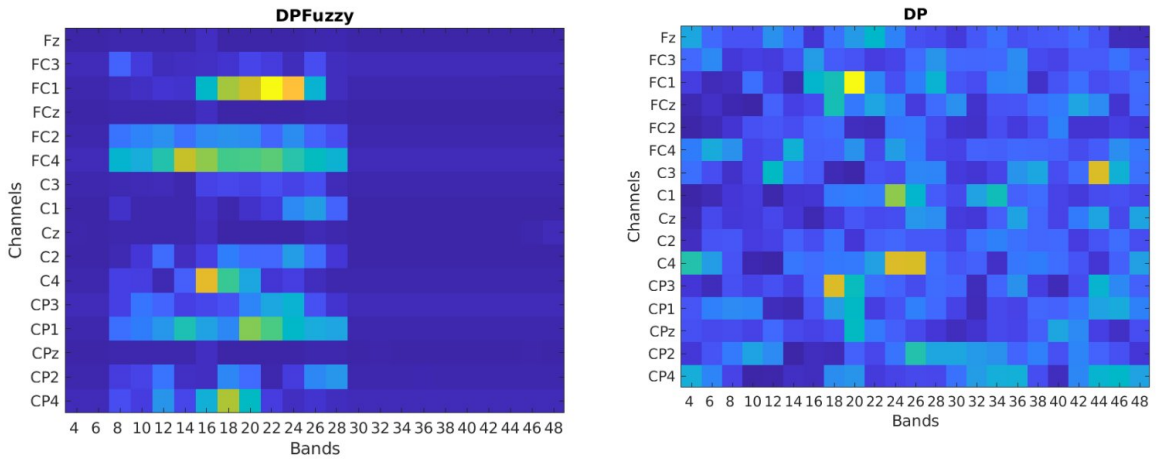


Fig. 4.16 Feature fitness heatmaps with the data-driven discriminant power method (right) and my fuzzy controller method (left). Blue indicates low fitness and yellow indicates good fitness. In this example, the fuzzy method successfully highlights the most relevant features allowing them to emerge as top-ranking and to be selected instead of arbitrary low-discriminant power features.

relevant features enough so that these can surface at the top of the modified feature ranking so that they can be automatically picked. Although the separability of these features is still low and will inevitably lead to compromised initial BCI performance, I hope that by imposing selected features to correspond to known MI correlates I can

facilitate the subjects' learning process during closed-loop training by permitting them to work within a "learnable" feature manifold, as discussed in [133]. Fig. 4.16 shows that my fuzzy controller is also effective in that regard.

Although these two goals have dictated most of the choices made here (i.e., number and type of inputs and outputs, the basic form of membership functions, number and type of fuzzy rules, etc.), it must be highlighted that, as it is often the case in FL system design, my controller's final parameterization and architecture has been to a large degree the result of "trial-and-error". The observant reader may note that the fuzzy rule set does not make any use of two of the defined fuzzy sets for the Feature Fitness output variable ("average", "good"), exploiting instead only the sets "bad" and "very good". This is a good example of the aforementioned trial-and-error approach: I originally intended for each fuzzy rule to map antecedents to a consequent as:

- (all) three "good" inputs lead to "very good" feature fitness
- (any) two (out of three) "good" inputs lead to "good" feature fitness
- (any) one (out of three) "good" input leads to "average" feature fitness
- (all) three "bad" inputs lead to "bad" feature fitness

However, I soon realized that this initially envisioned scheme would not lead to sufficient "spurious" discriminant power suppression which is my main goal. Conversely, requiring all three inputs to be "good" so as to infer "very good" feature fitness, and mapping all other cases to "bad" feature fitness delivered the desired outcome. As can be seen in Fig. 4.6- 4.13, in my final architecture, the activation of the first rule is "driving" the final crisp output towards high Feature Fitness, while the remaining 7 rules act as "penalizers" of different combinations of deficiencies (i.e., not-so-relevant location/band, low separability, etc.), dragging the crisp output towards lower fitness. In practice, this approach turned out to adequately fulfil the two main design targets set.

Similarly, the exact shape of the membership functions of the inputs was determined by studying the effects of different choices on the actual MI data. In certain cases, this led to final results that were counter-intuitive in the beginning, like the membership function for the "good" fuzzy set for the Frequency Band input, where $\beta$ features have been eventually assigned higher weight than $\mu$ ones. This is necessary mainly in order to serve my second goal (of meaningful/learnable selected features) for end-user participants, for whom $\beta$ features are prevalent.

### 4.3.8 Classification

The classification of PSD feature vectors is effectuated with a Linear Discriminant Analysis (LDA) model. Automatic shrinkage with the OAS method [139] is applied to all class-wise covariance matrices in case they are not positive semi-definite. The LDA's common covariance matrix is estimated as the average of the class-wise covariance matrices. I extract and report two types of accuracy: per run or per session. In both cases, for closed-loop (online) runs/sessions the LDA classifier used to classify the data has been trained on the data of the previous run/session, respectively. For the first online session, the classifier is trained on the data of the most recent calibration session. Classification accuracy for the calibration session is extracted through cross-validation on the session's own data, as no previous data exists in this case. Feature selection is naturally also done on the data of the previous run/session prior to training the LDA model.

### 4.3.9 Evaluation

I evaluate the performance of the proposed automatic feature selection algorithm across three different aspects: BCI performance, selected feature stability and avoidance of class bias. In all cases, the respective evaluation metric is calculated for the proposed FL-

based algorithm and compared to the conventional automatic feature selection method where the $N$-best features are selected automatically based on discriminant power $r^2$ ranking. We standardize the finally reported result as the difference $(M_{fuzzy} - M_{dp})$ for each metric $M$, so that positive values indicate the superiority of the fuzzy method over the conventional data-driven method. Furthermore, I present this difference across all combinations of a number of selected features $N_f = 2, 5, 10, 14, 20, 30, 50$ and noise level $p_{nl} \in [0 : 10 : 100]\%$. For statistical analysis, all sessions/runs executed by each subject are pulled together within each subject's dataset and averaged. Subsequently, averages and statistical testing are reported across subjects. Paired, two-sample t-tests $(\alpha = 0.0.05)$ are performed for each evaluated measure with Bonferroni correction to account for multiple comparisons due to canvassing several values of selected feature set cardinality and noise level.

The immediate effect on BCI performance is assessed through classification accuracy, computed as detailed above. Accuracy reflects the percentage of correctly classified samples (of both classes) over the total number of samples in the run/session.

Feature stability in the context of BCI systems refers to the consistency of the selected features across different trials or sessions. Stable features are crucial for the robustness and reliability of BCI systems. Feature stability is quantified thanks to the Jaccard similarity coefficient, a statistical measure assessing the similarity of two sets $A, B$ as the size of their intersection over the size of their union:

$$J(A, B) = \frac{|A \cap B|}{|A \cup B|} \tag{4.1}$$

Here, $J(S_i, S_{i+1})$ measures the similarity of the features selected in two consecutive runs/sessions, $S_i$ and $S_{i+1}$, and effectively communicates the percentage of selected features that were common. Hence, a Jaccard Index value close to $J = 1.0$ indicates high stability, meaning most of the features are consistent across consecutive runs/sessions,

while $J = 0.0$ signifies that the selected features tend to be entirely different every time a new feature selection round is performed.

I also report a measure of class bias as the distribution of accuracy across the two MI classes. My assumption is that, by promoting the selection of physiologically relevant features rather than only the most discriminant ones, the final feature set will be more balanced with respect to features that are responsive for both MI tasks. On the contrary, my observation is that, often, a subject's $N$ most separable features will tend to exhibit ERD/ERS only, or at least primarily, for one of the two MI tasks in the taskset. This leads to "biased" control during 2-class closed-loop BCI where a subject is able to deliver successfully one of the two mental commands, but struggles with the other one. The class balance metric offered here is derived by normalizing row-wise the standard confusion matrix of the classification outcome, so that the diagonal elements $c_{11}$ and $c_{22}$ of the normalized confusion matrix $C$ express the class-wise accuracy rates. The final balance $B$ is given by the absolute value of their difference: $B = |c_{11} - c_{22}|$.

## 4.4 Results

The results for this chapter highlight the performance gains of the proposed automatic FL-based neurophysiological knowledge-embedded feature selection algorithm over the regular, purely data-driven feature selection approach. All the comparisons presented here are based on the full database of 65 subjects made available to me.

### 4.4.1 Classification accuracy results

The heatmaps in Fig. 4.17 show the session-wise (Fig. 4.17a) and run-wise (Fig. 4.17b) average accuracy difference between the novel FL-based feature selection method and the discriminancy based method. In areas where the heatmap is green or, even more,

yellow, there is a high, statistically significant (paired, two-sample t-test at the 95% confidence interval with Bonferroni correction) average accuracy difference in favour of the fuzzy method. On the contrary, blue encodes a slight, not statistically significant difference. For both session-wise and run-wise plots, the heatmaps show that my FL controller approach delivers higher accuracy, especially for feature set cardinality greater than 5 features and noise levels within the interval 10%-50%. It is evident that the overall effect in accuracy changes with varying levels of noise and different numbers of features used, however, importantly, statistically significant and noteworthy gains are already observed for 0% noise (i.e., when the MI data are not artificially contaminated with artifacts at all). The effect of my algorithm on accuracy can reach 7% on average for the most susceptible combinations of feature number and noise level.

Fig. 4.18 and Fig. 4.19 visualize the histograms of per-subject average (across each subject's runs or sessions, respectively) accuracy difference between the fuzzy-based and the conventional method for 0%, 10% and 20% noise level and 10 selected features. It can be seen that individual subjects may in fact benefit much more from my algorithm than the average 7% with certain subjects exhibiting impressive accuracy enhancement of even 20%.

Equally (if not more) important, the few subjects that show no improvement would not suffer any adverse effect (i.e., there are no subjects where the application of the FL approach leads to reduced accuracy). In-depth inspection reveals that the non-improving subjects are mostly the already "good" participants whose selected features were already both strong and relevant; hence, the subset of users where the proposed approach has no ground for improvements (ceiling effect).

As shown in Fig. 4.20, several subjects whose performance was below the 58% chance-level accuracy threshold (at the 95% confidence interval [47]) and who were unable to control the BCI, my method is able to raise their performance above this

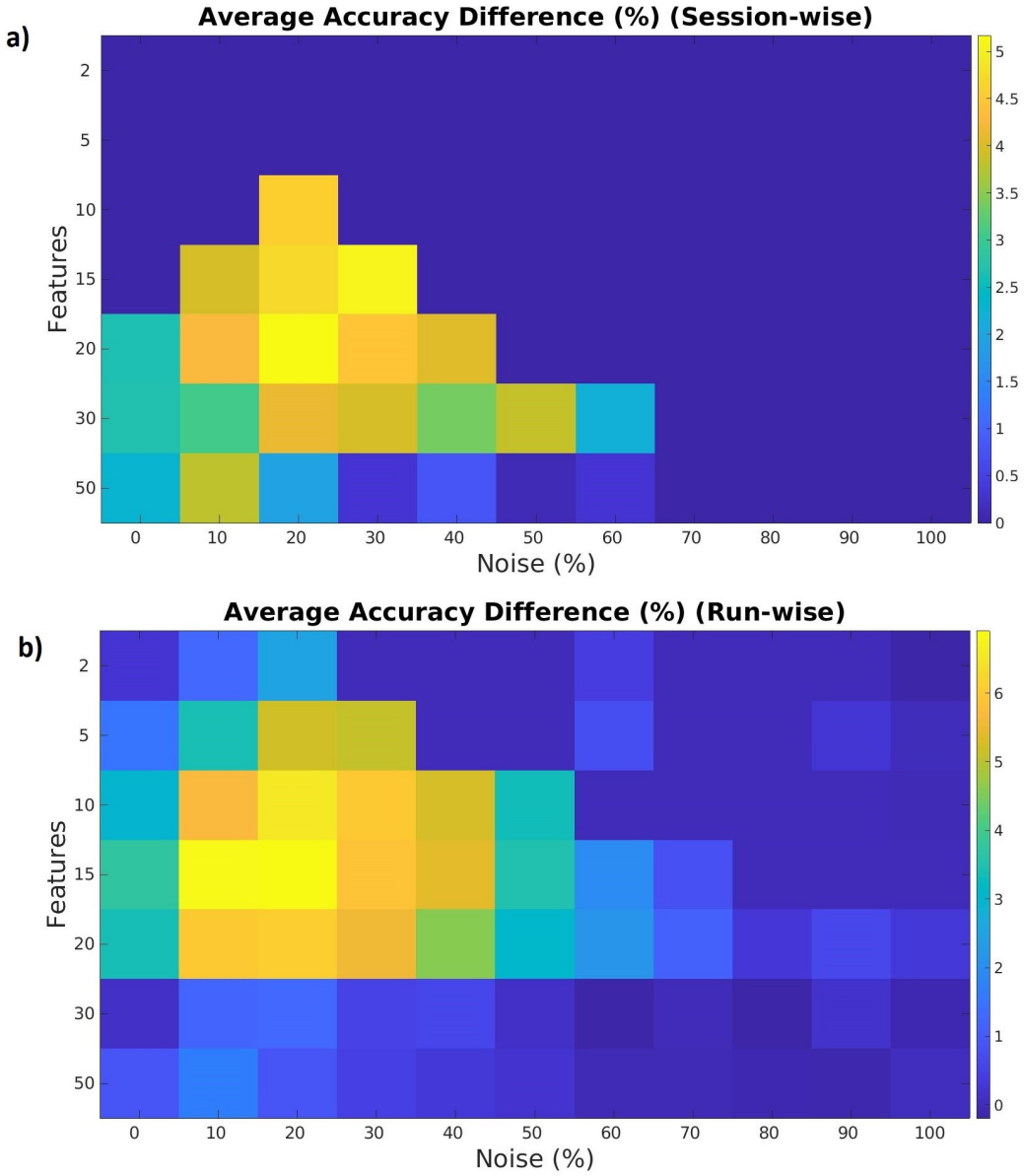


Fig. 4.17 Average (across participants) accuracy difference between the proposed feature selection method (neurophysiological knowledge-embedded feature selection) and the data-driven feature selection method. Positive values (yellow/orange) indicate the superiority of my FL-based method. Cells with 0 value (deep blue) indicate no statistical significance. All other cells indicate statistically significant differences at the 95% confidence interval after Bonferroni correction (paired, two-sample t-tests). (a) Session-wise average Accuracy difference. (b) Run-wise average accuracy difference.

threshold. Therefore, this approach also contributes to the alleviation of the serious issue of non-universal applicability to MI BCI, where several subjects fail to control

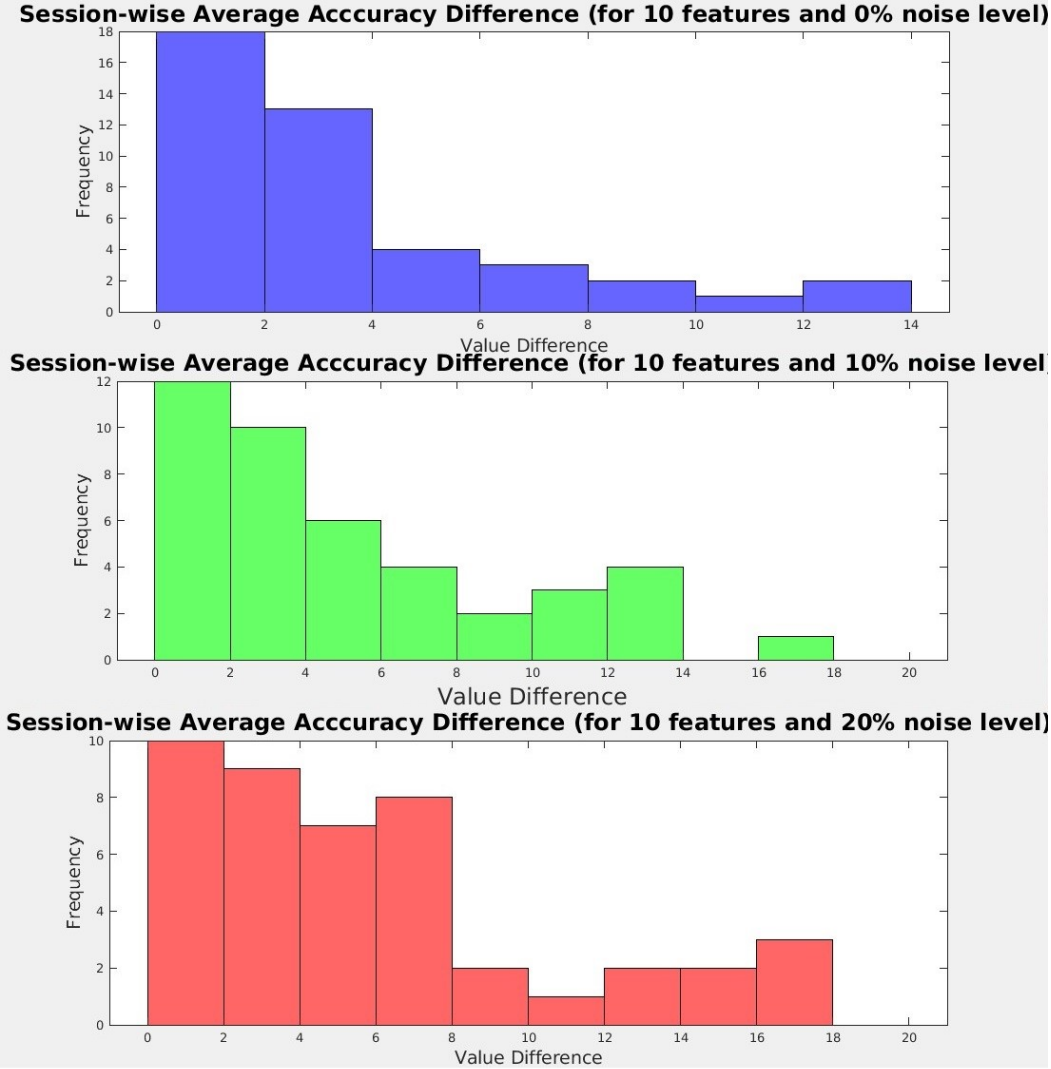


Fig. 4.18 Histogram of per-subject average (across sessions) classification accuracy for 10 selected features and 0% (top, blue), 10% (middle, green) or 20% (bottom, red) noise level.

the BCI system after training [22]. Such improvements are more pronounced for 2-30 features used and 0-50% noise level.

### 4.4.2 Feature stability results

Fig. 4.21 demonstrates that the proposed FL-based feature selection method has a strong effect also concerning feature stability. Again, only statistically significant

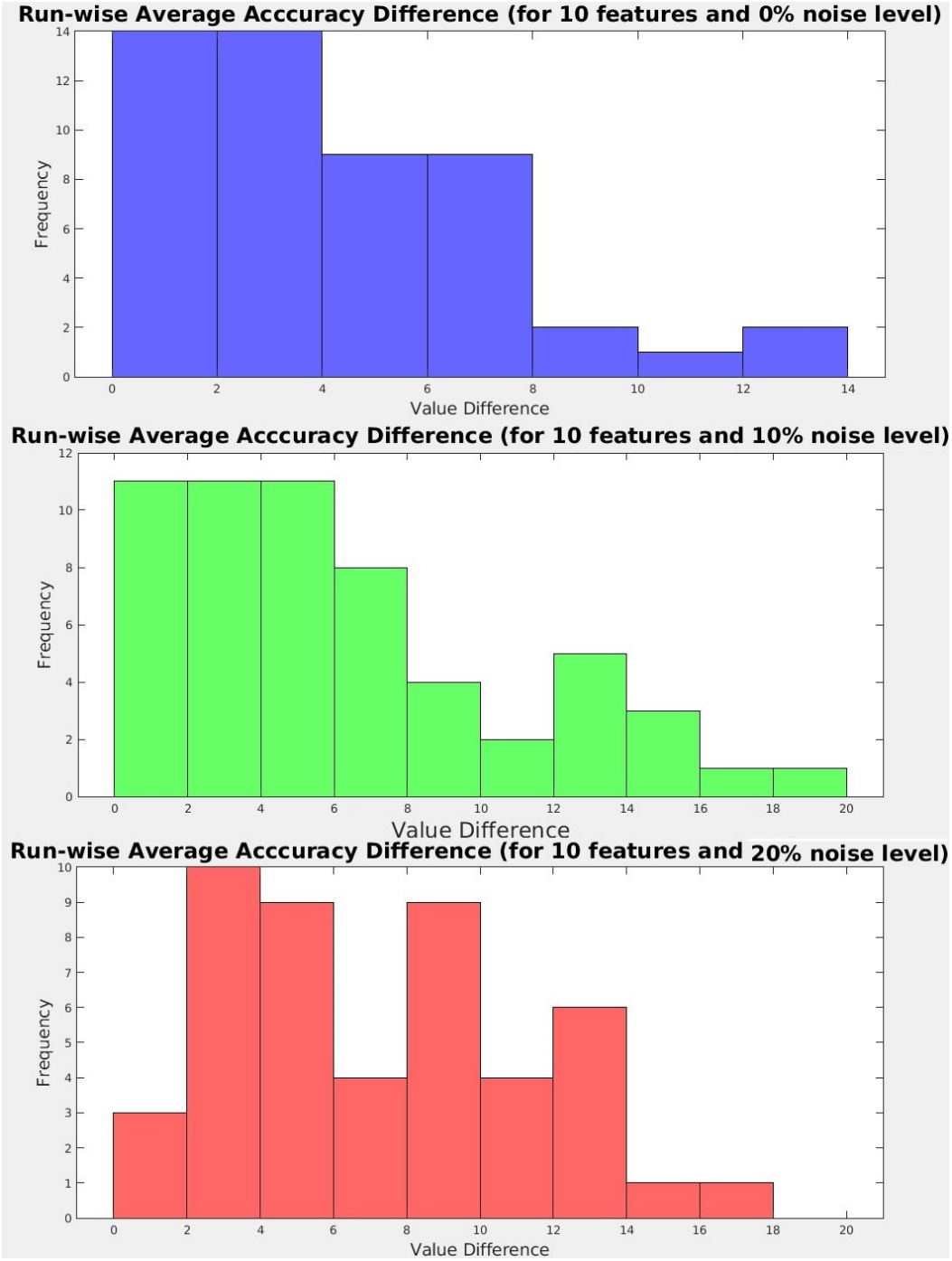


Fig. 4.19 Histogram of per-subject average (across runs) classification accuracy for 10 selected features and 0% (top, blue), 10% (middle, green) or 20% (bottom, red) noise level.

differences in Jaccard index values are visualised in the figure's heatmap, so that

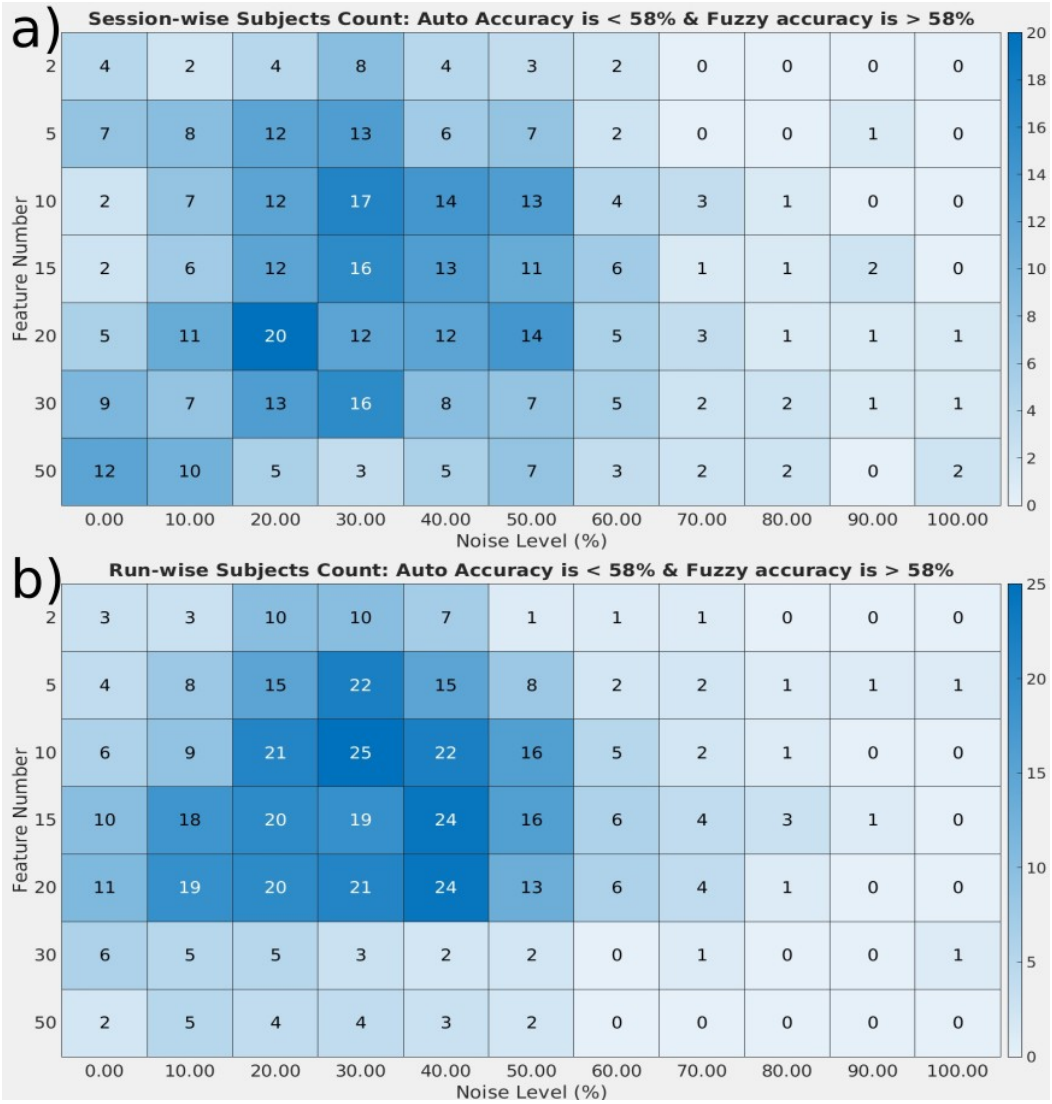


Fig. 4.20 Count of participants exceeding chance classification threshold after applying the proposed method. (a) Session-wise classification accuracy. (b) Run-wise classification accuracy.

0-valued cells indicate a small, insignificant difference between the two methods in terms of feature stability.

Feature stability improvement thanks to the FL method is greater when the noise level is below 60%. Statistically significant gains (2-5% in magnitude on average) are also noted for 0% noise level for cardinality above 20 features. Overall, the proposed method exhibits increased feature stability with a larger number of features, which

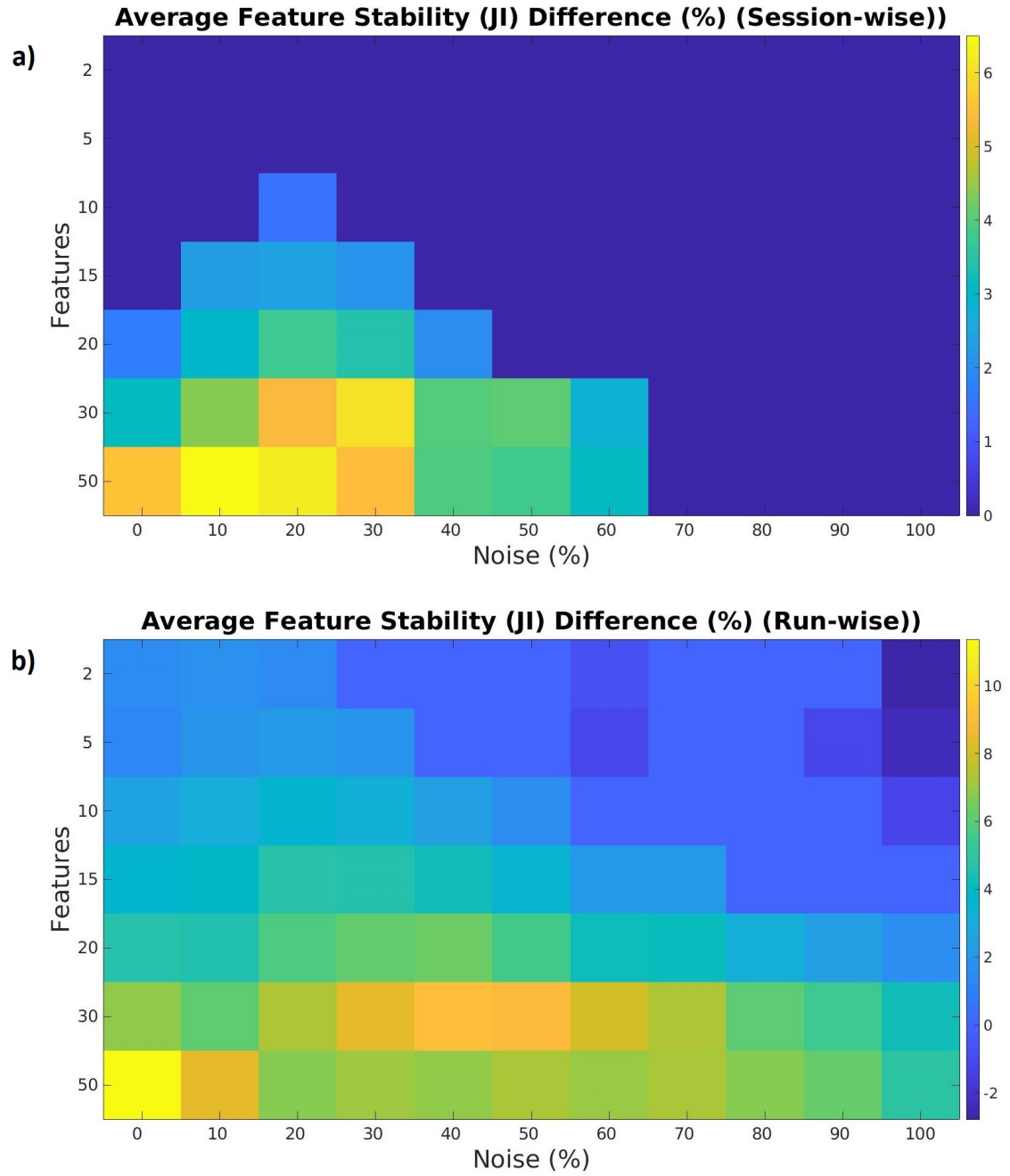


Fig. 4.21 Average (across participants) feature stability based on the Jaccard Index. Cells with 0 value (deep blue) indicate no statistical significance. All other cells indicate statistically significant differences at the 95% confidence interval after Bonferroni correction (paired, two-sample t-tests). (a) Session-wise average feature stability. (b) Run-wise average feature stability.

is reasonable, since the modified feature fitness in our approach mainly impacts the medium- and low-DP features (high-DP features will usually maintain high modified feature fitness unless found in a completely irrelevant EEG channel and band for a given taskset). It is interesting to observe that session-wise stability gains are much larger than run-wise gains; this could be anticipated, since non-stationarity effects, which may substantially alter the discriminant power of features, are known to mainly occur in-between sessions rather than within a BCI session [4]. In summary, Figure 4.21 reveals that my fuzzy method preserves a substantial overlap of features across runs and sessions, boosting stability in the selected features by as high as 7% in the best-case scenario. Additionally, it must be underlined that feature stability improves already at low levels of noise, as well as in the absence of (at least, artificially added) noise.

### 4.4.3 Class-balance results

Fig. 4.22 illustrates that the proposed FL-based feature selection method outperforms the data-driven approach also in maintaining class balance. A pronounced and statistically significant (always with paired, two-sample t-tests, Bonferroni corrected) difference in favour of the fuzzy method is evident when the number of features ranges from 5 to 30, particularly at lower noise levels. Notably, the proposed method manages to preserve class balance even under conditions with a high count of features and elevated noise levels. An impressive outcome is that class re-balancing in some scenarios reaches or exceeds 30%. Practically, this means that the fuzzy method is able to render a completely biased 2-class BCI into a very well-balanced system allowing the user to deliver both BCI commands with similar ease of use.

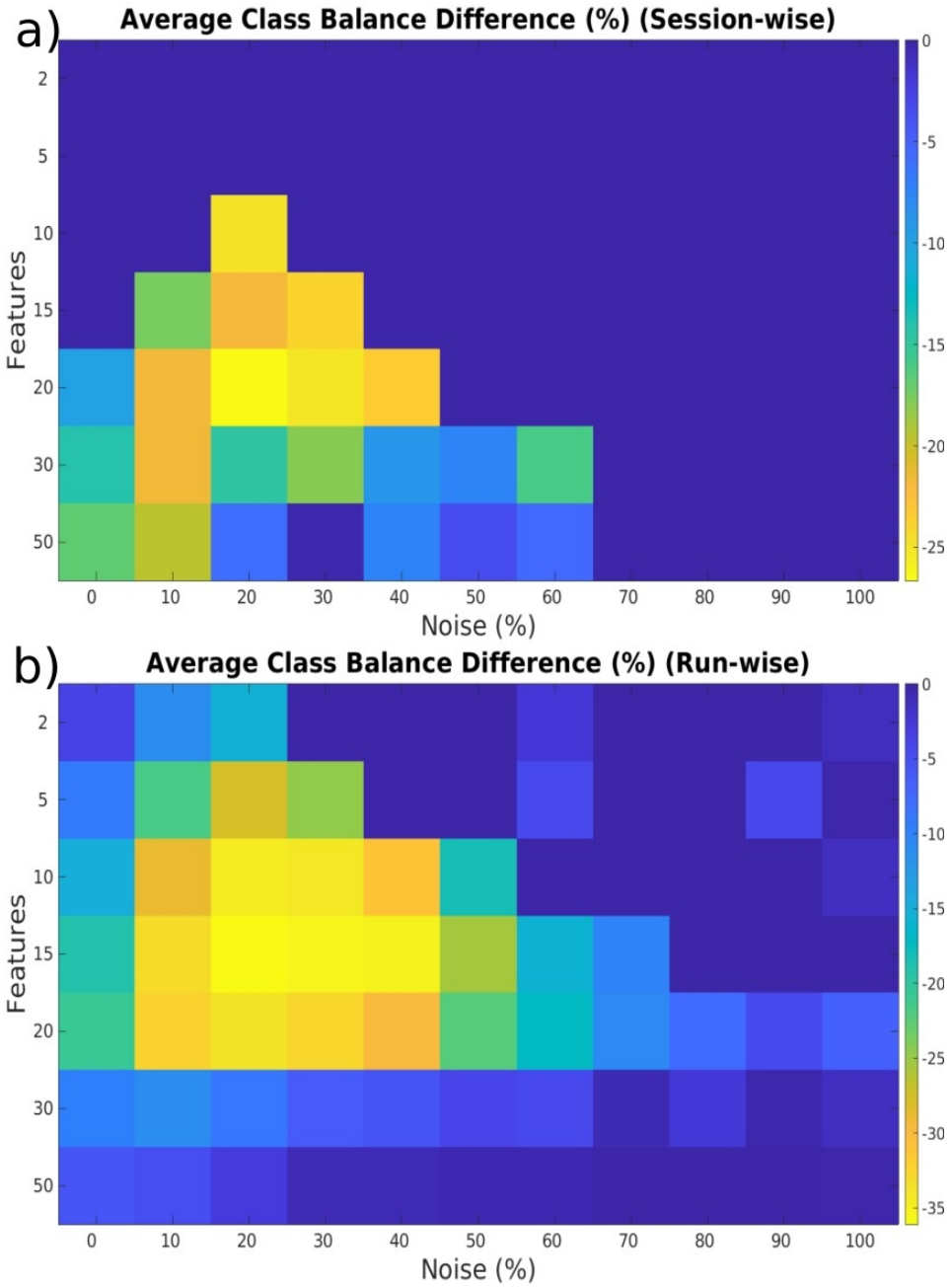


Fig. 4.22 Average (across participants) class-balance. (a) Session-wise average class-balance. (b) Run-wise average class-balance. Note that, in this case, yellow (i.e., large negative difference as shown in the colour bar) indicates the superiority of the fuzzy method in terms of class balance, while blue colour suggests similar performances between the two compared methods. Cells with 0 value (dark blue) indicate no statistical significance. All other cells indicate statistically significant differences at the 95% confidence interval after Bonferroni correction (paired, two-sample t-tests).

## 4.5 Discussion

The major research objective of this study has been to explore the feasibility of integrating expert knowledge with a data-driven approach via FL to enhance feature selection, thereby improving BCI performance and user learning. I have assumed that the proposed system could be beneficial in terms of classification accuracy, the prototypical and still most widely used BCI performance metric, feature stability and ability to "unbias" the BCI classifier. My results have confirmed these assumptions and show that the magnitude of the effects across all these performance aspects could make a real difference for closed-loop BCI control. For example, since up to 7% classification accuracy increase on average is retrieved, this means that several users with random performance could benefit from this algorithm to get in control of a MI BCI. I have also found a trend where the performance gains tend to be greater as the noise in the data increases and when the number of selected features is large.

More specifically, based on the run- and session-wise classification accuracy (for different numbers of features and noise levels), it appears that embedding expert knowledge has a positive impact on improving classification accuracy, especially when the source data is noisy. Thanks to the fuzzy logic-infused expert knowledge, the proposed method can eliminate noisy features that fully data-driven feature selection methods fail to identify. The average accuracy of the proposed feature selection method when no noise is added whatsoever is 56.5%, compared to 54.5% (for 10 features) for the data-driven method. While the accuracy gap between the two methods may not seem substantial in this case, the proposed system exhibits more consistent and stable features than its data-driven counterpart. Importantly, this 2% effect raises to 7% for the same number of features when there is artifact interference in 10-20% of trials, something that could be commonplace in real-world BCI [47].

All three performance facets checked here (classification accuracy, feature stability, class-balance) seem to be positively affected by my method as the noise level increases. However, it should also be highlighted that at very high noise levels (60% and above "noise level" as defined here through the % of artifact-contaminated trials), both methods collapse. This should be attributed to the difficulty of any method to select features on and classify extremely noisy data. I strongly believe that the range of 0-50% noise level where my method is impactful is within the spectrum of "natural" noise levels that could be observed in real-life BCI scenarios, also depending on the particularities of each application.

With regard to stability, I have underlined that gains are anticipated to be larger for session-wise selection, as my algorithm's demonstrated ability to maintain feature selection consistency finds profound applicability in session-wise feature selection where in-between session (i.e., longer-term) non-stationarity is known to greatly affect EEG feature distributions. It should also be noted that feature selection is more likely to happen in-between sessions, as too frequent feature exchange could disrupt the user's learning [47, 22]. That being said, my method's greater feature stability probably opens the road for more frequent feature selection at the initial stages of learning, where intense user learning may lead to different features naturally (i.e., not because of noise interference) emerging as optimal [61]. In other words, my method paves the way for effective online/adaptive feature selection algorithms. Of note, an adaptive version of this algorithm–if an unsupervised separability/data-driven metric can be defined–could be fully unsupervised, given that expert knowledge is embedded in the architecture of my model and does not need to be learned by data.

Importantly, it must be stressed that the added value in various types of BCI performance indicators shown and discussed here is merely the one that has been established by my "offline" analysis. It is reasonable to hypothesize that, up to the

extent that increased initial accuracy, feature stability and class-balance indeed yield improved subject learning through closed-loop feedback training, the actual effect of this algorithm when applied in actual mutual learning and/or co-adaptive user training protocols could in fact be much stronger. My future research will seek to answer this question, shedding further light on the benefits that can be reaped by fusing background knowledge with ML.

On a more conceptual note, this research makes a good effort to bridge the machine learning versus "human factors" gap in BCI literature by exemplifying how data-driven methods can be combined with neurophysiological insights and expert knowledge, as well as how subject learning objectives and facilitating factors can be taken into account. The proposed method is shown to be very successful in improving the feature selection process, incorporating both human judgment and machine intelligence to optimize inference.

## 4.6 Conclusion

In this study, I have developed a novel feature selection method that blends data-driven information with neurophysiological expert knowledge thanks to a fuzzy logic controller architecture. The proposed model not only leads to considerably higher and statistically significant classification accuracy over a conventional, purely data-driven feature selection method but also enforces greater feature stability coupled with improved class-balance. My method delivers its best in the presence of noisy EEG data but is already impactful for regular, "lab-quality" signals. Last but not least, the effect of applying this algorithm in real user training protocols will have a multiplicative impact on BCI performance because on top of the demonstrated machine learning gains, advantages like better feature stability, class-balance and keeping the feature set in a physiologically relevant manifold will additionally facilitate the subjects'

learning process. However, the proposed method currently lacks an online evaluation involving BCI users. Future work could focus on implementing the method within a proper closed-loop system. This would allow for testing the effects of the method across a larger group of subjects and more BCI sessions. Additionally, it would enable the monitoring of learning effects while ensuring the feature set remains within the physiologically relevant manifold.

# Chapter 5

# Towards calibration-less BCI-based rehabilitation

## 5.1 Introduction

Brain-computer interfaces (BCIs) are increasingly deployed in stroke rehabilitation. Most BCIs rely on batch, supervised parameter estimation which requires large, labelled brain data associated with the motor tasks to be performed during the therapy. Consequently, BCI-based rehabilitation regimes include an initial calibration session aimed at collecting the necessary data to train the BCI model. This calibration process is time-consuming and tedious, especially considering the strict logistical constraints in a clinical setting. This chapter investigates the possibility of calibration-free BCI regimes rendering re-calibration sessions entirely redundant.

## 5.2 Motivations

The main contribution of this chapter is to investigate the possibility of calibration-free BCI-based methods for stroke rehabilitation emphasizing the use of algorithms that

enable the immediate launch of therapy without imposing any prerequisite. In particular, the target is to discard the need for either previous patient data for adaptation, or subject-unspecific data for transfer learning. This analysis is based on a novel dataset of 26 sub-acute stroke patients undergoing 15 therapeutic sessions. The comparison is based on the classification accuracy obtained online by the conventional calibration method, to that of three different calibration-less schemes based on i) a supervised adaptive algorithm ii) Event-Related Spectral Perturbation (ERSP) extraction, and iii) Mahalanobis distance of SMR patterns from resting-state distributions. The findings indicate that calibration-less BCI for stroke treatments is not only possible, thus lifting a major practical barrier hindering the translation of this technology to clinics, but may also be superior to the standard, calibration-based methodology in terms of classification accuracy. The proposed method also promotes learning by escalating the therapy session without the need for any calibration sessions.

## 5.3 Materials and Methods

### 5.3.1 Participants

A total of 26 acute/sub-acute stroke patients (maximum 3 months after stroke incidence) with severe hemiplegia (16 male, 62 $\pm$ 11 years old) were recruited in 5 clinical centres in Germany, Switzerland and Italy. All patients signed informed consent and the study was approved by the local ethical committees.

### 5.3.2 Study and BCI protocols

Each patient underwent 15 therapeutic sessions over 3-5 weeks involving the training of a wrist/palm extension movement, and 3 screening sessions (pre-intervention, post-intervention, and 6-month follow-up) where the motor and resting-state tasks were

performed in open-loop with high-density EEG, and clinical assessments were carried out. Here, only the data derived from each participant's 15 therapy sessions are used. The primary outcome was Fugl-Meyer Assessment of the upper limb, with several other clinical scales (e.g., Medical Research Council scale of muscle strength) monitored at the three endpoints.

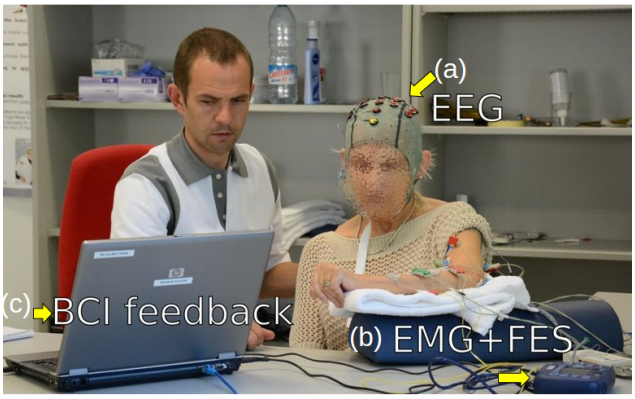


(a) Experimental setup of therapy sessions.

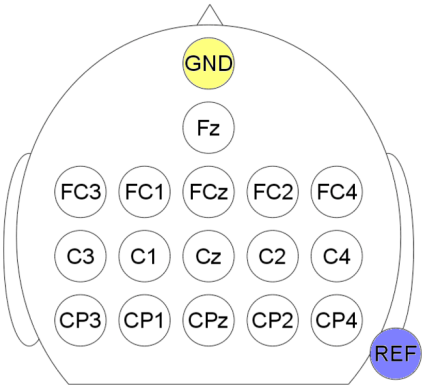


(b) EEG placement.

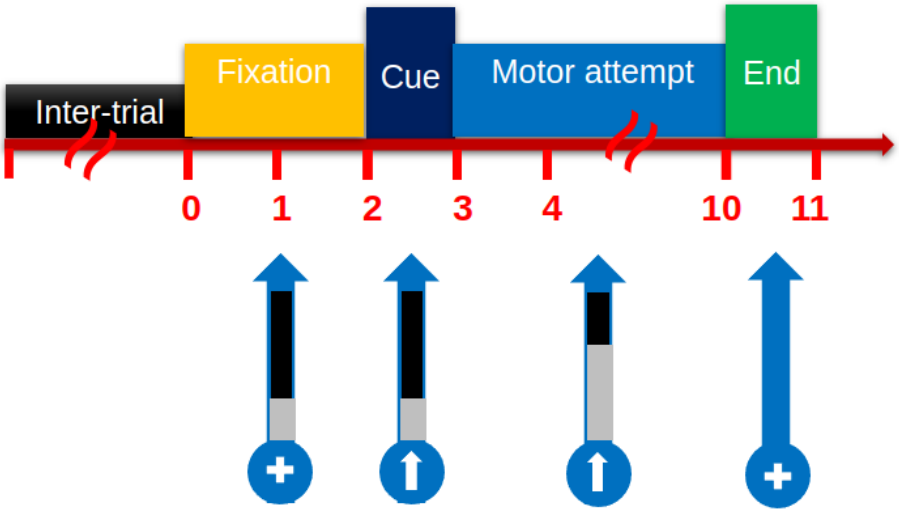


(c) Trial timeline of a therapeutic run.

Fig. 5.1 Experimental and protocol setup.

The therapy comprised repetitions of BCI-triggered, Functional Electrical Stimulation (FES)-actuated movements (wrist/palm extension of the affected upper limb

by stimulating the *extensor digitorum communis* muscle and nearby muscle sites of the forearm). The EEG and FES (Motionstim 8, Medel, Germany) hardware/software configuration (Fig. 5.1), the BCI processing, the group design (BCI vs Sham-BCI) and the experimental protocol are also partially reported in [99] and follow closely those described by Biasiucci et al. [5].

Fig. 5.1a and 5.1b illustrate the experimental setup of a therapeutic session. Brain activity acquisition during the therapeutic sessions followed the same process mentioned in Chapter 1 (1.5).

For each trial repetition, patients were requested to perform attempted wrist extension movements of the affected hand [5, 99], whose SMR EEG correlates have been shown to be similar to those elicited during MI (ERD) [8]. A therapy session included 3-7 runs (blocks) comprising 15 trials each. As shown in Fig. 5.1c, each trial started with a 2 s "fixation stimulus" epoch, during which patients were instructed to fixate a cross in the middle of the screen and prepare for the upcoming movement attempt, avoiding inducing any artifacts. This was followed by a 1 s "cue" epoch (arrow pointing upwards) instructing the user to commence their motor attempt. In the motor attempt epoch, the BCI was continuously classifying in closed-loop the patient's SMR as either "rest/no-movement" or "motor attempt". Consecutive classification decisions were integrated with an exponential smoothing filter, the output of which was visualised through a grey, "liquid-cursor" bar and fed back to the patient, as in [5, 47]; unlike its predecessor study in chronic stroke [5], in this case, patients were shown visual feedback, as depicted in Fig. 5.1c. The motor attempt epoch would successfully finish either when the patient was able to produce adequate and timely ERD in order to push the liquid cursor upwards enough so as to reach a re-configurable (by the therapist) threshold, or when the epoch would time-out (7 s). Only in the former case, reaching the threshold would trigger the FES wrist extension movement and show a

trial-end/decision-reached feedback for 1 s. The end of the motor attempt epoch was followed by an inter-trial interval lasting randomly between [3, 4] s, before the next trial takes place.

Before the therapy, a calibration session (3-4 runs) was imposed to collect data for training the BCI classifier. These runs interleaved, in random order, 15 motor attempts with 15 "rest"/no-movement trials, all of which lasted 4 s, with fake/positive feedback. The trial structure and feedback graphics were otherwise identical to those of the therapy runs. Importantly, as the results reported here refer to the online/therapy runs only, the fixation-cross epoch is used to derive instances of "rest"/"no-move" data.

A new BCI decoder was manually produced every week using data from the preceding week's therapeutic sessions so that the calibration-based benchmark already reflects a mild ("offline", periodic, subject-specific) adaptation. Of note, re-calibration was always performed by the same BCI expert and extended to Sham participants (for effective blinding). Participants in both groups underwent the exact same protocol, wearing the same apparatus; the only difference is that, in the Sham-BCI group, FES-based movement execution is triggered at random, and does not depend on the patient's SMR modulation. This was achieved by "playing back", for each participant in the Sham group, the EEG data of a matched patient in the BCI group.

### 5.3.3 EEG processing, feature extraction and selection

For this experiment, EEG processing has been done using the same method mentioned in Chapter 1 (1.5). For the actual therapy sessions, the most discriminant EEG spatio-spectral features were selected to build the BCI classifier as in [5, 34, 140].

For the calibration-less methods introduced here, to eliminate the supervised feature selection procedure that is part of conventional calibration and alleviate overfitting, the feature vectors has been reduced to 24 PSD features by considering only 12 lateral

channels–FC3, FC1, FC2, FC4, C3, C1, C2, C4, CP3, CP1, CP2, and CP4–and 2 broad–averaging the original feature space–frequency bands: $\mu$ (8-14 Hz) and $\beta$ (18-24 Hz).

### 5.3.4 Calibration-based and calibration-free methods

This work compares three calibration-less schemes to the calibration-based approach that was actually used during online BCI operation at the therapeutic sessions. The calibration-free methods concern i) a supervised adaptive algorithm relying on Quadratic Discriminant Analysis (QDA) ii) extraction and thresholding of ERSP, and iii) Mahalanobis distance of SMR patterns from resting-state distributions. The following sections describe each of these algorithms in greater detail.

### 5.3.5 Calibration-based classification

The calibration-based method is the one presented in [5]. PSD feature vectors were classified with a Gaussian mixture model (GMM) framework [34]. For each incoming PSD sample at time $t$, the output of the GMM resulted in a posterior probability distribution over the two mental classes $c$ (motor attempt "move", resting "no-move") $p_t(c|\mathbf{x_t}) = [p_t^{move}, p_t^{no-move}]$. Each mental class is represented by 4 Gaussian units. Uniform priors for the classes and mixture coefficients are assumed, as well as shared, diagonal covariance matrices. The centroids of the Gaussian units are initialized by means of self-organizing map clustering and their covariance matrices are subsequently computed as the pooled covariance matrices of the data closest to each prototype. Finally, the distribution parameters are, iteratively re-estimated through gradient descent so as to reduce the mean square error (MSE) [141]. The training of the Gaussian classifier stops, if the MSE change after each iteration is not improving, or after 20 iterations at maximum [34, 141]. As already described, during the actual therapy,

posteriors $p_t(c|\mathbf{x_t})$ were further processed with an evidence accumulation framework (exponential smoothing) to drive the feedback and the FES; for the purposes of this work, each sample $\mathbf{x_t}$ is classified as belonging to the mental class with the highest posterior probability, in order to extract classification accuracy.

### 5.3.6 Supervised adaptive QDA

Online parameter estimation of the BCI model discards the need for re-calibration sessions and presents what is probably the most straightforward avenue towards calibration-less BCI-based rehabilitation. Since in the context of a rehabilitation protocol motor tasks are instructed and not self-paced, BCI adaptation can proceed in a supervised manner, which simplifies the algorithmic design and guarantees convergence properties [24, 40]. To represent the BCI adaptation approach in the comparison, here this work devises an adaptive method based on QDA.

Specifically, by accumulating the latest available 2000 PSD samples $\mathbf{x_t}$ derived by elapsed motor attempt ("move") and fixation ("no-move") epochs in the ongoing and previous runs of a participant's data. $\mathbf{x_t}$ regards the 24 broad-band, lateral feature vectors employed also for the other calibration-less methods. The classifier is updated during the inter-trial interval every time 3 new trials are completed. The update consists in selecting the 5 (out of 24) best features according to $r^2$ separability and subsequently computing on these further reduced space $\mathbf{x'_t}$ the mental class-specific mean vectors/centroids $\mu_\mathbf{c}$ and full covariance matrices $\Sigma_c$ (with Oracle Approximating Shrinkage [142] to counteract overfitting, especially while the adaptation buffer is mostly empty at the beginning of adaptive learning). Effectively, a multivariate normal distribution $N_c(\mu_\mathbf{c}, \Sigma_c)$ is fitted to the data of each class ("move", "no-move"), which constitutes the generative dual of a QDA classifier. Similarly to the calibration-based approach (see Section 5.3.5), posteriors $p_t(c|\mathbf{x'_t}, \mu_\mathbf{c}, \Sigma_c)$ are derived at each time $t$, and

the class exceeding a probability of 0.5 "wins" the corresponding sample. The PSD samples of the first 3 trials of the simulation where no adaptive classifier exists are excluded from the calculation of classification accuracy.

### 5.3.7 ERSP-based movement detection

ERD refers to brain oscillatory activity responses in specific frequency bands and cortical locations that are widely used in SMR BCI. Strong ERD activation during motor tasks is distinguishable from the "resting" state [8]. ERSP refers to numerically stable approaches to quantify ERD phenomena describing the relative change in the EEG power following some endogenous motor task and reflecting a measure of the deviation of the bandpower relative to a baseline period. Here, ERSP definition has been adapted as:

$$ERSP_t^f = \frac{|x_t^f - \mu_{no-move}^f|}{s_{no-move}^f} \tag{5.1}$$

where $\mu_{no-move}^f$, $s_{no-move}^f$ are the mean and standard deviation of the PSD feature $f$ (for all $f$ among the aforementioned 24 features) retrieved in the preceding fixation epoch of the motor attempt trial where sample $\mathbf{x_t}$ belongs. Effectively, $ERSP_t^f$ represents the z-score of motor attempt samples with respect to the most recent estimate of the "rest" distribution for a particular spatio-spectral feature [61]. This metric relies on the notion that motor attempt periods should generate large z-score values, well outside of the high-density PSD value area corresponding to the no-movement distributions.

As $ERSP_t^f$ is a univariate metric calculated individually for each feature $f$, 3 final decision-making variants are examined, taking into account the evidence by all features: either thresholding the–across features–average (ERSP Mean), or the maximum (ERSP Max), or individually thresholding features and producing a final "move vs no-move" decision through majority voting (ERSP Majority Voting).

### 5.3.8 Mahalanobis distance movement detection

The third calibration-less approach tested resides on the same idea, but directly derives a multivariate metric to quantify the deviation of a sample $\mathbf{x_t}$ from the "resting state" through the sample's Mahalanobis distance [143] $D(\mathbf{x_t})$ from the (covariance-shrinked) multivariate normal distribution $N(\mu_{no-move}, \Sigma_{no-move})$ of the preceding fixation epoch, which is subsequently thresholded:

$$D(\mathbf{x_t}) = \sqrt{(\mathbf{x_t} - \mu_{no-move})^T * \Sigma_{no-move}^{-1} * (\mathbf{x_t} - \mu_{no-move})} \tag{5.2}$$

## 5.4 Results

Fig. 5.2 represents the average Fisher Score separability of PSD samples between the move and no-move mental classes in the $\mu$ (8-14 Hz) and $\beta$ (16-24 Hz) bands for the two patients exhibiting the highest (left) and lowest (right) classification accuracy with the calibration-based approach actually used during the therapy. It provides favourable evidence for the soundness of the motor tasks performed by patients in the study. Specifically, both patients showcase prominent SMR modulation in the anticipated $\mu$ and $\beta$ bands, which is lateralized (mostly contra-lateral–the affected hand is the right hand for Patient 1 and the left one for Patient 2–but, also with a strong ipsilateral component, especially for Patient 1), as expected for regular motor EEG correlates. Furthermore, the magnitude of SMR separability is consistent with the classification accuracy obtained for these two patients, where high accuracy is accompanied by neurophysiologically relevant SMR patterns of activity, similar to those manifesting in able-bodied and/or spinal cord injury BCI users performing motor imagery [24, 47].

With regard to the comparison among calibration-based and calibration-free methods, in order to account for the class imbalance between motor attempt and no-

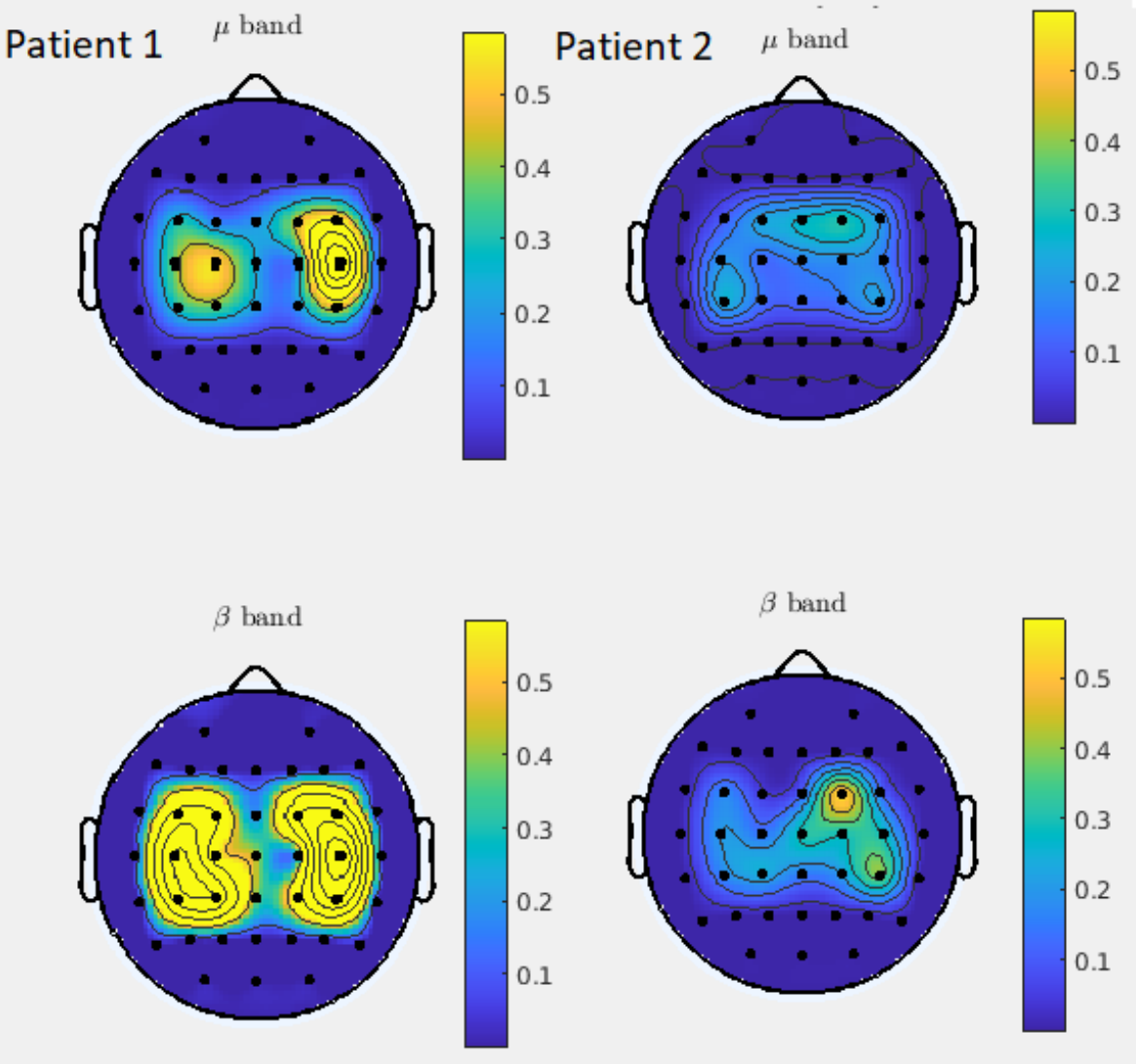


Fig. 5.2 Exemplary topographical SMR distribution for two patients with strong (left) and weaker (right) ERD.

movement intervals in terms of the number of samples available in each category in the used dataset, the investigation reports ”balanced” classification accuracy (average of the true positive and true negative rates of the obtained confusion matrix for each patient and algorithm). For each method, the results have been produced for a single, optimized threshold applied to all subjects and sessions, so that the proposed methods involve no learning of (hyper)-parameters other than what can be seamlessly computed in a standard protocol.

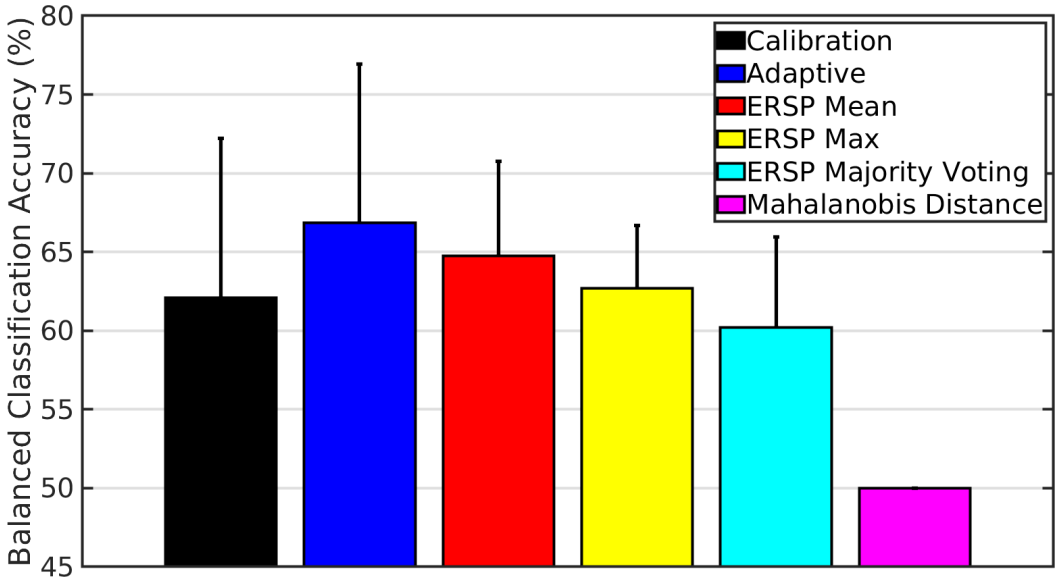


Fig. 5.3 Average and standard deviation of balanced accuracy for all methods.

Fig. 5.3 presents the average, method-wise balanced classification accuracy across patients. Evidently, the calibration-free algorithms proposed here are competitive to a standard, calibration-based approach. Specifically, the adaptive algorithm is statistically significantly superior ($p = 0.005$) to the standard approach and the ERSP-Mean marginally so ($p = 0.07$, paired, two-sided t-test). The Mahalanobis distance method did not perform better than a random classifier due to intense overfitting, in spite of using covariance shrinkage for regularization; however, the successful application of univariate ERSP, which shares the same underlying idea, suggests that it could work with a reduced feature space and/or longer resting epochs.

## 5.5 Conclusions

The results strongly indicate that a calibration phase for supervised training of SMR BCI classification models, currently the method-of-choice (also) in stroke rehabilitation protocols despite the logistic concerns raised, is not really necessary. Adaptive classification with virtually "zero" calibration needs (i.e., in this work, only 3 trials are

needed to output the first classifier; fake or no feedback provided for this short interval should be acceptable in the rehabilitation setting) is shown to significantly outperform, on average, the standard, calibration-based BCI. Importantly, methods based on simple ERSP-inspired movement intent detection from EEG are also competitive to the supervised classification model; this is a critical observation, as there can be occasions or individuals (e.g., increased artifact production due to concomitant deficits for certain stroke patients, such as spasticity or dyskinesia) where adaptive approaches may be ill-advised, due to their vulnerability of adapting to noise.

Necessary findings substantiate the claim that the calibration stage in BCI-based rehabilitation regimes, where the natural availability of labels and the seamless incorporation of short resting-state epochs allow for supervised adaptation and ERD-inspired methodologies, can be spared without detriment. This conclusion yields considerable impact on the design and logistics of BCI-based rehabilitation interventions. Furthermore, the findings have good potential and can be applied to other BCI-based motor rehabilitation regimes (e.g., for spinal cord injury patients). However, the proposed methods lack online evaluation, which is necessary to understand their impacts and monitor the long-term effects of learning. Proposed calibration-less methods should be implemented through a closed-loop, BCI-based rehabilitation regime to explore their full potential and establish these methods as an effective way to eliminate the need for calibration. Further work will focus on fine-tuning these approaches and extending their evaluation to larger datasets, along with conducting appropriate clinical trials for stroke patients.

# Chapter 6

# Discussion and future work

## 6.1 Summary and main findings

This thesis has presented an analysis of EEG correlates and methods that promote learning, of either the machine, the subject, or both, in a BCI context. It highlights how current MI BCI-based methods are biased towards data-driven approaches and still largely lack efficient and effective user-oriented methodologies. Here, I have attempted to partially fill this gap by conducting three different investigations.

The first experiment aimed to identify the EEG correlates of learning to drive a racing car. It further investigated the potential role of a neuromodulation technology, tDCS, in enhancing race-driving skills. The conducted experiments and analysis suggest that tDCS might affect the acquisition of complex motor learning skills like race driving. Additionally, this work determined that theta band EEG rhythms and functional connectivity in the alpha band are neuromarkers of acquiring race-driving skills.

The second study introduced a novel feature selection method that combines neurophysiological expert knowledge with a data-driven approach. FL is the basis of this algorithm, exploiting the suitability of FL theory for integrating different

information channels for decision-making. The results show that the proposed algorithm yields substantial benefits compared to purely data-driven feature selection methods. Specifically, it outperformed the conventional approach in terms of classification accuracy, stability, and class balance. I also showed that the proposed feature selection method provides larger gains when noisy MI BCI data are involved.

The third and final study explored possible ways to eliminate calibration sessions in the framework of BCI-based rehabilitation. Several calibration-free methods were compared. My analysis indicates that the calibration procedure is unnecessary and can be spared without compromising the BCI decoder's performance. The proposed algorithms could remove the major logistics barrier towards deploying BCI-based therapies in clinics.

## 6.2 Discussion of methods, limitations and future work

The common ground in the studies conducted during my thesis has been the introduction of analysis and BCI methods that take into account and shift the focus on subject learning, neuroplasticity effects and, in general, the human factor in the BCI loop. Irrespective of the inherently different nature and scope of the conducted investigations, I sincerely believe that my thesis has set some important stepping stones in that regard. Nevertheless, my work inevitably also suffers certain limitations, the main of which I attempt to identify here.

The racing driving study has singled out key biomarkers of learning to race. These findings could be used as the basis of modern racing protocols that rely on real-time EEG monitoring. However, it remains unclear how exactly this information could be exploited in that respect. One possible option could be the establishment of

neurofeedback-based protocols providing feedback on the identified neuromarkers so as to enforce and speed up their modulation, hoping that this will further promote learning to race. Assessing the effectiveness of this approach must be experimentally verified. Furthermore, this kind of learning protocol is known to be lengthy. In general, greater effort must be devoted to a solid plan for the exploitation of these findings.

Another limitation of this study is that the hints about a potential role of tDCS in speeding up learning are rather weak and must be also confirmed in bigger studies. Further work could also include redefining the metrics for assessing brake and throttle use and analyzing eye fixation potential through EOG data that are available but have not been analyzed so far.

My FL-based feature selection algorithm has shown great promise for improving classification accuracy, feature stability and class-bias in MI BCI. Nevertheless, I have posited that this kind of algorithm should yield even bigger impact once applied in actual mutual learning protocols and engage the user's learning capacity. Naturally, evidence for confirming this hypothesis can only be derived by additional, and exclusively closed-loop, experimentation. This investigation can also be expanded by generating additional rules in order to better model issues like stability (e.g., by explicitly requiring common feature subsets across sessions) and class-balance (e.g., by explicitly imposing a minimum number of features that are physiologically relevant for each of the classes, separately). Lastly, there is probably room for improving the defined membership functions so as to further increase the method's effect. This could be done either through further trial-and-error, or in a more data-driven approach: by creating exact profiles of the frequency with which various features emerge as separable in large subject databases and using these "selection frequency" profiles as membership functions.

Last but not least, the calibration-free algorithms introduced in my last investigation should be tested in practice in the clinic, either for stroke or spinal cord injury motor

therapies. In fact, an ongoing randomised clinical trial is already successfully using the adaptive method proposed therein. These approaches could also be fine-tuned, and the failure of the Mahalanobis-distance-based algorithm must be understood in-depth.

In general, future work could entail closed-loop application and testing of all of the proposed methods with larger numbers of subjects and BCI sessions so as to monitor long-term learning effects.

# References


[1] Leeb, R.; Perdikis, S.; Tonin, L.; Biasiucci, A.; Tavella, M.; Creatura, M.; Molina, A.; Al-Khodairy, A.; Carlson, T.; Millán, J. d. R. Transferring brain-computer interfaces beyond the laboratory: Successful application control for motor-disabled users. *Artificial Intelligence in Medicine* **2013**, *59*, 121–132.

[2] Yi, W.; Qiu, S.; Qi, H.; Zhang, L.; Wan, B.; Ming, D. EEG feature comparison and classification of simple and compound limb motor imagery. *Journal of neuroengineering and rehabilitation* **2013**, *10*, 1–12.

[3] Perdikis, S.; Tonin, L.; Saeedi, S.; Schneider, C.; Millán, J. d. R. The Cybathlon BCI race: Successful longitudinal mutual learning with two tetraplegic users. *PLoS biology* **2018**, *16*, e2003787.

[4] Perdikis, S.; Leeb, R.; Williamson, J.; Ramsay, A.; Tavella, M.; Desideri, L.; Hoogerwerf, E.-J.; Al-Khodairy, A.; Murray-Smith, R.; d R Millán, J. Clinical evaluation of BrainTree, a motor imagery hybrid BCI speller. *Journal of neural engineering* **2014**, *11*, 036003.

[5] Biasiucci, A.; Leeb, R.; Iturrate, I.; Perdikis, S.; Al-Khodairy, A.; Corbet, T.; Schnider, A.; Schmidlin, T.; Zhang, H.; Bassolino, M.; Viceic, D.; Vuadens, P.; Guggisberg, A.; Millan, J. d. R. Brain-actuated functional electrical stimulation elicits lasting arm motor recovery after stroke. *Nature Communications* **2018**, *9*, 2421.

[6] Chaudhary, U.; Birbaumer, N.; Ramos-Murguialday, A. Brain–computer interfaces for communication and rehabilitation. *Nature Reviews Neurology* **2016**, *12*, 513–525.

[7] Wolpaw, J. R.; Birbaumer, N.; McFarland, D. J.; Pfurtscheller, G.; Vaughan, T. M. Brain-computer interfaces for communication and control. *Clin. Neurophysiol.* **2002**, *113*, 767–91.

[8] Pfurtscheller, G.; da Silva., F. H. L. Event-related EEG/MEG synchronization and desynchronization: basic principles. Clinical Neurophysiology. 1999; pp 1842–1857.

[9] Birbaumer, N.; Ghanayim, N.; Hinterberger, T.; Iversen, I.; Kotchoubey, B.; Kübler, A.; Perelmouter, J.; Taub, E.; Flor, H. A spelling device for the paralysed. *Nature* **1999**, *398*, 297–298.

[10] Carmena, J. M.; Lebedev, M. A.; Crist, R. E.; O'Doherty, J. E.; Santucci, D. M.; Dimitrov, D. F.; Patil, P. G.; Henriquez, C. S.; Nicolelis, M. A. L. Learning to control a brain–machine interface for reaching and grasping by primates. *PLoS biology* **2003**, *1*, e42.

[11] Neuper, C.; Pfurtscheller, G. Neurofeedback training for BCI control. *Brain-Computer Interfaces: Revolutionizing Human-Computer Interaction* **2010**, 65–78.

[12] Ganguly, K.; Carmena, J. M. Emergence of a stable cortical map for neuroprosthetic control. *PLoS biology* **2009**, *7*, e1000153.

[13] Jarosiewicz, B.; Chase, S. M.; Fraser, G. W.; Velliste, M.; Kass, R. E.; Schwartz, A. B. Functional network reorganization during learning in a brain-computer interface paradigm. *Proceedings of the National Academy of Sciences* **2008**, *105*, 19486–19491.

[14] Wander, J. D.; Blakely, T.; Miller, K. J.; Weaver, K. E.; Johnson, L. A.; Olson, J. D.; Fetz, E. E.; Rao, R. P.; Ojemann, J. G. Distributed cortical adaptation during learning of a brain–computer interface task. *Proceedings of the National Academy of Sciences* **2013**, *110*, 10818–10823.

[15] Koralek, A. C.; Jin, X.; Long II, J. D.; Costa, R. M.; Carmena, J. M. Corticostriatal plasticity is necessary for learning intentional neuroprosthetic skills. *Nature* **2012**, *483*, 331–335.

[16] Dornhege, G.; Millan, J. d. R.; Hinterberger, T.; Mcfarland, D.; Müller, K.-R. *Toward Brain-Computer Interfacing*; 2007.

[17] Müller, J. S.; Vidaurre, C.; Schreuder, M.; Meinecke, F. C.; Von Bünau, P.; Müller, K.-R. A mathematical model for the two-learners problem. *Journal of neural engineering* **2017**, *14*, 036005.

[18] Millán, J. d. R. Brain-machine interfaces: the perception-action closed loop: a two-learner system. *IEEE Systems, Man, and Cybernetics Magazine* **2015**, *1*, 6–8.

[19] Orsborn, A. L.; Moorman, H. G.; Overduin, S. A.; Shanechi, M. M.; Dimitrov, D. F.; Carmena, J. M. Closed-loop decoder adaptation shapes neural plasticity for skillful neuroprosthetic control. *Neuron* **2014**, *82*, 1380–1393.

[20] Lotte, F.; Larrue, F.; Mühl, C. Flaws in current human training protocols for spontaneous Brain-Computer Interfaces: lessons learned from instructional design. *Frontiers in Human Neuroscience* **2013**, *7*, 568.

[21] Chavarriaga, R.; Fried-Oken, M.; Kleih, S.; Lotte, F.; Scherer, R. Heading for new shores! Overcoming pitfalls in BCI design. *Brain-Computer Interfaces* **2017**, *4*, 60–73.

[22] Perdikis, S.; d. R. Millán, J. Brain-Machine Interfaces: A Tale of Two Learners. *IEEE Systems, Man, and Cybernetics Magazine* **2020**, *6*, 12–19.

[23] Leeb, R.; Perdikis, S.; Tonin, L.; Biasiucci, A.; Tavella, M.; Creatura, M.; Molina, A.; Al-Khodairy, A.; Carlson, T.; dR Millán, J. Transferring brain–computer interfaces beyond the laboratory: successful application control for motor-disabled users. *Artificial intelligence in medicine* **2013**, *59*, 121–132.

[24] Perdikis, S.; Leeb, R.; Millán, J. d. R. Context-aware adaptive spelling in motor imagery BCI. *J. Neural Eng.* **2016**, *13*, 036018.

[25] Tonin, L.; Leeb, R.; Tavella, M.; Perdikis, S.; Millán, J. d. R. The role of shared-control in BCI-based telepresence. 2010 IEEE International Conference on Systems, Man and Cybernetics. 2010; pp 1462–1466.

[26] Leeb, R.; Tonin, L.; Rohm, M.; Desideri, L.; Carlson, T.; Millan, J. d. R. Towards independence: a BCI telepresence robot for people with severe motor disabilities. *Proceedings of the IEEE* **2015**, *103*, 969–982.

[27] Randazzo, L.; Iturrate, I.; Perdikis, S.; Millán, J. d. R. mano: A wearable hand exoskeleton for activities of daily living and neurorehabilitation. *IEEE Robotics and Automation Letters* **2017**, *3*, 500–507.

[28] Ethier, C.; Gallego, J.; Miller, L. E. Brain-controlled neuromuscular stimulation to drive neural plasticity and functional recovery. *Current opinion in neurobiology* **2015**, *33*, 95–102.

[29] Ramos-Murguialday, A.; Broetz, D.; Rea, M.; Läer, L.; Yilmaz, Ö.; Brasil, F. L.; Liberati, G.; Curado, M. R.; Garcia-Cossio, E.; Vyziotis, A.; others Brain–machine interface in chronic stroke rehabilitation: a controlled study. *Annals of neurology* **2013**, *74*, 100–108.

[30] Pichiorri, F.; Morone, G.; Petti, M.; Toppi, J.; Pisotta, I.; Molinari, M.; Paolucci, S.; Inghilleri, M.; Astolfi, L.; Cincotti, F.; others Brain–computer interface boosts motor imagery practice during stroke recovery. *Annals of neurology* **2015**, *77*, 851–865.

[31] Perdikis, S. A Critical Review of Adaptive Brain-Computer Interfaces. *Encyclopedia BRAIN* **2023**, 0136, to appear.

[32] Carmena, J. M. Advances in neuroprosthetic learning and control. *PLoS biology* **2013**, *11*, e1001561.

[33] Millan, J. R.; Mouriño, J. Asynchronous BCI and local neural classifiers: an overview of the adaptive brain interface project. *IEEE transactions on neural systems and rehabilitation engineering* **2003**, *11*, 159–161.

[34] Leeb, P. S. T.-L. B. A. T. M. . C. M. e. a., R. Transferring brain-computer interfaces beyond the laboratory: successful application control for motor-disabled users. Artificial Intelligence in Medicine. 2013; pp 121–132.

[35] Blumberg, J.; Rickert, J.; Waldert, S.; Schulze-Bonhage, A.; Aertsen, A.; Mehring, C. Adaptive classification for brain computer interfaces. 2007 29th Annual International Conference of the IEEE Engineering in Medicine and Biology Society. 2007; pp 2536–2539.

[36] Zhang, D.; Wang, Y.; Gao, X.; Hong, B.; Gao, S.; others An algorithm for idle-state detection in motor-imagery-based brain-computer interface. *Computational Intelligence and Neuroscience* **2007**, *2007*.

[37] Yoon, J. W.; Roberts, S. J.; Dyson, M.; Gan, J. Q. Bayesian inference for an adaptive ordered probit model: An application to brain computer interfacing. *Neural Networks* **2011**, *24*, 726–734.

[38] Vidaurre, C.; Sannelli, C.; Müller, K.-R.; Blankertz, B. Machine-learning-based coadaptive calibration for brain-computer interfaces. *Neural computation* **2011**, *23*, 791–816.

[39] DiGiovanna, J.; Mahmoudi, B.; Fortes, J.; Principe, J. C.; Sanchez, J. C. Coadaptive brain–machine interface via reinforcement learning. *IEEE transactions on biomedical engineering* **2008**, *56*, 54–64.

[40] Cunha, J. D.; Perdikis, S.; Halder, S.; Scherer, R. Post-Adaptation Effects in a Motor Imagery Brain-Computer Interface Online Coadaptive Paradigm. *IEEE Access* **2021**, *9*, 41688–41703.

[41] Birbaumer, N.; Murguialday, A.-R.; Weber, C.; Montoya, P. In *Neurofeedback and Brain–Computer Interface: Clinical Applications*; Summerer, L. R. D. I. L., Ed.; International Review of Neurobiology; Academic Press, 2009; Vol. 86; pp 107–117.

[42] Birbaumer, N.; Ghanayim, N.; Hinterberger, T.; Iversen, I.; Kotchoubey, B.; Kübler, A.; Perelmouter, J.; Taub, E.; Flor, H. A Spelling Device for the Paralyzed. *Nature* **1999**, *398*, 297–298.

[43] Lotte, F.; Bougrain, L.; Cichocki, A.; Clerc, M.; Congedo, M.; Rakotomamonjy, A.; Yger, F. A review of classification algorithms for EEG-based brain–computer interfaces: a 10 year update. *Journal of Neural Engineering* **2018**, *15*, 031005.

[44] Iturrate, I.; Chavarriaga, R.; del R. Millán, J. In *Brain-Computer Interfaces*; Ramsey, N. F., del R. Millán, J., Eds.; Handbook of Clinical Neurology; Elsevier, 2020; Vol. 168; pp 311–328.

[45] Chavarriaga, R.; Fried-Oken, M.; Kleih, S.; Lotte, F.; Scherer, R. *Brain-Computer Interfaces* **2017**, *4*, 60–73.

[46] Perdikis, S.; Leeb, R.; d. R. Millán, J. Subject-oriented training for motor imagery brain-computer interfaces. 2014 36th Annual International Conference of the IEEE Engineering in Medicine and Biology Society. 2014; pp 1259–1262.

[47] Perdikis, S.; Tonin, L.; Saeedi, S.; Schneider, C.; Millán, J. d. R. The Cybathlon BCI race: Successful longitudinal mutual learning with two tetraplegic users. *PLoS Biol.* **2018**, *16*, e2003787.

[48] Hehenberger, L.; Kobler, R. J.; Lopes-Dias, C.; Srisrisawang, N.; Tumfart, P.; Uroko, J. B.; Torke, P. R.; Müller-Putz, G. R. Long-Term Mutual Training for

the CYBATHLON BCI Race With a Tetraplegic Pilot: A Case Study on Inter-Session Transfer and Intra-Session Adaptation. *Frontiers in Human Neuroscience* **2021**, *15*, 70.

[49] Benaroch, C.; Sadatnejad, K.; Roc, A.; Appriou, A.; Monseigne, T.; Pramij, S.; Mladenovic, J.; Pillette, L.; Jeunet, C.; Lotte, F. Long-Term BCI Training of a Tetraplegic User: Adaptive Riemannian Classifiers and User Training. *Frontiers in Human Neuroscience* **2021**, *15*, 118.

[50] Bang, J.-S.; Lee, M.-H.; Fazli, S.; Guan, C.; Lee, S.-W. Spatio-Spectral Feature Representation for Motor Imagery Classification Using Convolutional Neural Networks. *IEEE Transactions on Neural Networks and Learning Systems* **2021**, *33*, 3038–3049.

[51] Rudin, C. Stop explaining black box machine learning models for high stakes decisions and use interpretable models instead. *Nature Machine Intelligence* **2019**, *1*, 206–215.

[52] Bernal, G.; Montgomery, S. M.; Maes, P. Brain-Computer Interfaces, Open-Source, and Democratizing the Future of Augmented Consciousness. *Frontiers in Computer Science* **2021**, *3*, 23.

[53] Hwang, H.-J.; Kim, S.; Choi, S.; Im, C.-H. EEG-Based Brain-Computer Interfaces: A Thorough Literature Survey. *International Journal of Human-Computer Interaction* **2013**, *29*, 814–826.

[54] Bhattacharyya, S.; Rakshit, P.; Konar, A.; Tibarewala, D. N.; Janarthanan, R. Feature Selection of Motor Imagery EEG Signals Using Firefly Temporal Difference Q-Learning and Support Vector Machine. Swarm, Evolutionary, and Memetic Computing. Cham, 2013; pp 534–545.

[55] Bhattacharyya, S.; Sengupta, A.; Chakraborti, T.; Konar, A.; Tibarewala, D. N. Automatic feature selection of motor imagery EEG signals using differential evolution and learning automata. *Medical & Biological Engineering & Computing* **2014**, *52*, 131–139.

[56] Joadder, M. A. M.; Myszewski, J. J.; Rahman, M. H.; Wang, I. A performance based feature selection technique for subject independent MI based BCI. *Health information science and systems* **2019**, *7*, 15–15.

[57] Molla, M. K. I.; Shiam, A. A.; Islam, M. R.; Tanaka, T. Discriminative Feature Selection-Based Motor Imagery Classification Using EEG Signal. *IEEE Access* **2020**, *8*, 98255–98265.

[58] Guyon, I.; Elisseeff, A. An Introduction to Variable and Feature Selection. *J. Mach. Learn. Res.* **2003**, *3*, 1157–1182.

[59] Ying, O. Z.; binti Awang, S. A.; Vijean, V. A. Optimization of Irrelevant Features for Brain-Computer Interface (BCI) System. *Journal of Physics: Conference Series* **2019**, *1372*, 012047.

[60] Bevilacqua, M.; Perdikis, S.; Millán, J. d. R. On Error-Related Potentials During Sensorimotor-Based Brain-Computer Interface: Explorations With a Pseudo-Online Brain-Controlled Speller. *IEEE Open Journal of Engineering in Medicine and Biology* **2020**, *1*, 17–22.

[61] Perdikis, S.; Leeb, R.; Williamson, J.; Ramsay, A.; Tavella, M.; Desideri, L.; Hoogerwerf, E.-J.; Al-Khodairy, A.; Murray-Smith, R.; Millán, J. d. R. Clinical evaluation of BrainTree, a motor imagery hybrid BCI speller. *J. Neural Eng.* **2014**, *11*, 036003.

[62] Fruitet, J.; McFarland, D. J.; Wolpaw, J. R. A comparison of regression techniques for a two-dimensional sensorimotor rhythm-based brain-computer interface. *Journal of neural engineering* **2010**, *7*, 16003–16003.

[63] Ang, K. K.; Chin, Z. Y.; Zhang, H.; Guan, C. Mutual information-based selection of optimal spatial–temporal patterns for single-trial EEG-based BCIs. *Pattern Recognition* **2012**, *45*, 2137–2144, Brain Decoding.

[64] Radman, M.; Chaibakhsh, A.; Nariman-zadeh, N.; He, H. Feature fusion for improving performance of motor imagery brain-computer interface system. *Biomedical Signal Processing and Control* **2021**, *68*, 102763.

[65] Faller, J.; Vidaurre, C.; Solis-Escalante, T.; Neuper, C.; Scherer, R. Autocalibration and Recurrent Adaptation: Towards a Plug and Play Online ERD-BCI. *Neural Systems and Rehabilitation Engineering, IEEE Transactions on* **2012**, *20*, 313–319.

[66] Faller, J.; Scherer, R.; Costa, U.; Opisso, E.; Medina, J.; Müller-Putz, G. R. A Co-Adaptive Brain-Computer Interface for End Users with Severe Motor Impairment. *PLOS ONE* **2014**, *9*, 1–10.

[67] Perdikis, S.; Leeb, R.; Chavarriaga, R.; Millán, J. d. R. Context-Aware Learning for Generative Models. *IEEE Transactions on Neural Networks and Learning Systems* **2020**, *32*, 3471–3483.

[68] *Fuzzy Logic with Engineering Applications*; John Wiley  Sons, Ltd, 2010; Chapter 11, pp 369–407.

[69] Shafer, G. *A Mathematical Theory of Evidence*; Princeton University Press: Princeton, 1976.

[70] Mitra, S.; Pal, S. K. Fuzzy sets in pattern recognition and machine intelligence. *Fuzzy Sets and systems* **2005**, *156*, 381–386.

[71] Xydeas, C.; Angelov, P.; Chiao, S.-Y.; Reoullas, M. Advances in classification of EEG signals via evolving fuzzy classifiers and dependant multiple HMMs. *Computers in biology and medicine* **2006**, *36*, 1064–1083.

[72] Fabien, L.; Anatole, L.; Fabrice, L.; Bruno, A. Studying the use of fuzzy inference systems for motor imagery classification. *IEEE transactions on neural systems and rehabilitation engineering* **2007**, *15*, 322–324.

[73] Aarabi, A.; Fazel-Rezai, R.; Aghakhani, Y. A fuzzy rule-based system for epileptic seizure detection in intracranial EEG. *Clinical Neurophysiology* **2009**, *120*, 1648–1657.

[74] Martinez-Leon, J.-A.; Cano-Izquierdo, J.-M.; Ibarrola, J. Feature Selection Applying Statistical and Neurofuzzy Methods to EEG-Based BCI. *Computational Intelligence and Neuroscience* **2015**, *2015*, 781207.

[75] Trofimov, A. G.; Shishkin, S. L.; Kozyrskiy, B. L.; Velichkovsky, B. M. A Greedy Feature Selection Algorithm for Brain-Computer Interface Classification Committees. *Procedia Computer Science* **2018**, *123*, 488–493, 8th Annual International Conference on Biologically Inspired Cognitive Architectures, BICA 2017 (Eighth Annual Meeting of the BICA Society), held August 1-6, 2017 in Moscow, Russia.

[76] Tao, Z. Classification-Oriented Fuzzy-Rough Feature Selection for the EEG-Based Brain-Computer Interfaces. Proceedings of the Thirteenth International Conference on Management Science and Engineering Management. 2020; pp 295–307.

[77] Chatterjee, R.; Sanyal, D. K.; Chatterjee, A. Fuzzy-Discernibility Matrix-based Efficient Feature Selection Techniques for Improved Motor-Imagery EEG Signal Classification. *bioRxiv* **2021**,

[78] Yang, Z.; Wang, Y.; Ouyang, G. Adaptive Neuro-Fuzzy Inference System for Classification of Background EEG Signals from ESES Patients and Controls. *The Scientific World Journal* **2014**, *2014*, 140863.

[79] Herman, P. A.; Prasad, G.; McGinnity, T. M. Designing an Interval Type-2 Fuzzy Logic System for Handling Uncertainty Effects in Brain–Computer Interface Classification of Motor Imagery Induced EEG Patterns. *IEEE Transactions on Fuzzy Systems* **2017**, *25*, 29–42.

[80] Gupta, A.; Kumar, D. Fuzzy clustering-based feature extraction method for mental task classification. *Brain informatics* **2017**, *4*, 135–145.

[81] Jiang, Y.; Deng, Z.; Chung, F.-L.; Wang, G.; Qian, P.; Choi, K.-S.; Wang, S. Recognition of Epileptic EEG Signals Using a Novel Multiview TSK Fuzzy System. *IEEE Transactions on Fuzzy Systems* **2017**, *25*, 3–20.

[82] Saleh, A. I.; Shehata, S. A.; Labeeb, L. M. A fuzzy-based classification strategy (FBCS) based on brain–computer interface. *Soft Computing* **2019**, *23*, 2343–2367.

[83] Saga, N.; Doi, A.; Oda, T.; Kudoh, S. N. Elucidation of EEG Characteristics of Fuzzy Reasoning-Based Heuristic BCI and Its Application to Patient With Brain Infarction. *Frontiers in Neurorobotics* **2021**, *14*, 123.

[84] Li, M.; Wang, R.; Xu, D. An Improved Composite Multiscale Fuzzy Entropy for Feature Extraction of MI-EEG. *Entropy (Basel, Switzerland)* **2020**, *22*, 1356.

[85] Cervera, M. A.; Soekadar, S. R.; Ushiba, J.; Millán, J. d. R.; Liu, M.; Birbaumer, N.; Garipelli, G. Brain-computer interfaces for post-stroke motor rehabilitation: a meta-analysis. *Annals of Clinical and Translational Neurology* **2018**, *5*, 651–663.

[86] Ramos-Murguialday, A. et al. Brain-machine interface in chronic stroke rehabilitation: A controlled study. *Annals of Neurology* **2013**, *74*, 100–108.

[87] Ang, K. K.; Guan, C.; Phua, K. S.; Wang, C.; Zhou, L.; Tang, K. Y.; Joseph, G. J. E.; Kuah, C. W. K.; Chua, K. S. G. Brain-computer interface-based robotic end effector system for wrist and hand rehabilitation: results of a three-armed randomized controlled trial for chronic stroke. *Frontiers in Neuroengineering* **2014**, *7*.

[88] Ang, K. K.; Chua, K. S. G.; Phua, K. S.; Wang, C.; Chin, Z. Y.; Kuah, C. W. K.; Low, W.; Guan, C. A Randomized Controlled Trial of EEG-Based Motor Imagery Brain-Computer Interface Robotic Rehabilitation for Stroke. *Clinical EEG and Neuroscience* **2014**, *46*, 310–320.

[89] Pichiorri, F.; Morone, G.; Petti, M.; Toppi, J.; Pisotta, I.; Molinari, M.; Paolucci, S.; Inghilleri, M.; Astolfi, L.; Cincotti, F.; Mattia, D. Brain-computer interface boosts motor imagery practice during stroke recovery. *Annals of Neurology* **2015**, *77*, 851–865.

[90] Frolov, A. A.; Mokienko, O.; Lyukmanov, R.; Biryukova, E.; Kotov, S.; Turbina, L.; Nadareyshvily, G.; Bushkova, Y. Post-stroke Rehabilitation Training with a Motor-Imagery-Based Brain-Computer Interface (BCI)-Controlled Hand Exoskeleton: A Randomized Controlled Multicenter Trial. *Frontiers in Neuroscience* **2017**, *11*.

[91] Vourvopoulos, A.; Pardo, O. M.; Lefebvre, S.; Neureither, M.; Saldana, D.; Jahng, E.; Liew, S.-L. Effects of a Brain-Computer Interface With Virtual Reality (VR) Neurofeedback: A Pilot Study in Chronic Stroke Patients. *Frontiers in Human Neuroscience* **2019**, *13*.

[92] Vidaurre C., C. R. S. R., Schlöogl A.; G., P. A fully on-line adaptive BCI. IEEE Transactions on Biomedical Engineering. 2006; pp 1214–1219.

[93] Krauledat M., B. B., Schroder M.; K., M. Calibration time for brain-computer interfaces: A clustering approach. Advances Neural Information Processing Syst. 2007; p 753.

[94] Fazli S., D. M. B. B. K. M. G. C., Popescu F. Subject independent mental state classification in single trials. Neural Networks. 2009; pp 1305–1312.

[95] Vidaurre C., M. K. R., Sannelli C.; B., B. Coadaptive calibration to improve BCI efficiency. Journal of Neural Engineering. 2011; p 025009.

[96] Arvaneh, M.; Guan, C.; Ang, K. K.; Quek, C. Omitting the intra-session calibration in EEG-based brain-computer interface used for stroke rehabilitation. 2012 Annual International Conference of the IEEE Engineering in Medicine and Biology Society. 2012; pp 4124–4127.

[97] Arvaneh, M.; Guan, C.; Ang, K. K.; Ward, T. E.; Chua, K. S. G.; Kuah, C. W. K.; Joseph, G. J. E.; Phua, K. S.; Wang, C. Facilitating motor imagery-based brain–computer interface for stroke patients using passive movement. *Neural Computing and Applications* **2016**, *28*, 3259–3272.

[98] Cao, L.; Chen, S.; Jia, J.; Fan, C.; Wang, H.; Xu, Z. An Inter- and Intra-Subject Transfer Calibration Scheme for Improving Feedback Performance of Sensorimotor Rhythm-Based BCI Rehabilitation. *Frontiers in Neuroscience* **2021**, *14*, 629572.

[99] Krueger, J. et al. Functional electrical stimulation driven by a brain–computer interface in acute and subacute stroke patients impacts beta power and long-range temporal correlation. 2022 IEEE Workshop on Complexity in Engineering (COMPENG). 2022; pp 1–5.

[100] Dhawale, A. K.; Smith, M. A.; Ölveczky, B. P. The role of variability in motor learning. *Annual review of neuroscience* **2017**, *40*, 479–498.

[101] Diedrichsen, J.; Kornysheva, K. Motor skill learning between selection and execution. *Trends in cognitive sciences* **2015**, *19*, 227–233.

[102] Ericsson, K. A.; Krampe, R. T.; Tesch-Römer, C. The role of deliberate practice in the acquisition of expert performance. *Psychological review* **1993**, *100*, 363.

[103] Park, J. L.; Fairweather, M. M.; Donaldson, D. I. Making the case for mobile cognition: EEG and sports performance. *Neuroscience & Biobehavioral Reviews* **2015**, *52*, 117–130.

[104] Bernardi, G.; Ricciardi, E.; Sani, L.; Gaglianese, A.; Papasogli, A.; Ceccarelli, R.; Franzoni, F.; Galetta, F.; Santoro, G.; Goebel, R.; others How skill expertise shapes the brain functional architecture: an fMRI study of visuo-spatial and motor processing in professional racing-car and naïve drivers. *PloS one* **2013**, *8*, e77764.

[105] Bernardi, G.; Cecchetti, L.; Handjaras, G.; Sani, L.; Gaglianese, A.; Ceccarelli, R.; Franzoni, F.; Galetta, F.; Santoro, G.; Goebel, R.; others It's not all in your car: functional and structural correlates of exceptional driving skills in professional racers. *Frontiers in human neuroscience* **2014**, *8*, 888.

[106] Lappi, O. The racer's brain–how domain expertise is reflected in the neural substrates of driving. *Frontiers in human neuroscience* **2015**, *9*, 635.

[107] Rito Lima, I.; Haar, S.; Di Grassi, L.; Faisal, A. A. Neurobehavioural signatures in race car driving: a case study. *Scientific reports* **2020**, *10*, 11537.

[108] Ericsson, K. A.; Lehmann, A. C. Expert and exceptional performance: Evidence of maximal adaptation to task constraints. *Annual review of psychology* **1996**, *47*, 273–305.

[109] Macnamara, B. N.; Moreau, D.; Hambrick, D. Z. The relationship between deliberate practice and performance in sports: A meta-analysis. *Perspectives on Psychological Science* **2016**, *11*, 333–350.

[110] Land, M. F.; Lee, D. N. Where we look when we steer. *Nature* **1994**, *369*, 742–744.

[111] Van Leeuwen, P. M.; De Groot, S.; Happee, R.; De Winter, J. C. Differences between racing and non-racing drivers: A simulator study using eye-tracking. *PLoS one* **2017**, *12*, e0186871.

[112] Reis, J.; Schambra, H. M.; Cohen, L. G.; Buch, E. R.; Fritsch, B.; Zarahn, E.; Celnik, P. A.; Krakauer, J. W. Noninvasive cortical stimulation enhances motor skill acquisition over multiple days through an effect on consolidation. *Proceedings of the National Academy of Sciences* **2009**, *106*, 1590–1595.

[113] Galea, J. M.; Vazquez, A.; Pasricha, N.; Orban de Xivry, J.-J.; Celnik, P. Dissociating the roles of the cerebellum and motor cortex during adaptive learning: the motor cortex retains what the cerebellum learns. *Cerebral cortex* **2011**, *21*, 1761–1770.

[114] Keeser, D.; Padberg, F.; Reisinger, E.; Pogarell, O.; Kirsch, V.; Palm, U. Prefrontal direct current stimulation modulates resting EEG and event-related potentials in healthy subjects: a standardized low resolution tomography (sLORETA) study. *Neuroimage* **2011a**, *55*, 644–657.

[115] Keeser, D.; Meindl, T.; Bor, J.; Palm, U.; Pogarell, O.; Mulert, C.; et al. "Prefrontal transcranial direct current stimulation changes connectivity of resting-state networks during fMRI. *Nature* **2011b**, *32*, 15284–15293.

[116] Chen, J. L.; Schipani, A.; Schuch, C. P.; Lam, H.; Swardfager, W.; Thiel, A.; Edwards, J. D. Does cathodal vs. sham transcranial direct current stimulation over contralesional motor cortex enhance upper limb motor recovery post-stroke? A systematic review and meta-analysis. *Frontiers in Neurology* **2021**, *12*, 626021.

[117] Jamil, A.; Batsikadze, G.; Kuo, H.-I.; Labruna, L.; Hasan, A.; Paulus, W.; Nitsche, M. A. Systematic evaluation of the impact of stimulation intensity on neuroplastic after-effects induced by transcranial direct current stimulation. *The Journal of physiology* **2017**, *595*, 1273–1288.

[118] Nitsche, M. A.; Paulus, W. Excitability changes induced in the human motor cortex by weak transcranial direct current stimulation. *The Journal of physiology* **2000**, *527*, 633.

[119] Fritsch, B.; Reis, J.; Martinowich, K.; Schambra, H. M.; Ji, Y.; Cohen, L. G.; Lu, B. Direct current stimulation promotes BDNF-dependent synaptic plasticity: potential implications for motor learning. *Neuron* **2010**, *66*, 198–204.

[120] Gellner, A.-K.; Reis, J.; Holtick, C.; Schubert, C.; Fritsch, B. Direct current stimulation-induced synaptic plasticity in the sensorimotor cortex: structure follows function. *Brain stimulation* **2020**, *13*, 80–88.

[121] Cantarero, G.; Spampinato, D.; Reis, J.; Ajagbe, L.; Thompson, T.; Kulkarni, K.; Celnik, P. Cerebellar direct current stimulation enhances on-line motor skill acquisition through an effect on accuracy. *Journal of Neuroscience* **2015**, *35*, 3285–3290.

[122] Kunaratnam, N.; Saumer, T. M.; Kuan, G.; Holmes, Z.; Swarbrick, D.; Kiss, A.; Mochizuki, G.; Chen, J. L. Transcranial direct current stimulation leads to faster acquisition of motor skills, but effects are not maintained at retention. *Plos one* **2022**, *17*, e0269851.

[123] Dosenbach, N. U.; Kristina; M.Visscher; D.Palmer, E.; M.Miezin, F.; K.Wenger, K.; C.Kang., H.; DarcyBurgund; L.Grimes, A.; L.Schlaggar, B.; E.Petersen, S. A core system for the implementation of task sets. *Neuron* **2006**, *50*, 799–812.

[124] Dayan, E.; Cohen, L. G. Neuroplasticity subserving motor skill learning. *Neuron* **2011**, *72*, 443–454.

[125] Cole, M. W.; Bassett, D. S.; Power, J. D.; Braver, T. S.; Petersen, S. E. Intrinsic and task-evoked network architectures of the human brain. *Neuron* **2014**, *83*, 238–251.

[126] Draganski, B.; Gaser, C.; Busch, V.; Schuierer, G.; Bogdahn, U.; May, A. Changes in grey matter induced by training. *Nature* **2004**, *427*, 311–312.

[127] Zatorre, R. J.; Fields, R. D.; Johansen-Berg, H. Plasticity in gray and white: neuroimaging changes in brain structure during learning. *Nature neuroscience* **2012**, *15*, 528–536.

[128] Chang, Y. Reorganization and plastic changes of the human brain associated with skill learning and expertise. *Frontiers in human neuroscience* **2014**, *8*, 35.

[129] Beeli, G.; Koeneke, S.; Gasser, K.; Jancke, L. Brain stimulation modulates driving behaviour. *Behav* **2008**, *34*, 4–34.

[130] Herwig, U.; Satrapi, P.; C, S.-L. Using the international 10-20EEG system for positioning of transcranial magnetic stimulation. *Brain Topogr* **2003**, *16*, 95–99.

[131] Daly, I.; Scherer, R.; Billinger, M.; Müller-Putz, G. FORCe: Fully online and automated artifact removal for brain-computer interfacing. *IEEE transactions on neural systems and rehabilitation engineering* **2014**, *23*, 725–736.

[132] Koo, T.-K. Construction of fuzzy linguistic model. Proceedings of 35th IEEE Conference on Decision and Control. 1996; pp 98–103.

[133] Sadtler, P. T.; Quick, K. M.; Golub, M. D.; Chase, S. M.; Ryu, S. I.; Tyler-Kabara, E. C.; Yu, B. M.; Batista, A. P. Neural constraints on learning. *Nature* **2014**, *512*, 423–426.

[134] Jin, Z.; Bourban, F.; Leeb, R.; Perdikis, S. Quantifying the impact and profiling functional EEG artifacts. 2022 IEEE International Conference on Systems, Man, and Cybernetics (SMC). 2022; pp 629–634.

[135] G, P.; C., N. Motor imagery and direct brain–computer communication. Proceedings of the IEEE. 2001; pp 1123–1134.

[136] Pfurtscheller, G.; Brunner, C.; Schlögl, A.; Da Silva, F. L. Mu rhythm (de) synchronization and EEG single-trial classification of different motor imagery tasks. *NeuroImage* **2006**, *31*, 153–159.

[137] Avdeenko, T.; Makarova, E. Integration of case-based and rule-based reasoning through fuzzy inference in decision support systems. *Procedia Computer Science* **2017**, *103*, 447–453.

[138] Zadeh, L. A.; Aliev, R. A. *Fuzzy logic theory and applications: part I and part II*; World Scientific Publishing, 2018.

[139] Chen, Y.; Wiesel, A.; Eldar, Y. C.; Hero, A. O. Shrinkage algorithms for MMSE covariance estimation. *IEEE transactions on signal processing* **2010**, *58*, 5016–5029.

[140] Galán F., O. F. G. J. M. J., Ferrez P. W. Feature extraction for multi-class BCI using canonical variates analysis. In Proc. IEEE Int Symp Intell Signal. 2007.

[141] Millán JdR, M. J. G. W., Renkens F Noninvasive brain-actuated control of a mobile robot by human EEG. IEEE Transactions on Biomedical Engineering. 2004; pp 1026–1033.

[142] Chen, Y.; Wiesel, A.; Eldar, Y. C.; Hero, A. O. Shrinkage Algorithms for MMSE Covariance Estimation. *IEEE Transactions on Signal Processing* **2010**, *58*, 5016–5029.

[143] R. De Maesschalck, D. M., D. Jouan-Rimbaud The Mahalanobis distance. Chemometrics and Intelligent Laboratory Systems. 2000; pp 1–18.